Online Appendix for 'Capital Inflow Shocks and Convenience Yields'

Nadav Ben Zeev*
Ben-Gurion University of the Negev

Noam Ben-Ze'ev†
Bank of Israel and Ben-Gurion University of the Negev

Daniel Nathan‡
Bank of Israel

June 15, 2025

Abstract

This online appendix consists of the following four appendices: an institutional background appendix; a forecast error variance (FEV) and historical decomposition analysis appendix; an appendix depicting a simple model that serves as theoretical motivation for the paper; and a robustness appendix.

*Department of Economics, Ben-Gurion University of the Negev, Beer-Sheva, Israel. *E-mail:* nadavbz@bgu.ac.il.

†Research Department, Bank of Israel, Jerusalem, Israel, and the Department of Economics, Ben-Gurion University of the Negev, Beer-Sheva, Israel. *E-mail:* Noam.ben-zeev@boi.org.il.

‡Research Department, Bank of Israel, Jerusalem, Israel. *E-mail:* daniel.nathan@boi.org.il.

Appendix A Institutional Background

This section provides an overview of the MAKAM market in Israel and the role of FFIs in this market. We begin by detailing the structure and purpose of MAKAM, short-term securities issued by the Bank of Israel (BOI).

MAKAM: Israel's BOI-Issued Short-Term Risk-Free Bond Market. MAKAM are short-term zero-coupon securities issued by the BOI that were introduced on a meaningful scale in 1995. The BOI issues MAKAM to large primary dealers as 3- or 12-month maturity bonds, with monthly issuances resulting in 12 series traded concurrently, each with a term up to 1 year.[1]

Why would there be a constraint on a central bank's security issuance in the presence of large capital inflow shocks? Section B addresses this question, presenting a simple structural model that provides a conceptual base and motivation for the empirical analysis of this paper. Our theoretical framework captures the general idea that a whenever a central bank faces a cost from supplying the large amounts of the risk-free bonds demanded by FFIs, its supply of such bonds would be imperfectly elastic and a convenience yield would thus emerge in the presence of FFIs' large demand flows. This idea applies to both the case where the central bank is an issuer of such bonds as well as to the case where the government—and not the central bank—is the issuer. For the government-as-issuer case, the model captures the idea that while governments could theoretically issue more bonds in response to foreign demand pressures, they face their own constraints—debt management considerations prevent arbitrary increases in short-term funding. As such, the model and mechanism we highlight have broad external validity beyond our empirical setting of central bank securities.

MAKAM Market Liquidity and Trading. The MAKAM market is highly liquid and centrally traded on the Tel Aviv Stock Exchange (TASE). Its liquidity significantly surpasses that of comparable short-term Israeli government bonds. Over our sample period, MAKAM's average daily trading volume was ILS 305.2 million, 3.3 times higher than the ILS 91.6 million for maturity-comparable short-term government bonds. Moreover, the MAKAM market has an average bid-ask spread of 0.025%, 40% tighter than that of government bonds, contributing to it being

[1] It is noteworthy that issuance of central bank securities is by no means unique to the BOI: over one third of central banks issue or have issued central bank securities (Gray and Pongsaparn (2015)), including economies such as Chile, Korea, Thailand, Switzerland, and Japan.

the preferred choice for FFIs engaging in USD/ILS CIP arbitrage. The crucial contributor to this superiority—on top of the aforementioned increased liquidity feature—will be explained below after providing a formal definition of FFIs and elucidating the CIP arbitrage trade.

Definition of FFIs. FFIs are global financial intermediaries, including commercial banks, investment banks, hedge funds, and asset managers, that pool funds from various investors and invest in financial assets. In the MAKAM market, FFIs are major players due to the opportunities for CIP arbitrage. The BOI's daily MAKAM flow data treats FFIs as any foreign financial institution involved in trading these short-term instruments.

MAKAM Market and CIP Arbitrage. MAKAM plays a crucial role in USD/ILS CIP arbitrage, where FFIs borrow at the risk-free dollar rate and tap into the FX swap market, investing the proceeds in local currency in the MAKAM market. To illustrate a hypothetical CIP arbitrage opportunity, consider a simplified example. An FFI borrows $100 million for one year at a USD LIBOR rate of 10%. This borrowing represents the funding leg of the FFI's CIP arbitrage trade. It then converts this to ILS at a spot rate of 4 ILS/USD and invests the resulting 4 million ILS in one-year MAKAM yielding 10%. The MAKAM investment represents the investment leg of the FFI's CIP arbitrage trade. Simultaneously, it enters a one-year forward contract at 3.9 ILS/USD for both the 440 million ILS (principal and interest proceeds from the MAKAM investment).

At maturity, the ILS investment grows to 440 million ILS, equivalent to $112.82 million when converted back to USD at the forward rate. After repaying the $110 million loan (principal plus interest), the FFI earns an arbitrage profit of $2.82 million, or 2.82%. This positive return represents the cross-currency basis in absolute terms (the basis is defined as the minus of this return as it is equal to the difference between the USD LIBOR rate (10% in our example) and the CIP-implied rate (12.82% in our example). MAKAM plays a crucial role in USD/ILS CIP arbitrage, where FFIs borrow at the risk-free dollar rate and tap into the FX swap market, investing the proceeds in local currency in the MAKAM market.

MAKAM Versus Government Bonds in CIP Arbitrage. As discussed above, the MAKAM market is significantly more liquid than the maturity-comparable government bond market, contributing to MAKAM being the preferred investment leg of FFIs' CIP arbitrage trades. But the most crucial contributor to this superiority is that, unlike short-term government bonds, MAKAM

offers a risk-free investment that is readily available across a rich spectrum of short-term maturities, making it ideal for being used as the investment leg in CIP arbitrage. Specifically, over our sample there are available for trading, on average, only 2 short-term (under one-year maturity) government bond securities as opposed to 12 MAKAM securities with month-specific maturities. This stark difference in availability and flexibility makes MAKAM the clearly superior choice over short-term government bonds for the implementation of CIP arbitrage.[2]

Importantly, the MAKAM market allows FFIs to access risk-free BOI-issued assets without needing local banking subsidiaries, which are typically required for access to central bank deposit facilities (Rime et al. (2022)). Specifically, to invest in a central bank's deposit facility, an FFI is required to own a local banking subsidiary with access to this facility. (Such associated local branching activity from FFIs' is a rarity in Israel.) In contrast, a local central bank securities market such as the MAKAM market circumvents this requirement, thus rendering effectively unlimited access to holding a risk-free central bank asset for all FFIs.

Sectoral Comparison of MAKAM Holdings as Shares of Outstanding MAKAM. Figure A.1 shows the evolution of monthly MAKAM holding shares of total outstanding MAKAM bonds held by various sectors, including FFIs. Note that total outstanding MAKAM level is determined by both the BOI's issuance activity, which it implements once every month, as well as the maturing of bonds. Figure A.1 indicates that over the course of our sample period FFIs have replaced local banks as the dominant MAKAM holders, with the former steadily reaching a roughly 50% share of the market from a single digit share and the latter correspondingly dropping from a similar such high share all the way to a single digit share. Local banks mostly substituted MAKAM holding with central bank deposits during our sample, which stresses the important link between the interbank and MAKAM markets. Notably, as discussed in Section 4.5 in the main text, mutual funds—and not local banks—are FFIs' counterparty in their secondary market MAKAM purchasing activity; local banks play a counteracting role only in the primary market, taking direct purchasing orders from FFIs prior to MAKAM auctions.

The figure clearly demonstrates that our FFIs were engaged in significant investment activity in the MAKAM market. The cross-currency basis dynamics in Figure A.2— which we discuss in

[2]On top of this crucial advantage, an additional edge - as relayed to us from conversations with market participants - that MAKAM enjoys is its perception by traders as being an even safer investment than short-term government bonds due to the BOI (rather than the government) being the issuer of legal tender.

detail below—explains the main point of attraction for FFIs' meaningful presence as buyers in the MAKAM market and in particular their increased presence from early March of 2020 onwards. Our identification design is based on capturing shocks to this persistent buying activity while purging them of a rich array of global and local shocks including COVID-induced financial shocks. FFIs' delayed entrance into the MAKAM market—relative to the already meaningful CIP arbitrage profit available from the beginning of the sample—is consistent with theories of slow-moving capital where there are institutional frictions such as search costs and time to raise capital (see, e.g., Mitchell et al. (2007) and Duffie (2010)).

USD/ILS Cross-Currency Basis. Figure A.2 shows the USD/ILS cross-currency basis (i.e., deviation from CIP) for our baseline sample period defined in the usual way as the difference between the USD LIBOR rate and CIP-implied rate. This basis is the average over the 1-, 3-, 6-, and 12-month bases. For completeness and comparison purposes, the figure shows the latter for both the Tel Aviv Inter-Bank Offered Rate (TELBOR), which is based on interest rate quotes by a number of commercial banks in the Israeli inter-bank market (i.e., TELBOR is the local interbank rate) rate as well as the MAKAM rate. The negative MAKAM-based basis for our sample period - which is on average -33.7 basis points - proxies for the CIP arbitrage profit that was obtained by FFIs.[3]

The USD/ILS negative basis for this period—long after the adverse credit supply shocks from the 2008-2009 global financial crisis and 2011-2012 European sovereign debt crisis—is not unique but rather a reflection of a salient such negative basis for a host of other currencies vis-a-vis the dollar, as established by the burgeoning CIP deviations literature described above.

MAKAM Versus TELBOR in CIP Arbitrage. That the MAKAM-based basis from Figure A.2 was less negative than the TELBOR-based basis, which is on average -39.5 basis points or 5.2 basis points lower than the average MAKAM-based basis,[4] is precisely due to the convenience yield embodied in MAKAM rates and speaks to the segmentation existing between these two mar-

[3]While FFIs tend to use short-term FX swaps in their CIP arbitrage activity and roll over these swap positions, thus making the 1-month basis the best measure of FFIs' actual arbitrage profit from their various transactions in the MAKAM market, we nevertheless show here the averaged and much smoother basis series for presentational purposes.

[4]From 2021 onwards, i.e., for the period when the convenience yield prevails, the average TELBOR-based basis is -68.6 basis points or nearly 25 basis points lower than the corresponding -44 basis point average of the MAKAM-based basis.

kets: FFIs view the latter rates as less risky (they are essentially risk-free) than the local interbank rates and hence tap into the MAKAM market rather than the interbank market when conducting CIP arbitrage, where they are willing to accept a lower MAKAM rate relative to the interbank rate so long that the MAKAM-based basis is still negative.

FFIs' preference for MAKAM as the CIP arbitrage's investment leg over the local interbank markets is not only due to internal risk management practices but also due to Basel III regulation concerning the Liquidity Coverage Ratio (LCR) which is defined as the ratio between high-quality liquid assets (HQLA) and the projected upcoming 30 days' net cash outflows under a stress scenario specified by supervisors (BCBS and BIS (2013)).[5] In particular, this regulation requires global banks to have an LCR that is at least 100% and imposes on assets haircuts that are increasing in the non-liquid and risky nature of the assets. Since unsecured wholesale funding, the text-book funding leg of CIP arbitrage trades, has an assumed outflow rate equal to 100% under distress, the global bank's only choice that does not worsen its LCR is to invest in HQLA in the CIP arbitrage trade's investment leg (Anderson et al. (2024)).[6] Marketable CB-issued securities such as MAKAM count as 'Level 1' HQLA and thus do not get penalized by any haircut while interbank term deposits—being excluded from all categories of HQLA ('Level 1 (0% haircut), 'Level 2A (15% haircut), and 'Level 2B (25%-50% haircut))—receive the maximal 100% haircut, making tapping into the local ILS interbank market as the investment leg of global banks' CIP arbitrage completely inferior to the MAKAM option.[7]

Convenience Yield. Figure A.3 shows the daily evolution of the MAKAM convenience yield. For completeness, we also show the MAKAM and TELBOR rate series. All series are averages

[5]Since cash inflows are capped by 75% of outflows, these net outflows in our setting are 25% of the expected outflow payment of the global bank on the funding leg of the CIP arbitrage, i.e., the principal and interest to be paid on the global interbank USD loan funding the FX swap.

[6]Using secured wholesale funding - such as repo loans - for the funding leg of the trade does not resolve this problem. Specifically, although assigning a 0% outflow rate under distress, secured wholesale funding also implies that the collateral used to obtain the funding be excluded from HQLA, thus making once more investing in HQLA the global bank's only choice not to worsen its LCR.

[7]Even when MAKAM rates are negative, as they are in 7.2% of our sample, it will still not be desirable by global banks to hold the ILS proceeds from the FX swap's first leg (i.e, spot trade) in a checking account with an Israeli bank. The reason for this is that such accounts still get assigned a 100% haircut as they are also excluded from all of the HQLA categories (like interbank term deposits). Since the negative rates on MAKAM never exceeded -20 basis points over our sample and averaged a modest -3.1 basis points, even in this negative rate environment the 100% haircut from regulators on local interbank checking accounts makes the latter assets undesirable for the CIP arbitrage's investment leg relative to MAKAM.

over the individual 1-12 monthly maturity-specific series. The 1-month TELBOR series effectively represents the *current* monetary policy stance (see more on this fact below) whereas later (2-12) maturity-specific TELBOR rates represent the near-term *future* stance of monetary policy. Hence, the MAKAM convenience yield constitutes a sound measure of the convenience yield and associated monetary policy transmission impairment: it precisely captures the difficulty of the central bank to perfectly align the short-term bond market rate with the corresponding interbank rate.

The close-to-zero TELBOR and MAKAM rates for the majority of the sample (up to April 2022) emphasize the corresponding zero lower bound (ZLB) state characterizing the BOI's policy stance from the beginning of our sample through April 2022 when the BOI began raising their policy rate. For our purposes, it is important to focus on the MAKAM convenience yield's dynamics and in particular its persistent shift into meaningful positive territory from early January of 2021 onwards, averaging 25.3 basis points. It is noteworthy that before this shift, there was no convenience yield in MAKAM with this yield averaging an effectively null -0.4 basis points.

While the MAKAM convenience yield clearly widens considerably further in tandem with the monetary-policy-induced rise in the MAKAM yield from April 2022 onwards, there is also a meaningful widening that takes place concurrently with the ZLB period (the average convenience yield from truncating the sample at 4/11/21—the start of rate hikes from the BOI—is 12 basis points).

Our econometric analysis, by focusing on exogenous capital inflow shocks and the MAKAM convenience yield as the outcome variable which in turn purges the effects of the current and future stance of monetary policy from the estimation, will be able to cleanly identify the convenience yield's response. A risk-free rate based convenience yield mechanism is likely to apply to MAKAM in the non-ZLB period when higher interest rates amplify MAKAM's role as a local near-money asset (Nagel (2016)).[8] Our identification approach and the fact that the bulk of our period is characterized by the ZLB make us confident that our results shed light on an additional convenience yield mechanism—distinct from the above-mentioned non-ZLB mechanism—by which capital inflow shocks drive local convenience yields. This confidence is further bolstered by our confirming the robustness of our results to excluding the non-ZLB period in Section D.2 of this

[8]The ZLB period began prior to our sample already from September 2014. The MAKAM convenience yield was a modest -3.8 basis points on average from this period until the beginning of our sample, while averaging 13.8 basis points for the non-ZLB period of January 2005 (the period when TELBOR data became available) to August 2014.

online appendix.

Figure A.1: **Time Series of MAKAM Holding Shares' Distribution by Sector.**

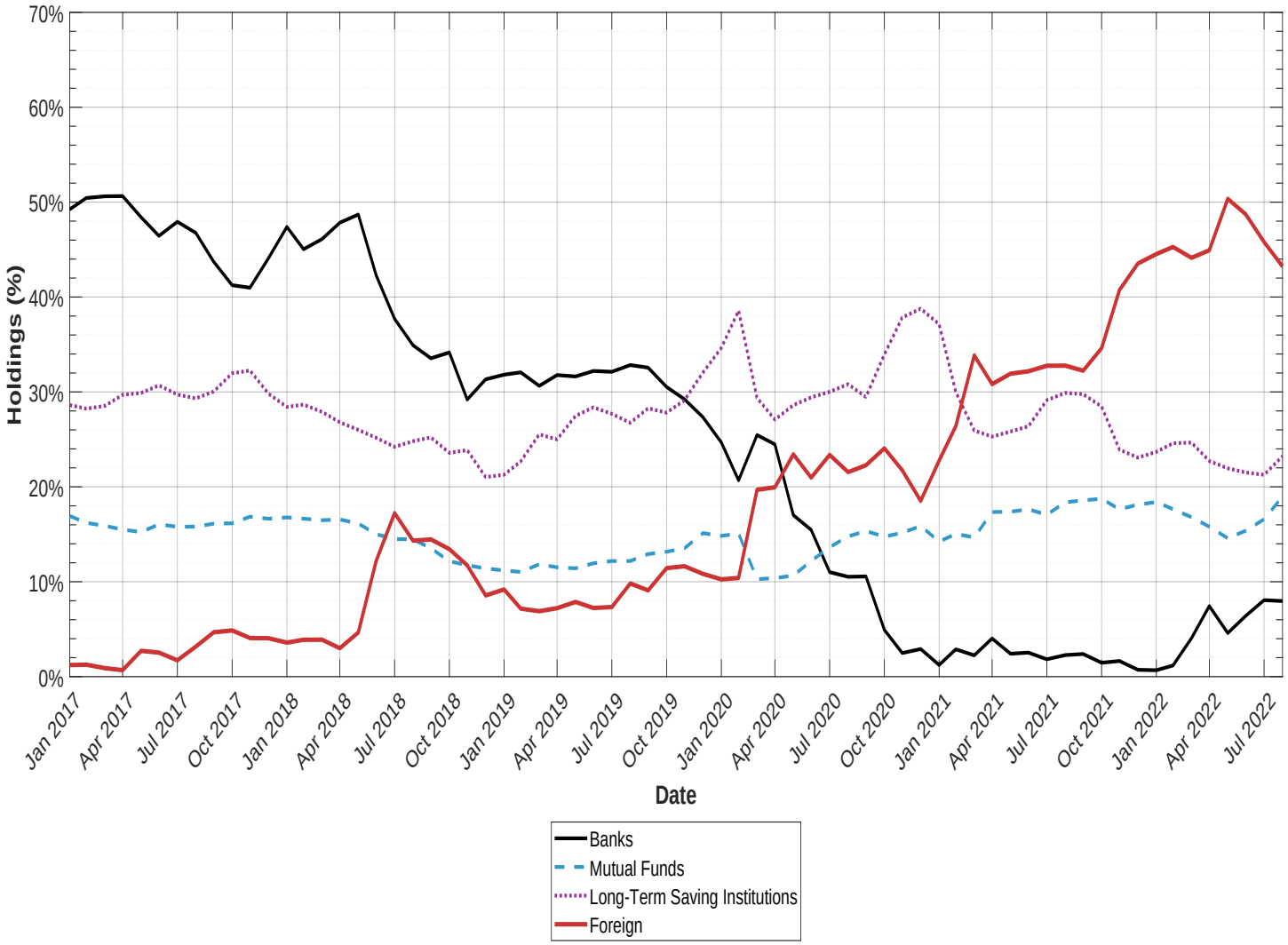

Notes: This figure presents the time series of MAKAM market holding shares by sector. On top of the FFI sector (which is represented by red solid line), this figure includes three additional sectors: Israeli mutual fund sector (dashed blue line); long-term savings sector (dotted purple line), which includes Israeli pension, provident, and advanced training funds as well as insurance companies; and Israeli commercial banks sector (black solid line). Data are from the BOI and cover 1/2017-8/2022. Time (in monthly dates) is on the x-axis. Values are in percentage terms.

Figure A.2: **Time Series of USD/ILS Cross-Currency Basis.**

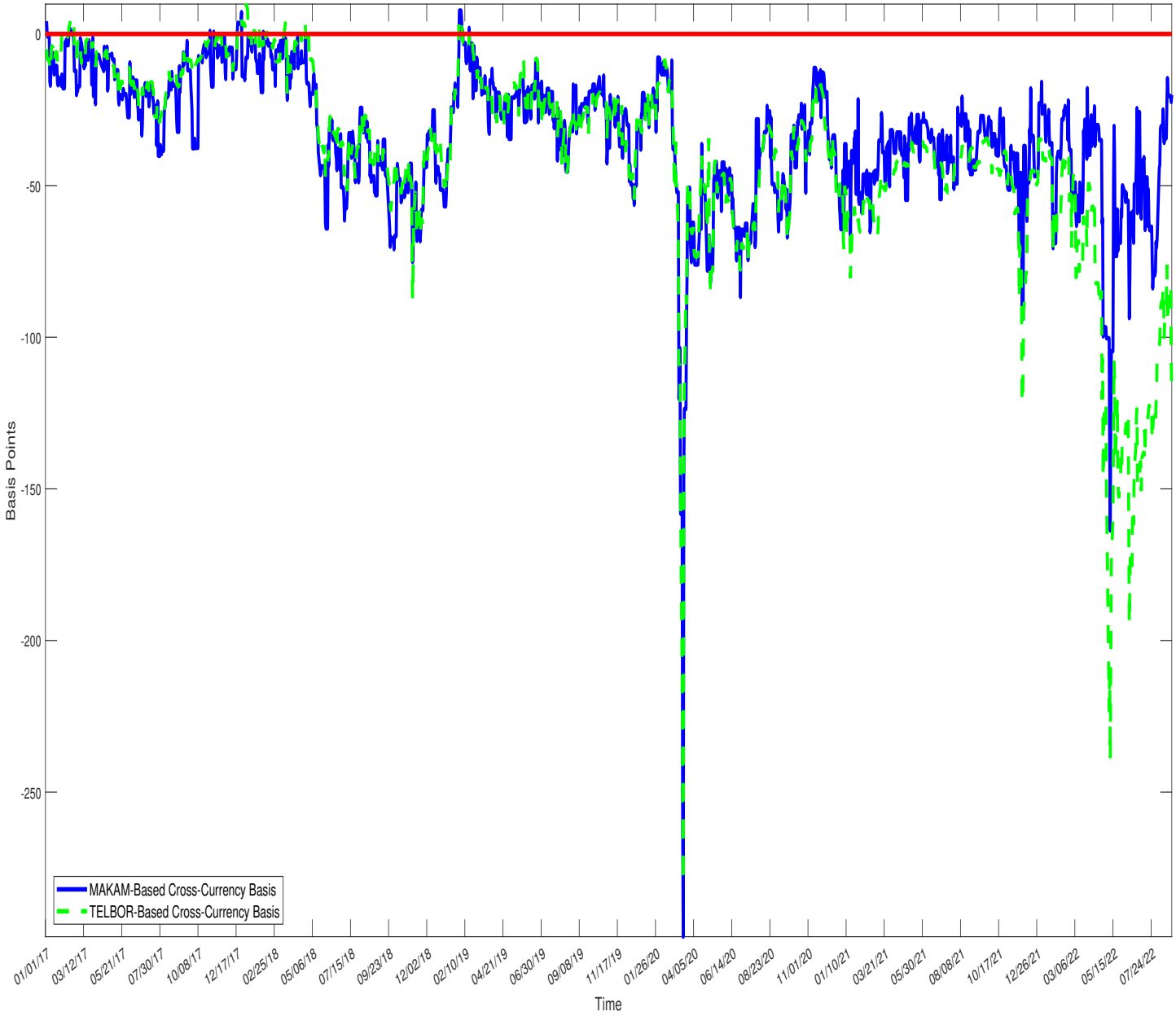

Notes: This figure presents the time series of the daily USD/ILS cross-currency basis calculated as the difference between LIBOR and CIP-implied dollar rate, where the local risk-free rate is either the MAKAM rate (solid line case) or TELBOR rate (dashed line case). The basis is computed as the average over the 1-, 3-, 6-, and 12-month bases. Data are from Bloomberg and cover 1/1/201-8/31/2022. Time (daily dates) is on the x-axis. The bases (in basis points) are on the left y-axis.

Figure A.3: **Time Series of MAKAM Convenience Yield.**

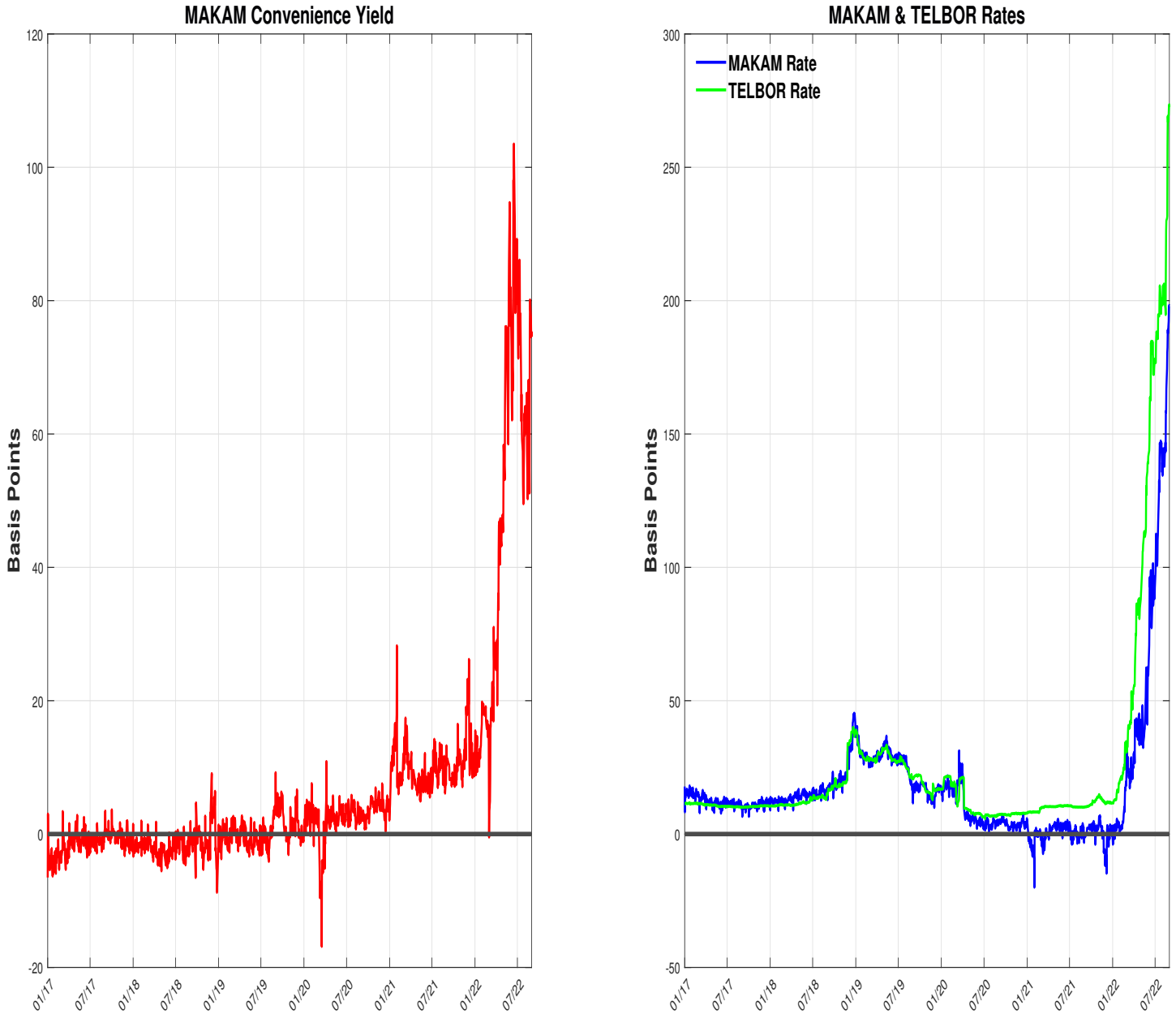

Notes: This figure presents the time series of the MAKAM Convenience Yield (red line) as well as its underlying MAKAM rate (blue line) and TELBOR rate (green line). MAKAM rate data are from the TASE and TELBOR rate data are from the BOI. The data cover 1/1/2017-8/31/2022. Time (daily dates) is on the x-axis. Values on the y-axis are in basis point units.

Appendix B Theoretical Motivation

This section presents a simple structural framework which is meant to fix ideas and form a suitable conceptual base for this project's empirical analysis. The framework we will use is a partial equilibrium of the local risk-free bond market consisting of two time periods (t and $t+1$) and two agents.

The first agent is a risk-averse foreign financial institution (FFI) who demands local risk-free bond as part of its covered interest parity (CIP) arbitrage trade. The second is a local central bank (CB) who supplies risk-free bonds as part of the operation and management of monetary policy. Our setting does not necessitate that the CB is the issuer of the bonds; an unmodeled government can be assumed to issue the bonds while the CB supplies them out of its given inventory. Moreover, and more generally, our setting's external validity can be easily broadened by replacing the CB with an explicitly modeled government that governs the model's supply side (see Section B.2 for more details).

We start our depiction of the model with a concise presentation of the demand side of the local risk-free bond market by presenting the FFI's demand for local risk-free bonds. We then briefly depict the supply of these bonds by the local CB. We end the section by defining equilibrium and presenting the model's main prediction.

B.1 Demand for Risk-Free Bonds

General Setting. There is a risk-neutral FFI that represents the demand side of the local risk-free bond market. The FFI funds its bond purchase through an FX swap. Specifically, the FFI's bond trade can be broken down into two parts. First, it buys spot $Q_{t,FFI}$ local currency units and sells spot $\frac{Q_{t,FFI}}{S_t}$ foreign currency units in period t which it borrows frictionlessly at the foreign risk-free interest rate $i_{t+1,W}$. Second, it sells forward $Q_{t,FFI}(1+i_{t+1,L})$ local currency units at forward rate $F_{t,t+1}$. $Q_{t,FFI}$ represents FFI's demand for local risk-free bonds and $i_{t+1,L}$ represents the local risk-free bond interest rate which it earns from investing $Q_{t,FFI}$ in the local risk-free bond market.[9]

[9] One may wonder why the FFI does not choose to deposit the funds with a local commercial bank in lie of, or in combination with, the investment in the local risk-free bond. Our choice to ignore this possibility comes from institutional information for Israel, which we believe applies to other developed SOEs as well, that such deposit investment is largely avoided by FFIs as it entails a regulatory capital surcharge due to the local commercial banks' perceived non-riskiness in the eyes of the FFI's regulators. This in contrast to the investment in the local risk-free bond, which bears no such surcharge.

For simplicity, we assume both $Q_{t,FFI}$ (i.e., the principal underlying FFI's FX swap trade) and $Q_{t,FFI}i_{t+1,L}$ (i.e., the interest related amount underlying FFI's FX swap trade) are sold forward to some (unmodeled) broker-dealer institution.

Haircut. Following Ivashina et al. (2015), we assume that a haircut is applied to FFI's FX swap trade in the amount of $\kappa Q_{t,FFI}$. That is, the FFI's FX swap trade requires it to incur a linear haircut-induced cost through the depositing of share κ of its swap position to the above-mentioned (unmodeled) broker-dealer institution.

FFI's Alternative Investment Activity. By allocating $\kappa Q_{t,FFI}$ for local risk-free bond investment, the FFI has to take these funds away from its pre-determined investment capital A_t (denoted here in foreign currency units). In other words, $A_t - \kappa \frac{Q_{t,FFI}}{S_t}$ represents the FFI's available capital for another investment activity which we assume to be risky (e.g., loans to foreign firms) and whose expected return is denoted by $\mathbb{E}_t i_{t+1,FFI}$, where $\mathbb{E}_t$ is the expectation operator conditional on period t information.

Expectation and Variance of FFI's Profit. We can write FFI's next period's expected profit (in foreign currency terms) from its investment activity (both local risk-free bond and alternative risky investment activity), which we assume to be positive and denote by $\mathbb{E}_t \Pi_{t+1,FFI}$, as

$$\mathbb{E}_t \Pi_{t+1,FFI} = \frac{Q_{t,FFI}(1+i_{t+1,L})}{F_{t,t+1}} - \frac{Q_{t,FFI}}{S_t}(1+i_{t+1,W}) + \left(A_t - \kappa \frac{Q_{t,FFI}}{S_t}\right)(1+\mathbb{E}_t i_{t+1,FFI}). \tag{B.1}$$

The FFI's total expected profit consists of that from the swap trade that funds FFI's investment in the local risk-free bond ($\frac{Q_{t,FFI}(1+i_{t+1,L})}{F_{t,t+1}} - \frac{Q_{t,FFI}}{S_t}(1+i_{t+1,W})$), which is not restricted to zero as it would be in a frictionless setting (i.e., without the haircut cost) in which covered interest parity would prevail, and that from the alternative risky investment ($\left(A_t - \kappa \frac{Q_{t,FFI}}{S_t}\right)(1+\mathbb{E}_t i_{t+1,FFI})$. And the variance of FFI's profit ($\mathbb{V}_t \Pi_{t+1,FFI}$) can be written as $\mathbb{V}_t \Pi_{t+1,FFI} = \left(A_t - \kappa \frac{Q_{t,FFI}}{S_t}\right)^2 \mathbb{V}_t(i_{t+1,FFI})$, where $\mathbb{V}_t$ is the variance operator conditional on period t information.

Mean-Variance Optimization Problem. We assume the FFI chooses its demand for local risk-free bonds $Q_{t,FFI}$ so as to maximize

$$\mathbb{E}_t\Pi_{t+1,FFI} - \frac{e^{\epsilon_t}}{2}\mathbb{V}_t\Pi_{t+1,FFI} = \frac{Q_{t,FFI}(1+i_{t+1,L})}{F_{t,t+1}} - \frac{Q_{t,FFI}}{S_t}(1+i_{t+1,W}) + \left(A_t - \kappa\frac{Q_{t,FFI}}{S_t}\right)(1+\mathbb{E}_t i_{t+1,FFI}) - \frac{e^{\epsilon_t}}{2}\left(A_t - \kappa\frac{Q_{t,FFI}}{S_t}\right)^2\mathbb{V}_t(i_{t+1,FFI}), \tag{B.2}$$

where ϵ_t represents a white noise shock to the FFI's demand for local risk-free bonds, which in turn determines the level of FFI's risk aversion with respect to the alternative risky investment activity the FFI undertakes. This shock should be interpreted as an idiosyncratic shift in the FFI's preference for holding the local risk-free bond, i.e., a shock which makes the risk-free local bond more appealing to the FFI relative to the alternative risky investment opportunity facing the FFI. Importantly, as formally shown below, a positive (negative) ϵ_t induces a rightward (leftward) shift in FFI's demand for local risk-free bonds.

The FOC that results from maximizing the objective function from Equation (B.2) with respect to $Q_{t,FFI}$ is

$$Q_{t,FFI} = \frac{S_t^2}{\kappa^2\mathbb{V}_t(i_{t+1,FFI})e^{\epsilon_t}}\left(\frac{1+i_{t+1,L}}{F_{t,t+1}} - \frac{1+i_{t+1,W}}{S_t} - \frac{\kappa}{S_t}(1+\mathbb{E}_t i_{t+1,FFI})\right) + \frac{S_t A_t}{\kappa\mathbb{V}_t(i_{t+1,FFI})}. \tag{B.3}$$

Equation (B.3) essentially represents FFI's demand for local risk-free bonds. Note that allocating one local currency unit to the risk-free, swap-funded investment in the local bond would produce profit $\frac{1+i_{t+1,L}}{F_{t,t+1}} - \frac{1+i_{t+1,W}}{S_t}$ while allocating it to the alternative risky investment (which would free up κ local currency units) would produce expected profit $\frac{\kappa}{S_t}(1+\mathbb{E}_t i_{t+1,FFI})$. We assume that the latter profit is greater than the former as otherwise the risky investment's existence would be unjustifiable.

Relation between $Q_{t,FFI}$ and $i_{t+1,L}$. Given that the local risk-free bond return $i_{t+1,L}$ is inversely related to its price ($\frac{1}{1+i_{t+1,L}}$), we should expect to have a positive relation between this return and demand for local risk-free bonds. To show this positive return-demanded-quantity relation (i.e., a downward sloping local risk-free bond demand curve in the bond price-quantity plane), let us differentiate Equation (B.3) with respect to $i_{t+1,L}$:

$$\frac{\partial Q_{t,FFI}}{\partial i_{t+1,L}} = \frac{S_t^2}{\kappa^4\mathbb{V}_t(i_{t+1,FFI})^2 e^{2\epsilon_t}F_{t,t+1}^2} > 0. \tag{B.4}$$

Relation between $Q_{t,FFI}$ and ϵ_t. We argued above that a positive (negative) realization for ϵ_t represents a rightward (leftward) shift in FFI's local risk-free bond demand curve. To show this formally, let us differentiate Equation (B.3) with respect to e^{ϵ_t}:

$$\frac{\partial Q_{t,FFI}}{\partial e^{\epsilon_t}} = -\frac{\kappa^2 \mathbb{V}_t(i_{t+1,FFI}) S_t^2}{\kappa^4 \mathbb{V}_t(i_{t+1,FFI})^2 e^{2\epsilon_t}} \left(\frac{1+i_{t+1,L}}{F_{t,t+1}} - \frac{1+i_{t+1,W}}{S_t} - \frac{\kappa}{S_t}(1+\mathbb{E}_t i_{t+1,FFI}) \right) > 0, \tag{B.5}$$

where the positive sign of Equation (B.5) comes from the fact that, as noted above, we assume that $\frac{1+i_{t+1,L}}{F_{t,t+1}} - \frac{1+i_{t+1,W}}{S_t} - \frac{\kappa}{S_t}(1+\mathbb{E}_t i_{t+1,FFI}) < 0$ as otherwise there is no justifiable existence for FFI's alternative risky investment opportunity.

B.2 Supply of Risk-Free Bonds

General Setting. There is a local central bank (CB) which supplies local risk-free bonds $Q_{t,CB}$ to regulate liquidity in the economy such that this supply generates a risk-free bond rate that aligns as much as possible with the CB's targeted monetary policy rate $i_{t+1,P}$. The latter rate can be viewed as the deposit rate earned by local depository institutions depositing funds with the CB; for simplicity, we abstract from modeling the associated deposit market and treat $i_{t+1,P}$ as exogenous where there is some level of local depository institutions' reserves consistent with $i_{t+1,P}$.

Since supply of $Q_{t,CB}$ mechanically draws down local depository institutions' reserves—as the payment to the CB by the FFI for the issuance must be through these reserves —, the CB guides its choice of $i_{t+1,L}$ with its intention to be as close as possible to $i_{t+1,P}$ while also avoiding large bond sales as these will have to be offsetted by corresponding large interbank/open market operations. I.e., we assume the CB has disutility from having to conduct large such operations to counter events in the local risk-free bond market. This assumed disutility is based on the notion that the CB wishes to avoid large swings in reserves coming from the bond market which in turn would have to be offsetted in an interbank market which may lack the depth for such offsetting.

As already mentioned above, the CB's bond supply can be viewed as either coming from its role as issuer of the bonds or seller of government-issued-bonds—where the government is unmodeled—out of its given inventory. Moreover, and more generally, the CB can be replaced by an explicitly modeled government that wishes to minimize quadratic deviations of some target rate sought after by the government from the actual market rate while also trying to avoid large fluctuations in its bond issuance. Since this bond issuance ultimately funds the government's

activity, the cost of such large fluctuations can be viewed to reflect political constraints on making large changes in the government's provision of public services. (This cost can also reflect economic constraints related to the government's desire to minimize disruptions to the government bond market coming from large supply changes.) Whichever setting is used, the model results in an imperfectly elastic supply curve and the emergence of increased convenience yield in the presence of large capital inflow shocks.[10]

Optimization Problem. The CB optimally chooses $i_{t+1,L}$ to minimize a quadratic loss function of the deviation between $i_{t+1,L}$ and $i_{t+1,P}$ as well as the cost of large bond sales (this cost is governed by $\zeta \geq 0$):

$$\min_{i_{t+1,L}} \quad (i_{t+1,L} - i^*_{t+1,P})^2 + \zeta Q^2_{t,CB}. \tag{B.6}$$

The FOC with respect to $i_{t+1,L}$ is

$$2(i_{t+1,L} - i^*_{t+1,P}) + 2\zeta Q_{t,CB} = 0. \tag{B.7}$$

Equation (B.7) implies an upward-sloping bond supply curve of the CB in the bond price-quantity plane where, so long that $\zeta > 0$—i.e., the CB incurs a cost from having to offset large reserve swings—there will be a segmentation between the local CB deposit and risk-free bonds markets as manifested by an inequality between $i_{t+1,L}$ and $i^*_{t+1,P}$.

B.3 Model Equilibrium

We define equilibrium in the local risk-free bond market as the equality $Q_{t,FFI} = Q_{t,CB} = Q_t$, where Q_t denotes the equilibrium level of local risk-free bonds. The latter equilibrium equation, when substituted into FOCs (B.4) and (B.7) produce two equations in two unknowns $i_{t+1,L}$ and Q_t. (A proof that relies on a fixed-point argument for the existence and uniqueness of a solution to this demand-supply equation system is available upon request from the authors.) We can use our previous results on the nature of the bond demand and supply curves to deduce the main prediction of our model.

[10] This is true even in the explicitly modeled government case because, given some risk- and convenience-free rate determined by a now unmodeled CB, a favorable capital inflow shock shifts the demand for risk-free bonds rightwards along an upward-sloping supply curve and thus results in increased convenience yield, i.e., a lower government bond rate relative to the CB-determined rate.

Equilibrium Prediction. Since we know from Equation (B.5) that a positive realization of ϵ_t produces a rightward shift in FFI's demand for local risk-free bonds, and it does so along an upward-sloping supply curve that is unaffected by ϵ_t, we obtain that a favorable shock to FFI's demand for local risk-free bonds results in an increase in bonds' equilibrium price ($\frac{1}{1+i_{t+1,L}}$), i.e., a decrease in the bond rate both in absolute terms as well as relative terms with respect to the monetary policy rate.

Appendix C Forecast Error Variance and Historical Decomposition Analyses

This section presents the estimation method and results from the forecast error variance (FEV) and historical decomposition analyses.

C.1 FEV Estimation Method and Results

For the forecast error variance (FEV) decomposition estimation, we utilize the estimated impulse responses to compute the FEV contributions of our capital inflow shock as follows (without loss of generality, we take those for the convenience yield variable):

$$\mathbb{C}_h = \frac{\hat{\Xi}_0^2 + ... + \hat{\Xi}_h^2}{\mathbb{V}(conv\_yield_{t+h} - conv\_yield_{t-1})}, \tag{C.1}$$

where $\hat{\Xi}_h$ is the estimated impulse response coefficient from Equation (3) from the text; and $\mathbb{V}(conv\_yield_{t+h} - conv\_yield_{t-1})$ represents the variance of accumulated differences of the convenience variable.[11] Recall that the unconditional variance of the GIV capital inflow shock is unit and hence does not appear in Equation (C.1). In other words, $\mathbb{C}_h$ represents the estimated contribution of a one-standard-deviation GIV capital inflow shock to the dynamic variation in the

[11] Following Gorodnichenko and Lee (2020)'s FEV method for local projections (termed LP-B in their paper) which ensures that the computed FEV share does not exceed one, we compute the denominator in Equation (C.1) as the sum of the corresponding numerator and the variance of the residual from the main text's Equation (3)'s implied moving average decomposition. (As in the empirical results whose presentation follows next, this moving average decomposition is based on estimated impulse responses up to the 500th horizon, which covers roughly 2 years of calendar years after accounting for non-trading days on the TASE.) While asymptotically this alternative way of computing the variance in the denominator is equivalent to computing it from the actual data, the latter computation in finite samples can lead to estimated FEV shares that exceed one.

convenience yield variable. Figures C.1-C.6 presents the main outcome variables' FEV shares explained by a one-standard-deviation GIV capital inflow shock. All of these figures and their results are discussed in Section 4 in the main text.

C.2 Historical Decomposition

To reinforce the notion that the GIV capital inflow shocks played a crucial role in driving the unconditional behavior of FFIs' Accumulated Net Capital Inflows and MAKAM convenience yield variables, it is helpful to compute the contributions of the actual realizations of our GIV capital inflow shocks to the change in FFIs' accumulated net capital inflows as share of MAKAM outstanding and MAKAM convenience yield over the run-up period in the former variable. We use as specific trough and peak dates 02/27/20 and 08/02/22, respectively; on 08/02/22 this variables reached its peak of the sample while from 02/27/20 it began its remarkable and steady rise. The historical decomposition calculation exploits the moving average representation of the accumulated changes in net capital inflows as share of outstanding MAKAM and MAKAM convenience yield in the run-up period. In particular, using the terminology from Section 3 of the main text, the contributions of our shocks to these changes (in terms of these changes' share)—which we denote as $\mathbb{HD}_{accum\_net\_inflows}$ and $\mathbb{HD}_{conv\_yield}$, respectively—are

$$\mathbb{HD}_{accum\_net\_inflows} = \frac{\hat{\Omega}_0 \varrho_{GIV,t+h} + ... + \hat{\Omega}_h \varrho_{GIV,t}}{(accum\_net\_inflows_{t+h} - accum\_net\_inflows_{t-1})/outstanding_{t-1}}, \tag{C.2}$$

$$\mathbb{HD}_{conv\_yield} = \frac{\hat{\Xi}_0 \varrho_{GIV,t+h} + ... + \hat{\Xi}_h \varrho_{GIV,t}}{conv\_yield_{t+h} - conv\_yield_{t-1}}, \tag{C.3}$$

where $t-1$ and $t+h$ correspond to 02/27/20 and 08/02/22, respectively; and $\hat{\Omega}_j$ and $\hat{\Xi}_j$ for $j = 0, ..., h$ are the dynamic effects of the GIV capital inflow shocks on the accumulated net capital inflows and convenience yield variables, respectively, i.e., they are the estimated impulse response coefficients from Equations (2) and (3) of the main text, respectively.

The historical decomposition results are shown in Table C.1, indicating that the actual realizations of our GIV capital inflow shocks have accounted for above and beyond of the run-up in FFIs' net capital inflows as share of MAKAM outstanding. In particular, our GIV capital inflows shocks have increased FFIs' accumulated net capital inflows as share of MAKAM outstanding by 124.4 percentage points, or 145.2% of the actual 85.6-percentage-point increase over the run-up period (02/27/20-08/02/22), pointing to a dominating presence of favorable such shocks during

this period.[12] The historical decomposition results for the MAKAM convenience yield over this period are staggering as well: our GIV capital inflow shocks have increased this spread by 82.5 basis points, or 135.5% of the actual 60.9-basis-point decline over this period.

[12] As discussed in Footnote 3 from the main text, some of FFI's MAKAM activity is done through a foreign custodian bank and is thus unobserved at the FFI-level. (See Section D.4 for a confirmation that our results are unaffected by these unobserved custody-based flows.) These flows amount to -64.2 billion ILS, mainly representing bond redemptions done by FFIs through this custodian's checking accounts with local banks. Hence, if one wanted to compute the precise market share of FFIs from our daily data, she would be required to sum the observed FFI-level flows used for identification and the custody-based flows that are observed in the aggregate but the not at the FFI-level which is what is required for our identification approach. This summation puts the daily market share at a nearly 50% peak compared to a peak 96.1% net capital inflows share of outstanding MAKAM.

Table C.1: **Contribution of GIV Capital Inflow Shock to FFIs' Accumulated Net Capital Inflows and MAKAM Convenience Yield Variables in Run-Up Period.**

	Accumulated Net Capital Inflows	MAKAM Convenience Yield
Change	85.6 Percentage Points	60.9 Basis Points
Contribution	124.4 Percentage Points [145.2%]]	82.5 Basis Points [135.5%]

Notes: This table presents the estimated contribution (in raw form as well as in terms of share of actual change in brackets) of the GIV capital inflow shock to the change in FFIs' accumulated net capital inflows as share of MAKAM outstanding and MAKAM convenience yield in the run-up period of the former variable (02/27/20-08/02/22). For completeness, the two variables' actual changes are also shown in the first row of the table.

Figure C.1: **FEVs Attributable to GIV Capital Inflow Shock: MAKAM Convenience Yield and FFIs' Accumulated MAKAM Net Capital Inflows.**

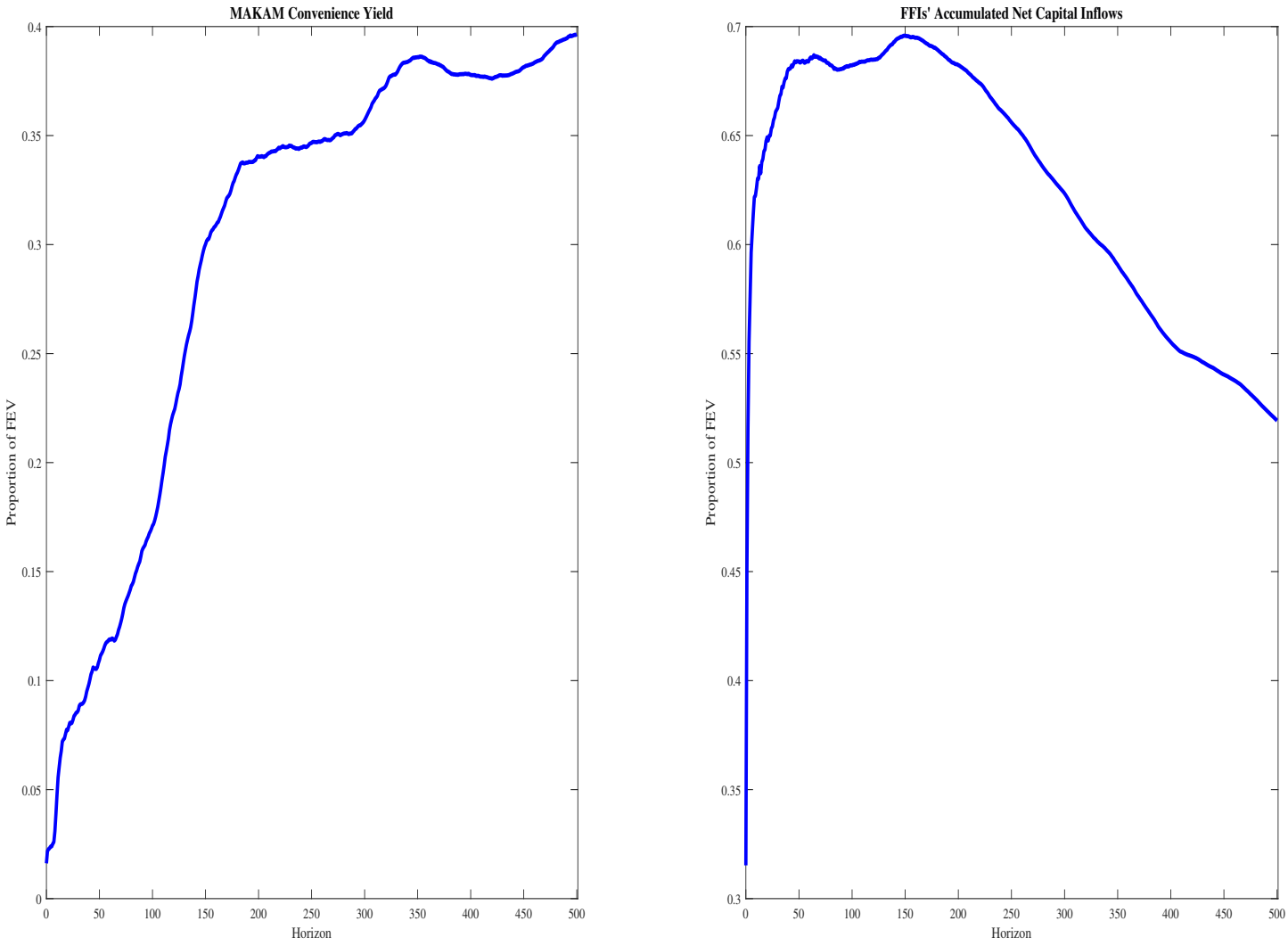

Notes: This figure presents the FEV shares of the variation in the MAKAM convenience yield and FFIs' accumulated MAKAM net capital inflow (as share of outstanding MAKAM) variables attributable to a one-standard-deviation GIV capital inflow shock. Horizons are on the x-axis (impact horizon (0) to 500th horizon). FEV share is on the y-axis (in fractional terms).

Figure C.2: **FEVs Attributable to GIV Capital Inflow Shock: Government Bond Yield Spreads.**

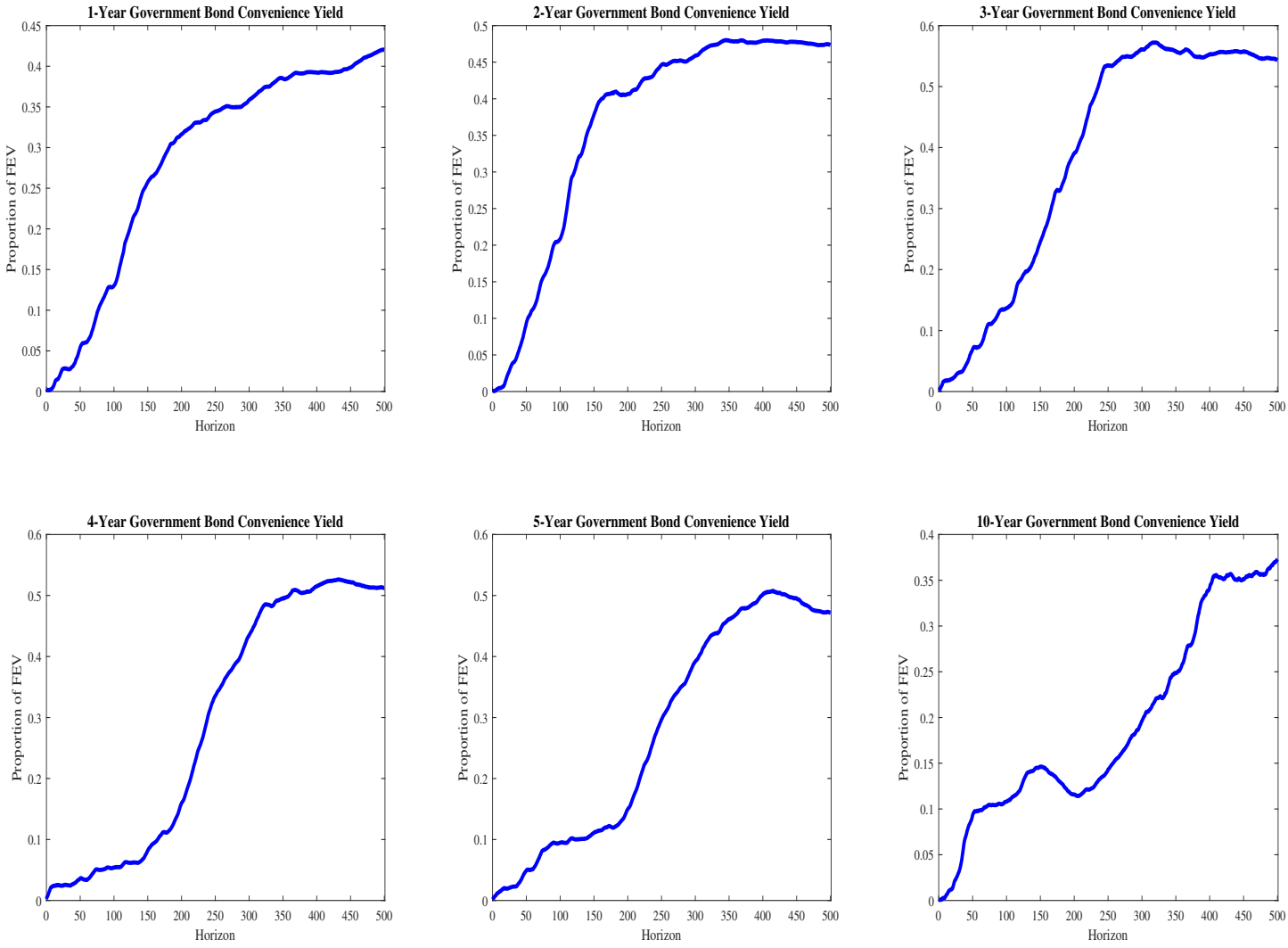

Notes: This figure presents the FEV shares of the variation in the government bond spread variables attributable to a one-standard-deviation GIV capital inflow shock. Horizons are on the x-axis (impact horizon (0) to 500th horizon). FEV share is on the y-axis (in fractional terms).

Figure C.3: **FEVs Attributable to GIV Capital Inflow Shock: Corporate Bond Yield Spreads.**

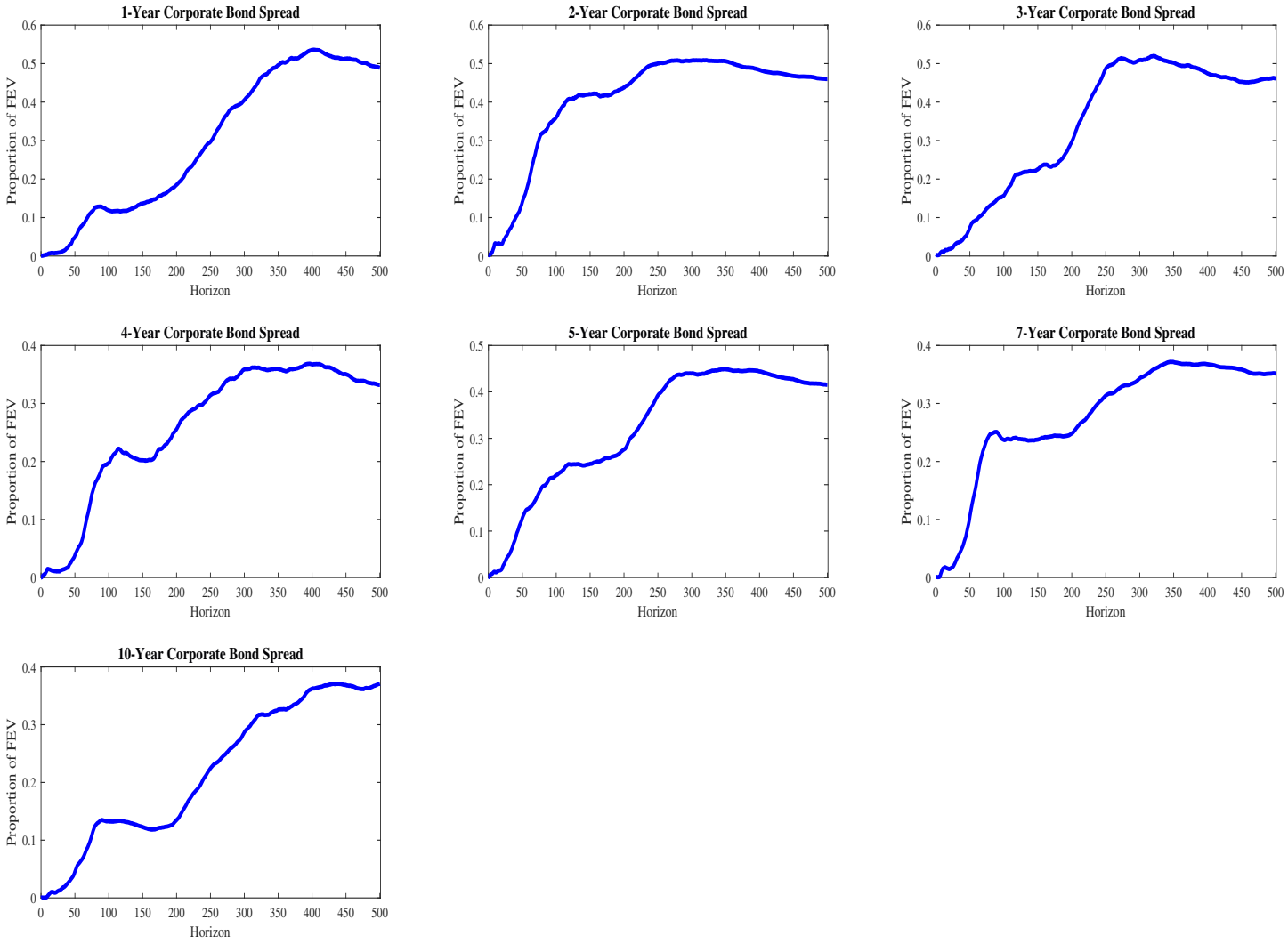

Notes: This figure presents the FEV shares of the variation in the corporate bond spread variables attributable to a one-standard-deviation GIV capital inflow shock. Horizons are on the x-axis (impact horizon (0) to 500th horizon). FEV share is on the y-axis (in fractional terms).

Figure C.4: **FEVs Attributable to GIV Capital Inflow Shock: TA-35 Index.**

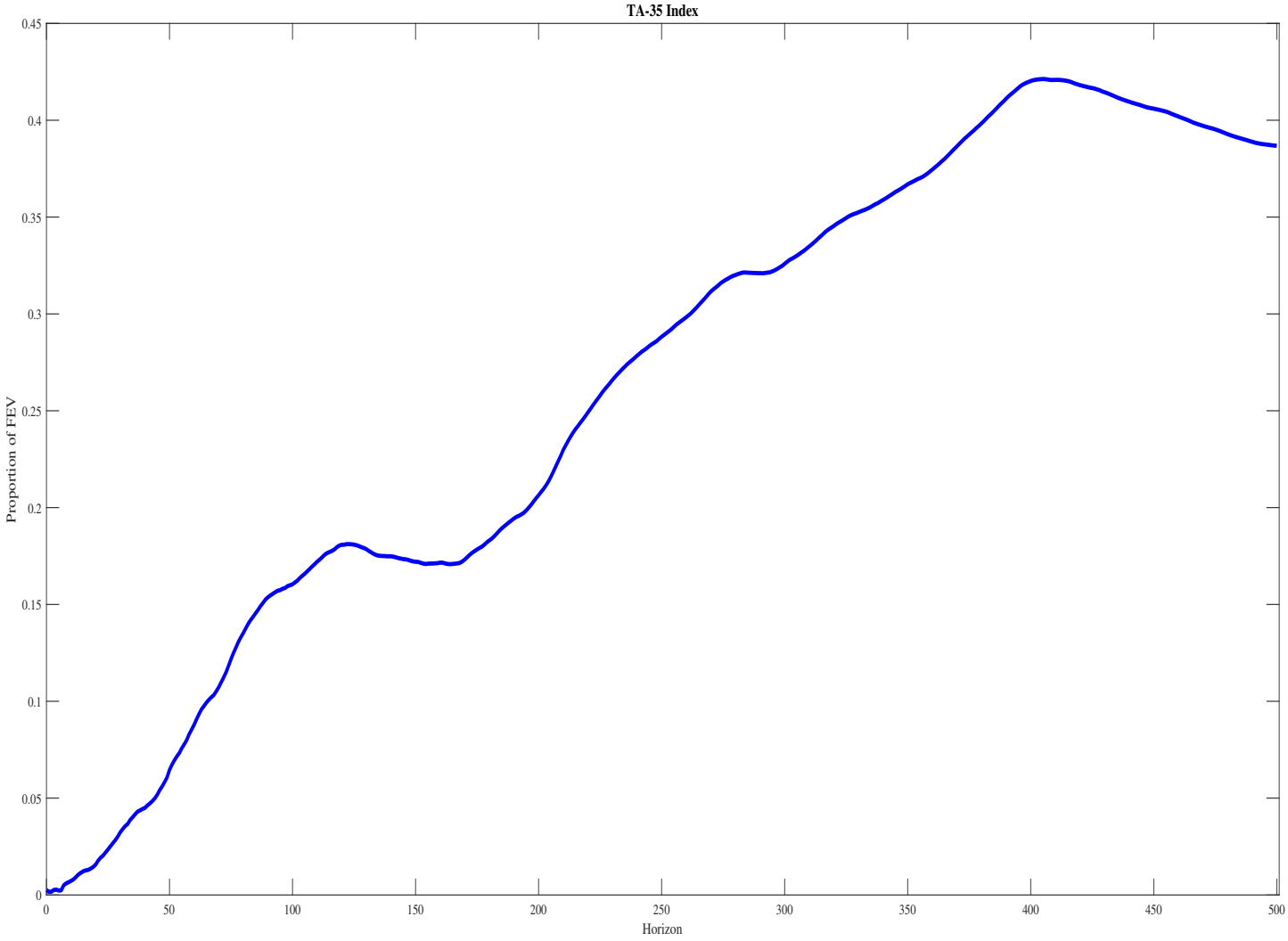

Notes: This figure presents the FEV shares of the variation in the TA-35 stock price index variable attributable to a one-standard-deviation GIV capital inflow shock. Horizons are on the x-axis (impact horizon (0) to 500th horizon). FEV share is on the y-axis (in fractional terms).

Figure C.5: **FEVs Attributable to GIV Capital Inflow Shock: MFs' and FFIs' Accumulated Secondary Market MAKAM Flows.**

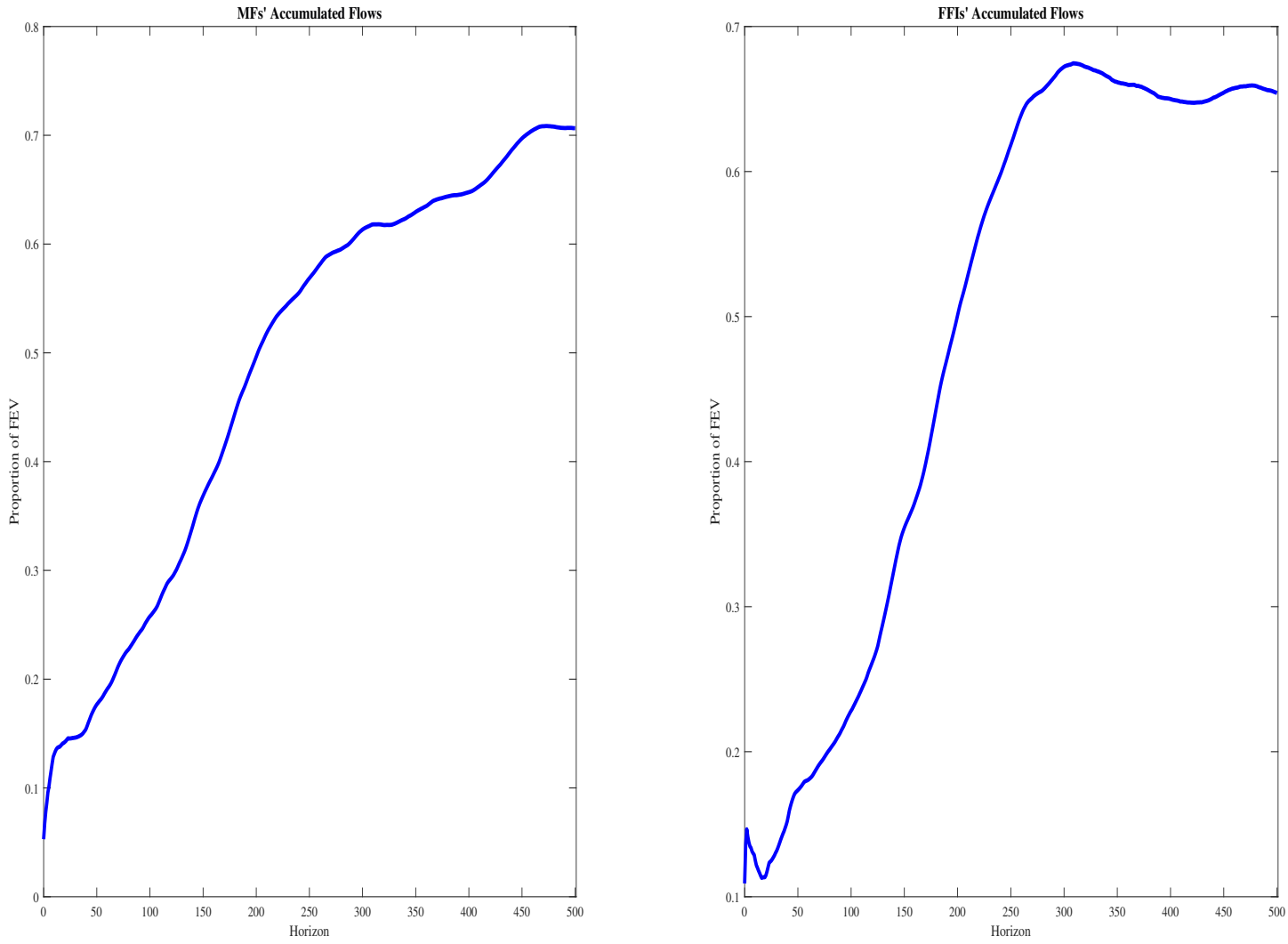

Notes: This figure presents the FEV shares of the variation in HFs' and FFIs' accumulated secondary market MAKAM flows as share of outstanding MAKAM attributable to a one-standard-deviation GIV capital inflow shock. Horizons are on the x-axis (impact horizon (0) to 500th horizon). FEV share is on the y-axis (in fractional terms).

Figure C.6: **FEVs Attributable to GIV Capital Inflow Shock: MFs' and FFIs' Accumulated Secondary Market Rebalancing Flows.**

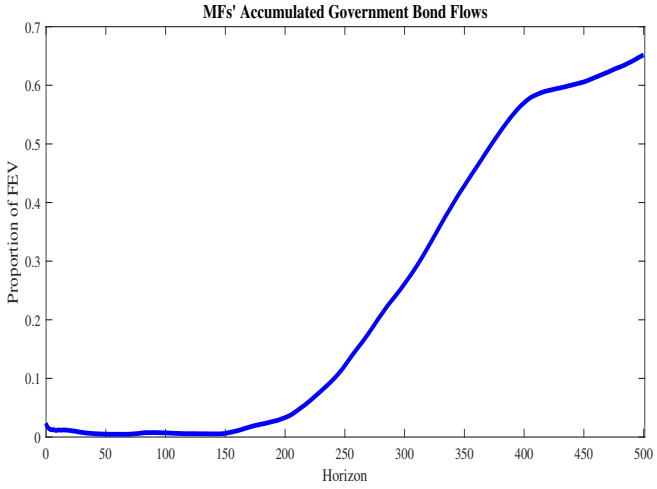

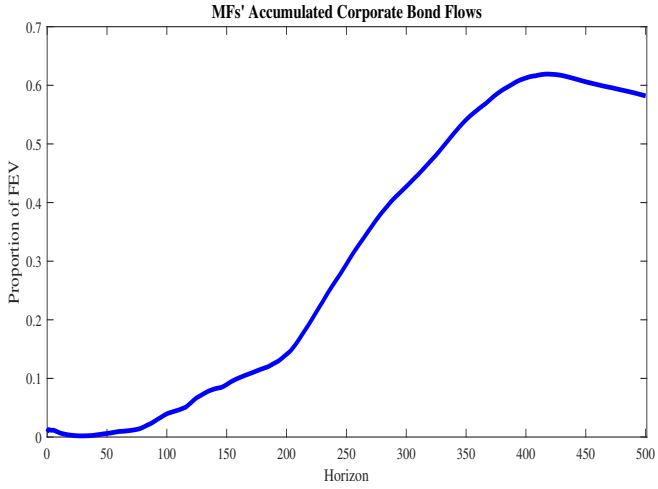

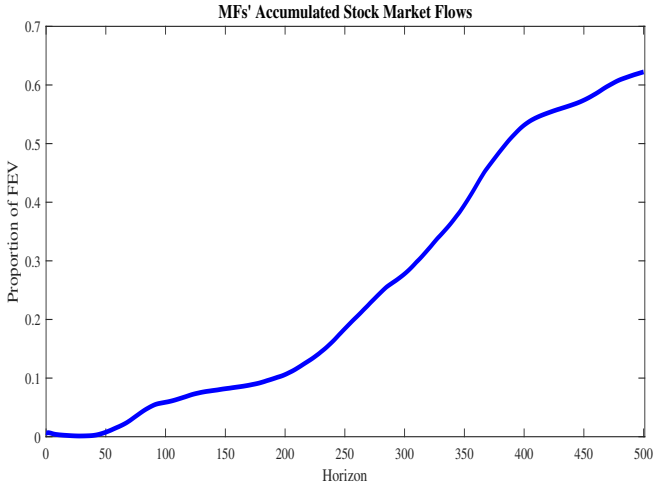

Notes: This figure presents the FEV shares of the variation in MFs' accumulated secondary market government bond, corporate bond, and equity flows as shares of outstanding MAKAM attributable to a one-standard-deviation GIV capital inflow shock. Horizons are on the x-axis (impact horizon (0) to 500th horizon). FEV share is on the y-axis (in fractional terms).

Appendix D Robustness Checks

This section examines the robustness of the baseline results discussed in the main text—and presented in Figures 3-8 from the main text (impulse response figures) and in Figures C.1-C.6) (FEV figures)—along four dimensions. First, using different lag specifications for the FFI-level regressions. Second, truncating the baseline sample at 4/11/2022 so as to confirm that the baseline results are robust to omission of the monetary tightening period part of our sample. The third replaces the inverse-variance-weighted-average shock component in the GIV construction with the equally-weighted-average one. And the fourth adds the flows of the removed significant (custodian bank) FFI as a control in the FFI-level regressions. The presentation of all of the results follows the same exposition and structure underlying the baseline results presented in the above-mentioned figures.

D.1 Alternative Lag Specifications

The lags for the FFi-level regressions from the main text (Equation (1)) were chosen optimally as the average of the chosen lag specifications from the AIC, corrected AIC, BIC, and HQIC lag length criteria tests for each FFi-level regression. To asses the sensitivity of our baseline results to alternative lag specifications, we present our baseline results for two additional lag specification cases: one that halves all lags in the FFI-level regressions and one that raises them by 50%. The results from these two cases are shown Figures D.1-D.8 (shorter lag case) and D.9-D.16 (longer lag case).

The results are very similar to the baseline ones, for both the impulse responses and the FEVs. The monetary transmission imperfection continues to be significant and persistent. And this imperfection continues to significantly and persistently spill over into government and corporate bonds markets as well as the equity market in similar fashion to the baseline case.

D.2 Excluding the Monetary Tightening Period

Theory implies that our results should hold regardless of the monetary stance in place locally or globally. In practice, however, since the last five months of our sample saw a shift in both local and global monetary stance, it is of value to confirm that our results are robust to omitting this part of our sample. Toward this end, Figures D.17-D.24 show the baseline results for a sample that

truncates at 4/11/2022 which is the date at which the BOI began its recent monetary tightening cycle.

The results confirm the robustness of the baseline results to the omission of the recent monetary tightening cycle. There continues to be a significant and persistent increase in the MAKAM convenience yield, which in turn appears to significantly spill over into the government and corporate bond markets as well as the equity market as manifested through the significant and persistent responses of government bond convenience yields and corporate bond spreads as well as the significant and persistent responses of equity prices. Furthermore, the GIV capital inflow shocks continues to account for meaningful FEV shares of the variation in all considered variables.

D.3 Common Component Removal in GIV

Our granular econometric approach to studying monetary transmission imperfection constructs the GIV as the difference between the size-weighted- and inverse-variance-weighted-average of the FFI-level shocks. Our choice of the latter inverse-variance-based component is based on the result from Gabaix and Koijen (2024) that such common component removal is optimal in the sense that the resulting estimation possesses the highest precision. However, a viable and unbiased alternative such removal subtracts the equally-weighted-average of the shocks from the size-weighted one. Figures D.25-D.32 shows the baseline results from this alternative removal choice.

It is clear that results are very similar to the baseline ones, indicating that our paper's main message about a meaningful transmission imperfection is insensitive to the choice to common component removal choice in the construction of the GIV.

D.4 Controlling for Unobserved Custody-Based Flows

As discussed in the main text, 10.3% of FFIs' MAKAM flows volume is done through a custodian bank. In accordance with our granular identification framework which requires that each FFI acts as a producer of positive accumulated net capital inflows, we have removed this custodian bank FFI since it accumulated a total of -64.2 billion ILS over our sample period. Since our data does not enable us to attribute this custodian bank's flows to our individual 18 FFIs', one may argue that our results can be affected by the omission of these unobserved flows; specifically, we may confoundedly identify as a capital inflow shock the mere desire of an FFI to buy MAKAM in

response to such unobserved flows.

To remove this concern, we show in Figures D.33-D.40 results from controlling for these custodian bank flows in the FFI-level regressions. I.e., these results are based on a capital inflow shock which is orthogonal by construction to the custodian bank FFI's activity; hence, robustness of the results to this orthogonalization would demonstrate that our baseline results are not driven by such unobserved custody-based activity. It is clear that results are very similar to the baseline ones, indicating that our paper's main message about a meaningful monetary transmission imperfection is insensitive to our inability to attribute custody-based flows to our individual FFIs.[13]

[13]We also confirmed that results from regressing our convenience yield variable on our baseline aggregate FFIs' flows (i.e., excluding the omitted significant FFI's flows) and on aggregate FFIs' flows inclusive of the omitted significant custodian bank FFI are similar. While such a plain vanilla aggregate OLS estimation raises the very problem of endogeneity that our granular identification approach sets out to resolve, we view the robustness of the results from this exercise to the inclusion of the omitted significant FFI's flows as additional evidence - on top of the robustness check described above - for these flows' neutrality for the convenience yield variable, which in turn further invalidates the worry cited in the beginning of this section.

Figure D.1: **Shorter Lag Specification: Impulse Responses to GIV Capital Inflow Shock: MAKAM Convenience Yield and FFIs' Accumulated MAKAM Net Capital Inflows.**

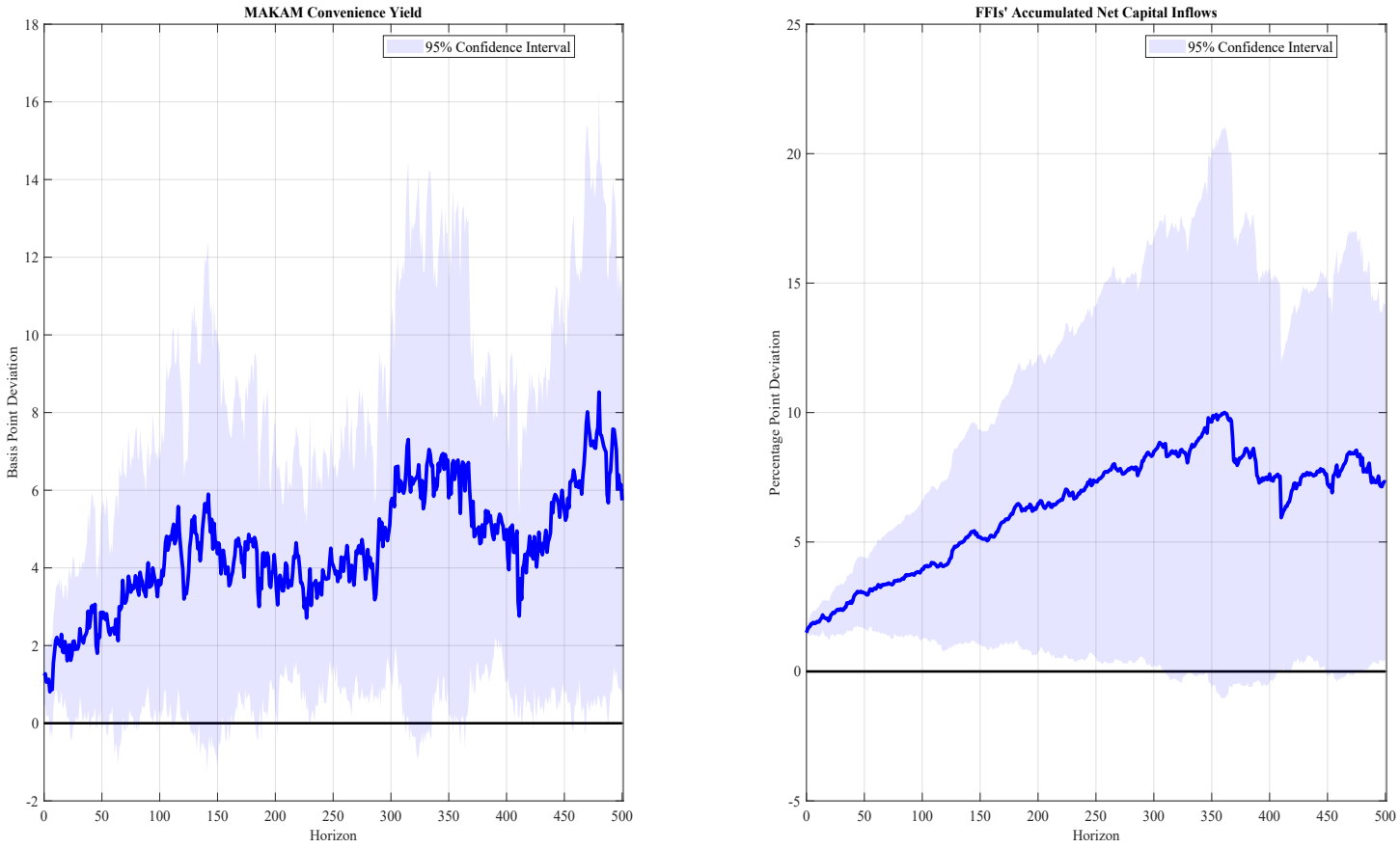

Notes: This figure presents the impulse responses (solid lines) to a GIV capital inflow shock of the MAKAM convenience yield and FFIs' accumulated MAKAM net capital inflows as share of outstanding MAKAM, where number of lags in each FFI-level regression is halved. Responses are normalized such that the peak response of the latter variable is 10 (i.e., 10-percentage-point increase as share of outstanding MAKAM), implying a 3.7-standard-deviation GIV capital inflow shock size. 95% confidence bands (shaded areas) are based on standard errors computed from the heteroskedasticity- and autocorrelation-consistent procedure of Newey and West (1987) with the truncation lag equal to $h+1$ (where $h = 0, 1, ..., 500$ is the local projection horizon). Horizons are on the x-axis (impact horizon (0) to 500th horizon). Values for MAKAM convenience yield variable are in basis point change units relative to the pre-shock value of the spread; those for the FFIs' accumulated MAKAM net capital inflows variable are in percentage-point change units relative to the pre-shock value of FFIs' market share.

Figure D.2: **Shorter Lag Specification: FEVs Attributable to GIV Capital Inflow Shock: MAKAM Convenience Yield and FFIs' Accumulated MAKAM Net Capital Inflows.**

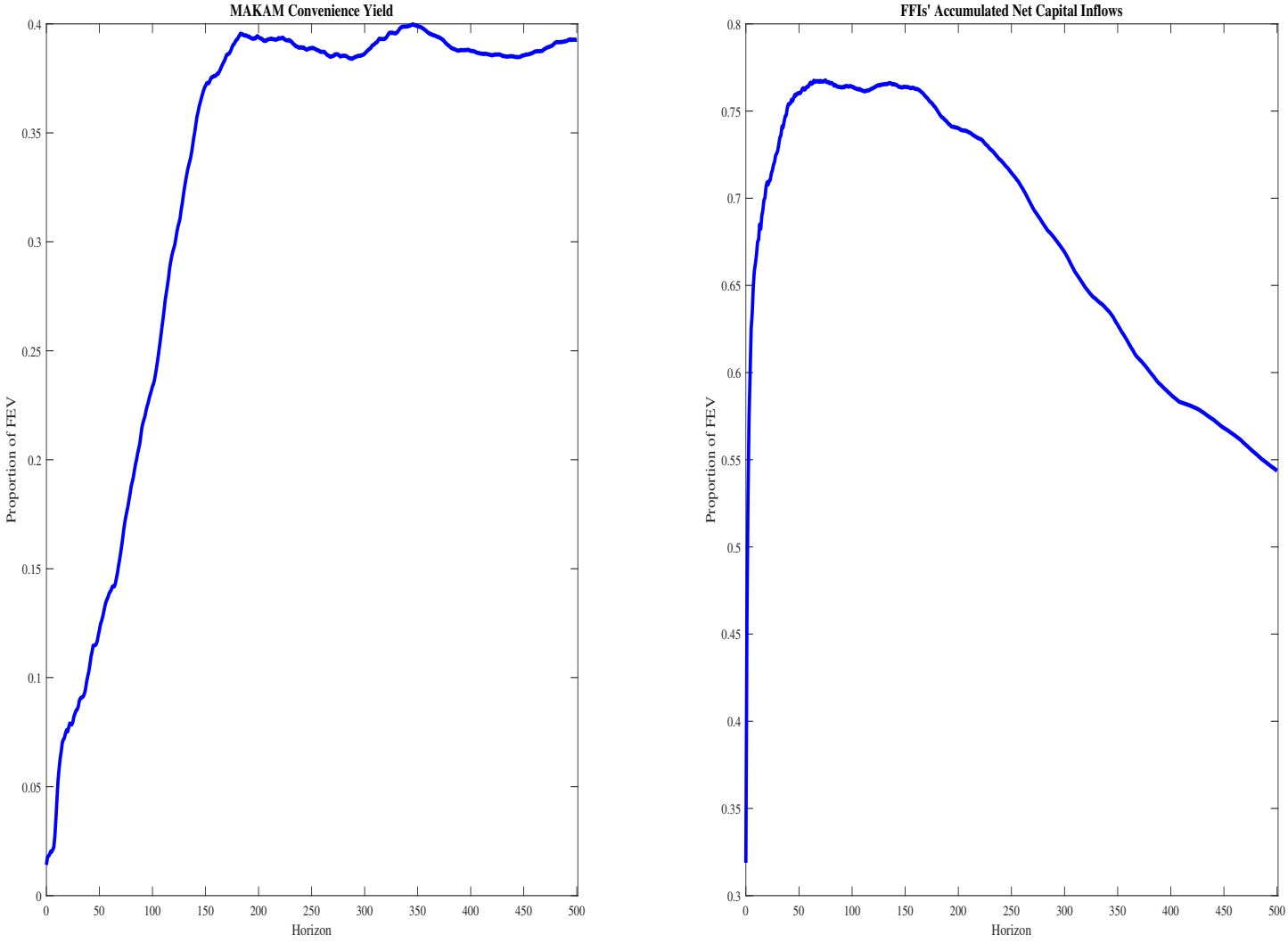

Notes: This figure presents the FEV shares of the variation in the MAKAM convenience yield and FFIs' accumulated MAKAM net capital inflow (as share of outstanding MAKAM) variables attributable to a one-standard-deviation GIV capital inflow shock, where the number of lags in each FFI-level regression is halved. Horizons are on the x-axis (impact horizon (0) to 500th horizon). FEV share is on the y-axis (in fractional terms).

Figure D.3: **Shorter Lag Specification: Impulse Responses to GIV Capital Inflow Shock: Government Bond Yield Spreads.**

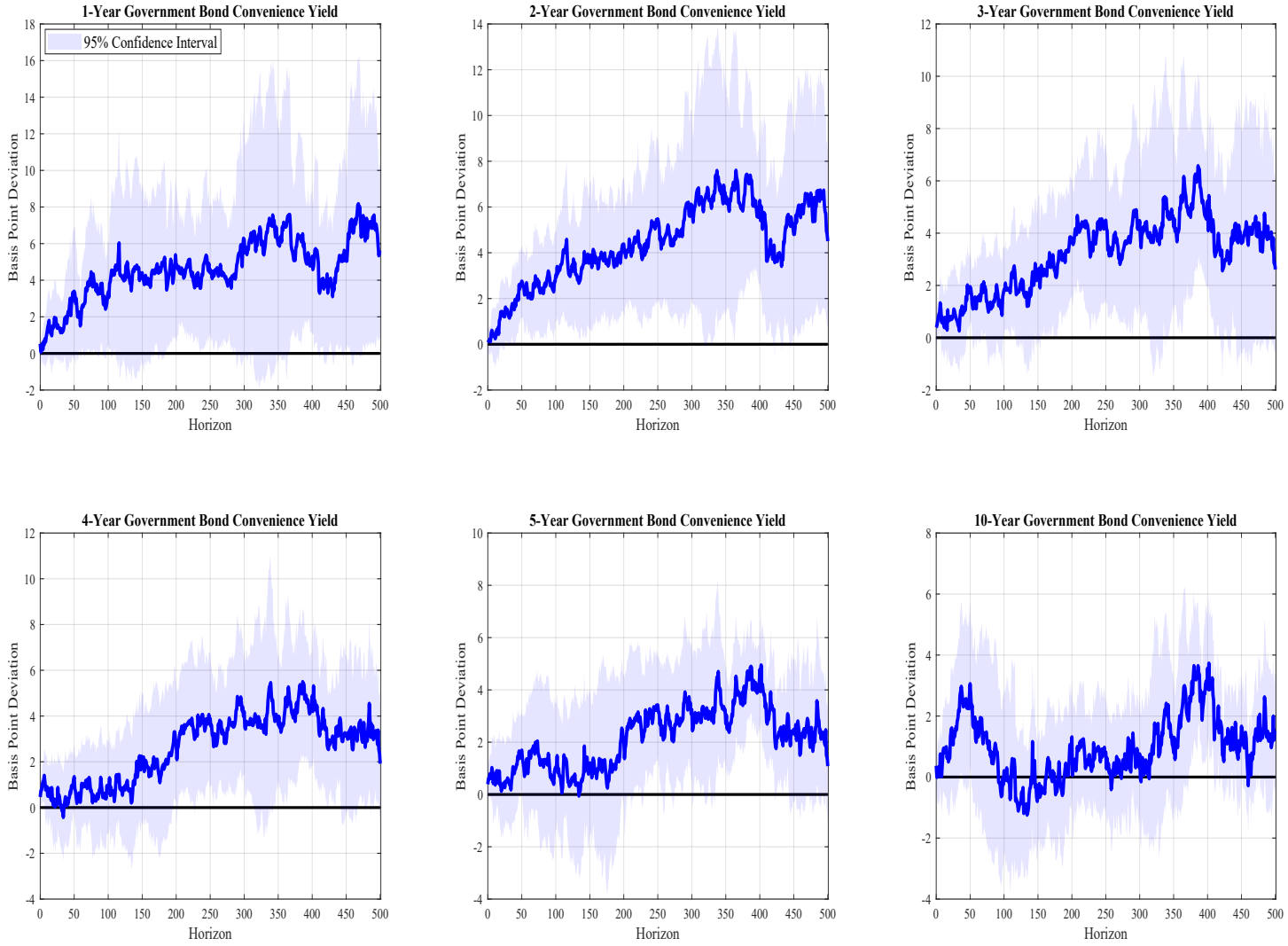

Notes: This figure presents the impulse responses (solid lines) to a GIV capital inflow shock of the 1- through 5-year and 10-year government bond convenience yields, where the number of lags in each FFI-level regression is halved. Responses are normalized such that the peak response of the latter variable is 0.1 (i.e., 10-percentage-point market share increase), implying a 3.7-standard-deviation GIV capital inflow shock size. 95% confidence bands (shaded areas) are based on standard errors computed from the heteroskedasticity- and autocorrelation-consistent procedure of Newey and West (1987) with the truncation lag equal to $h+1$ (where $h = 0, 1, ..., 500$ is the local projection horizon). Horizons are on the x-axis (impact horizon (0) to 500th horizon). Values are in basis point change units relative to the pre-shock value of the spread variable.

Figure D.4: **Shorter Lag Specification: FEVs Attributable to GIV Capital Inflow Shock: Government Bond Yield Spreads.**

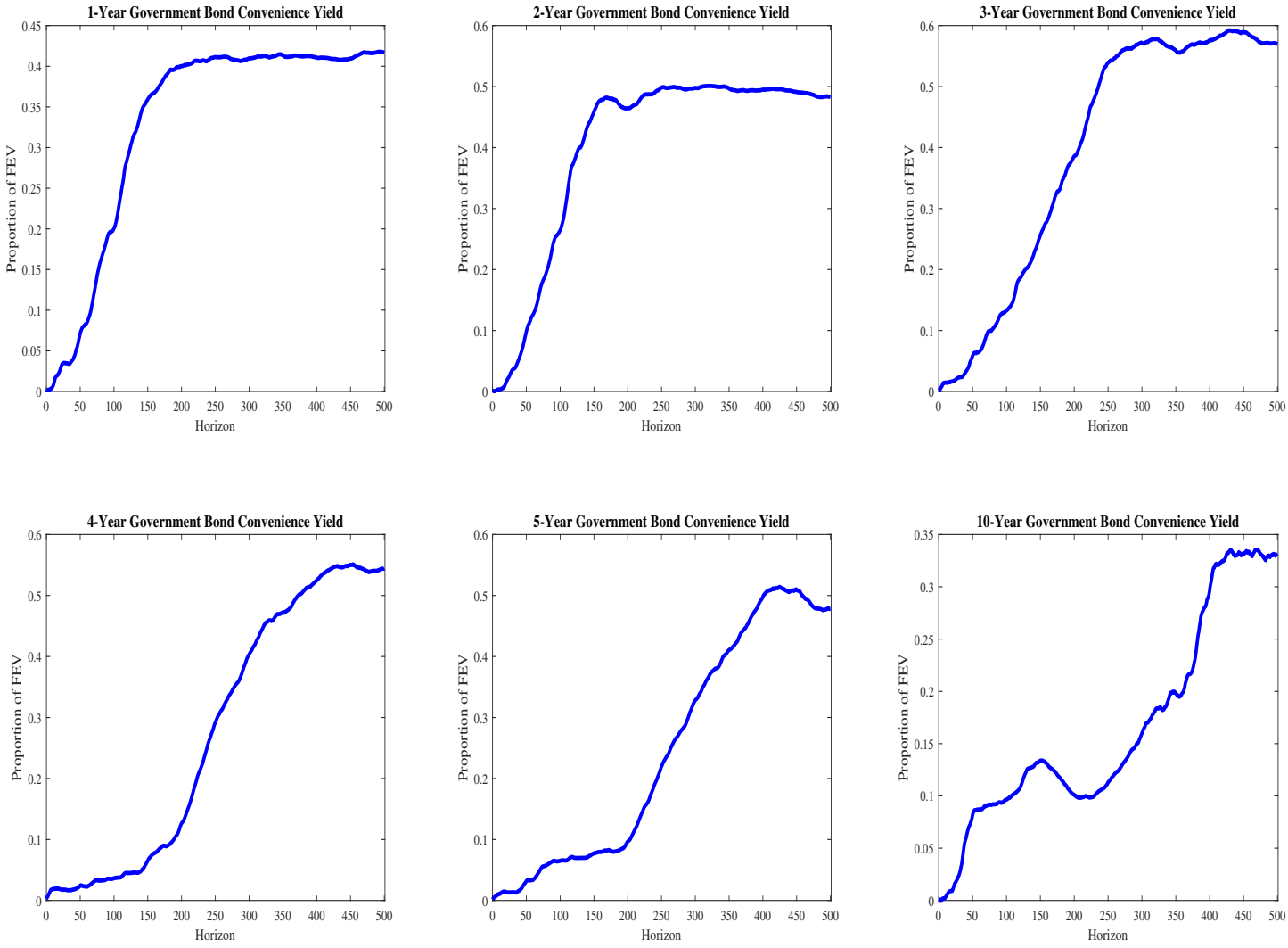

Notes: This figure presents the FEV shares of the variation in the government bond convenience yields attributable to a one-standard-deviation GIV capital inflow shock, where the number of lags in each FFI-level regression is halved. Horizons are on the x-axis (impact horizon (0) to 500th horizon). FEV share is on the y-axis (in fractional terms).

Figure D.5: **Shorter Lag Specification: Impulse Responses to GIV Capital Inflow Shock: Corporate Bond Yield Spreads.**

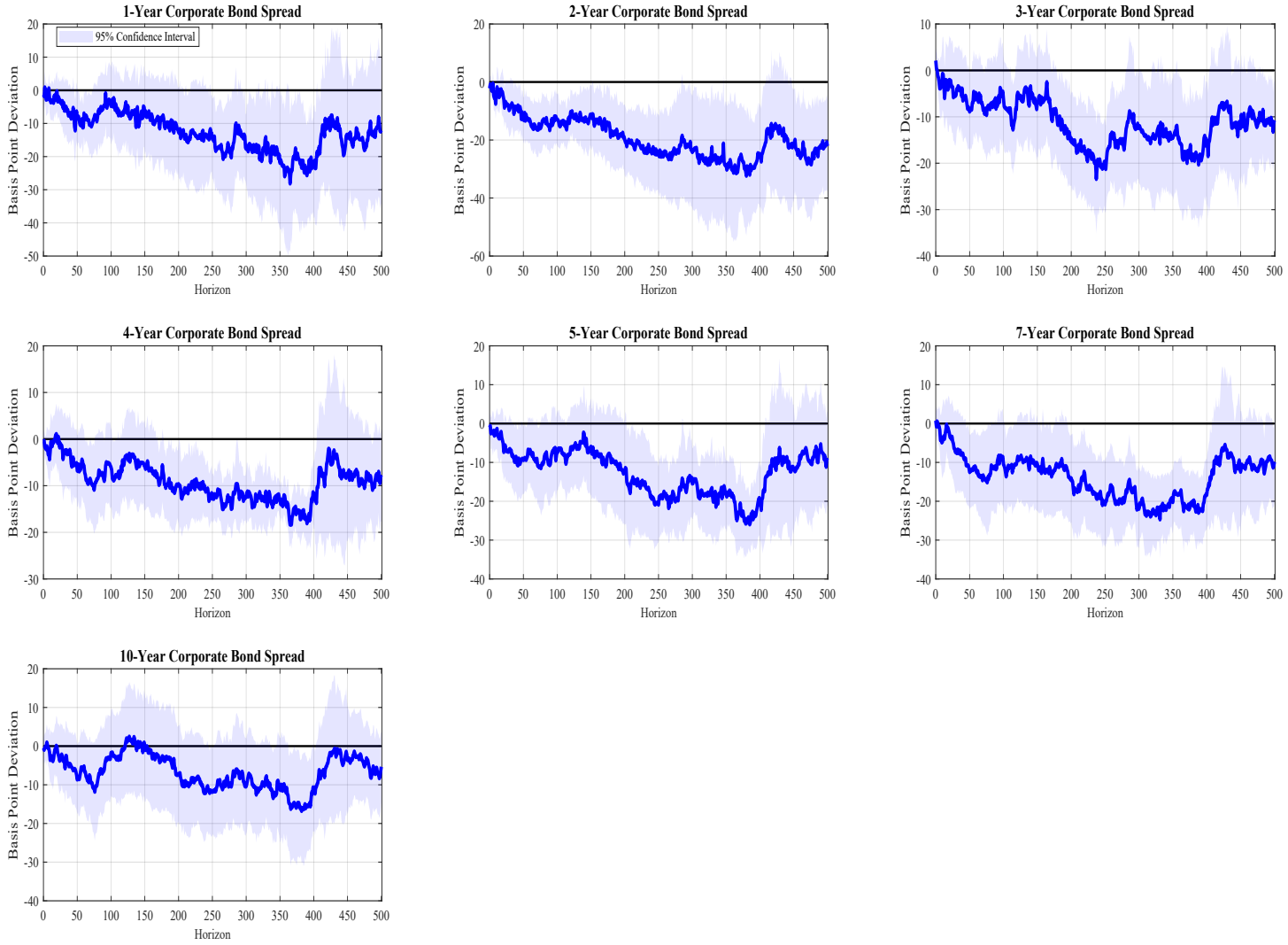

Notes: This figure presents the impulse responses (solid lines) to a GIV capital inflow shock of the 1- through 5-year and 7- and 10-year investment-grade corporate bond yield spreads (with respect to maturity-comparable IRS rates), where the number of lags in each FFI-level regression is halved. Responses are normalized such that the peak response of FFIs' accumulated net capital inflows variable is 10 (i.e., 10-percentage-point increase as share of outstanding MAKAM), implying a 3.7-standard-deviation GIV capital inflow shock size. 95% confidence bands (shaded areas) are based on standard errors computed from the heteroskedasticity- and autocorrelation-consistent procedure of Newey and West (1987) with the truncation lag equal to $h+1$ (where $h = 0, 1, ..., 500$ is the local projection horizon). Horizons are on the x-axis (impact horizon (0) to 500th horizon). Values are in basis point change units relative to the pre-shock value of the spread variable.

Figure D.6: **Shorter Lag Specification: FEVs Attributable to GIV Capital Inflow Shock: Corporate Bond Yield Spreads.**

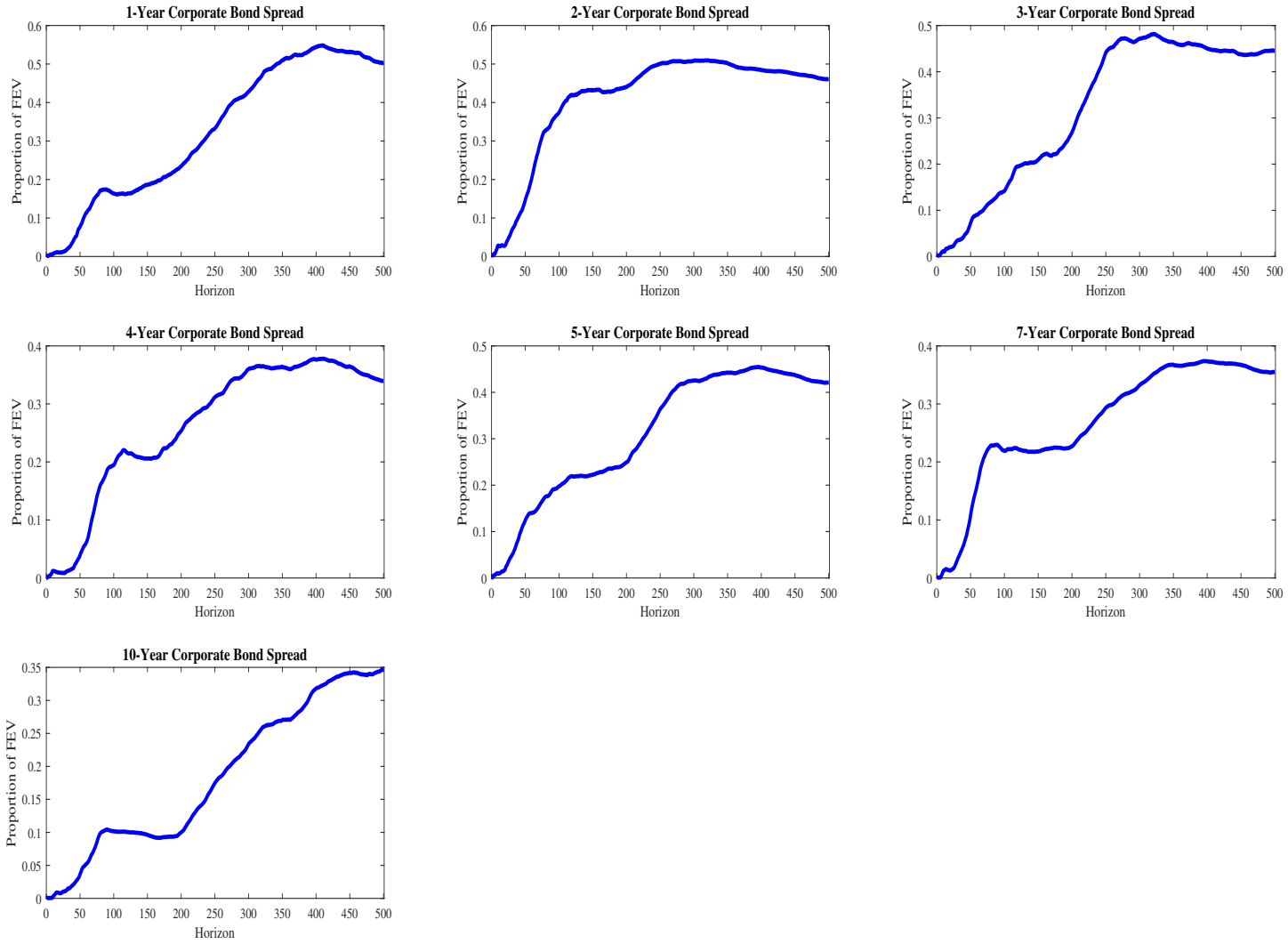

Notes: This figure presents the FEV shares of the variation in the corporate bond spread variables attributable to a one-standard-deviation GIV capital inflow shock, where the number of lags in each FFI-level regression is halved. Horizons are on the x-axis (impact horizon (0) to 500th horizon). FEV share is on the y-axis (in fractional terms).

Figure D.7: **Shorter Lag Specification: Impulse Responses to GIV Capital Inflow Shock: TA-35 Index.**

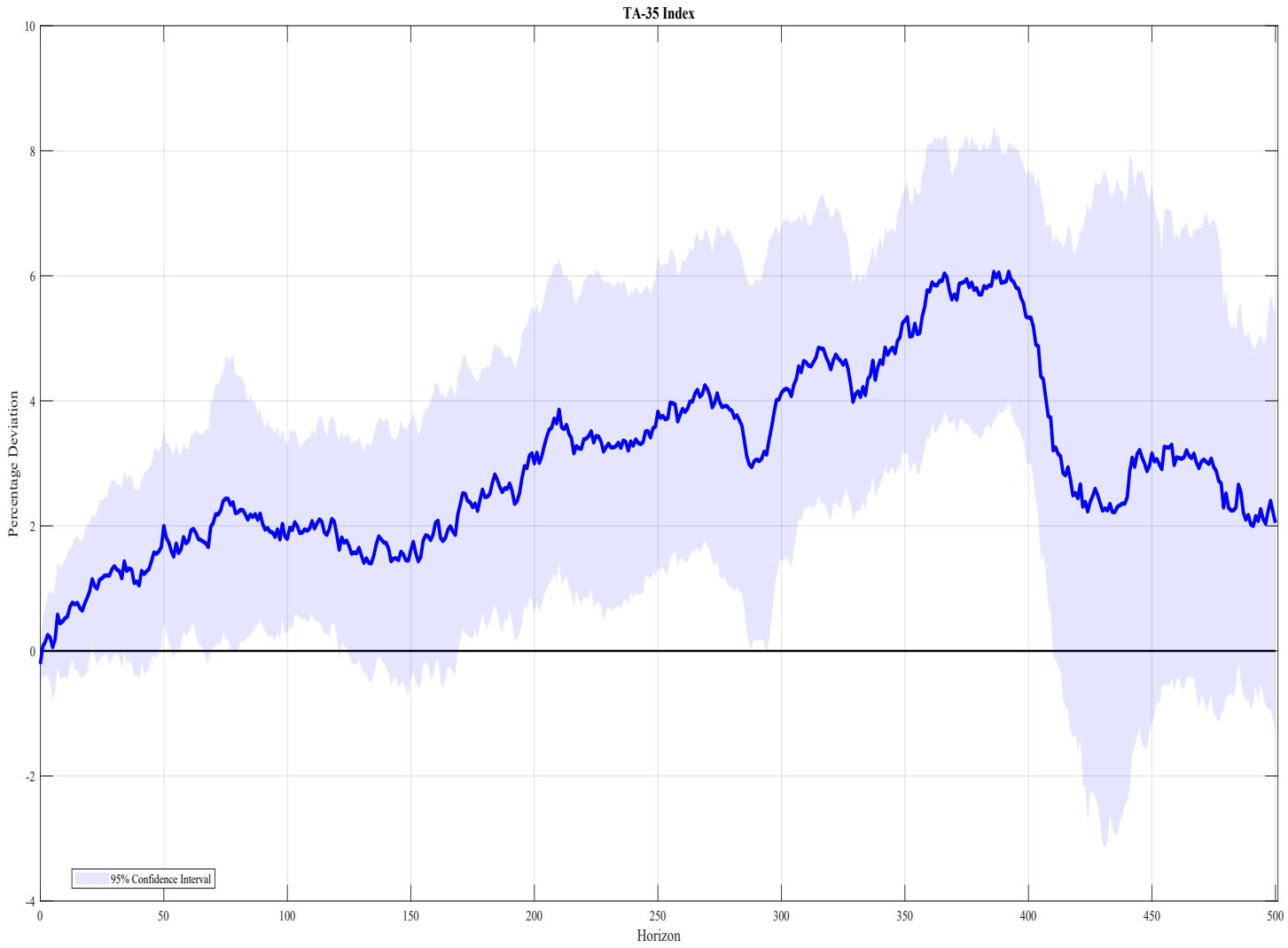

Notes: This figure presents the impulse responses (solid line) to a GIV capital inflow shock of the TA-35 stock price index, where the number of lags in each FFI-level regression is halved. Responses are normalized such that the peak response of FFIs' accumulated net capital inflows variable is 10 (i.e., 10-percentage-point increase as share of outstanding MAKAM), implying a 3.7-standard-deviation GIV capital inflow shock size. 95% confidence bands (shaded area) are based on standard errors computed from the heteroskedasticity- and autocorrelation-consistent procedure of Newey and West (1987) with the truncation lag equal to $h+1$ (where $h = 0, 1, ..., 500$ is the local projection horizon). Horizons are on the x-axis (impact horizon (0) to 500th horizon). Values are in percentage point change units relative to the pre-shock value of the stock price index variable.

Figure D.8: **Shorter Lag Specification: FEVs Attributable to GIV Capital Inflow Shock: TA-35 Index.**

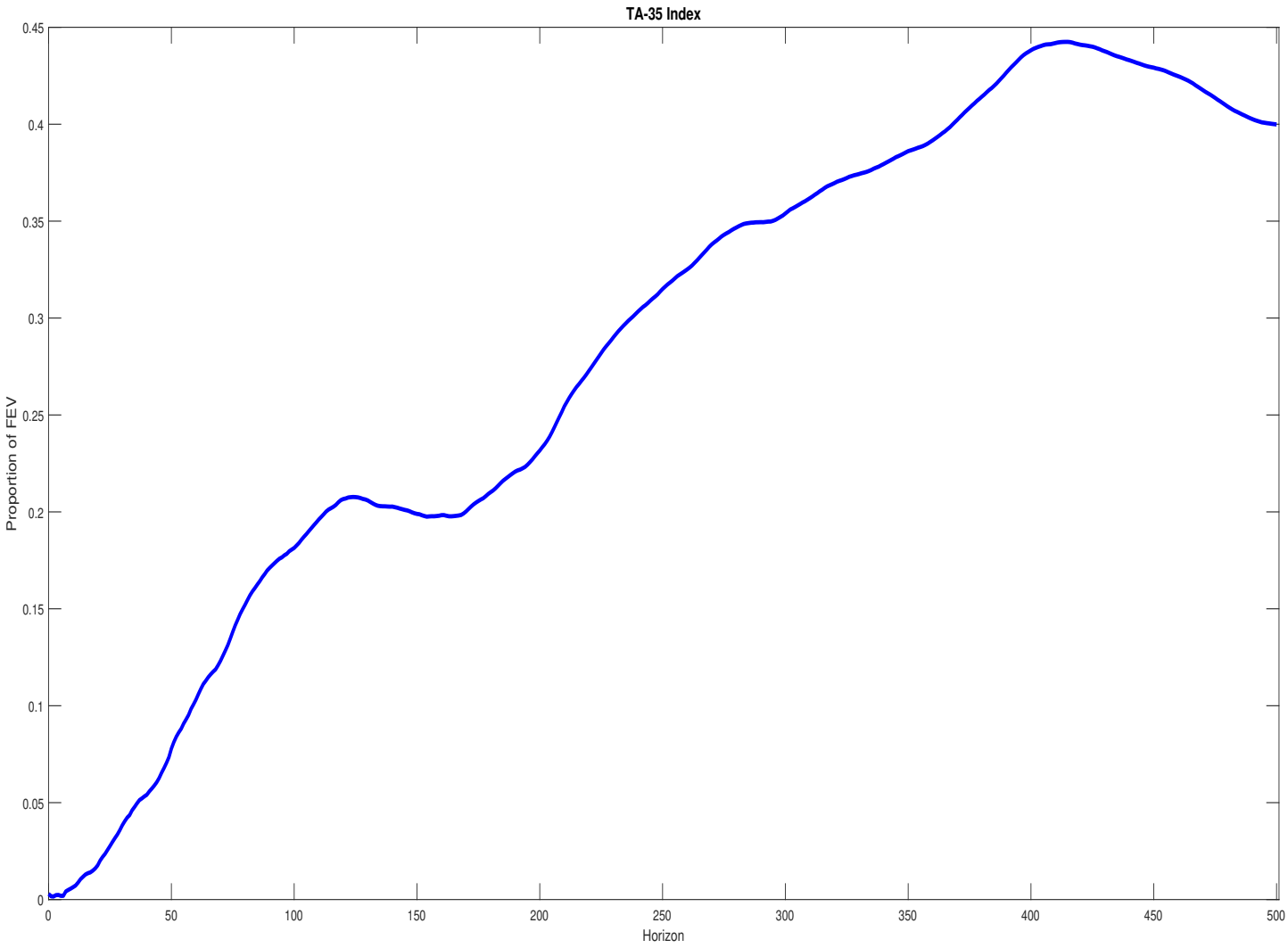

Notes: This figure presents the FEV shares of the variation in the TA-35 stock price index variable attributable to a one-standard-deviation GIV capital inflow shock, where the number of lags in each FFI-level regression is halved. Horizons are on the x-axis (impact horizon (0) to 500th horizon). FEV share is on the y-axis (in fractional terms).

Figure D.9: **Longer Lag Specification: Impulse Responses to GIV Capital Inflow Shock: MAKAM Convenience Yield and FFIs' Accumulated MAKAM Net Capital Inflows.**

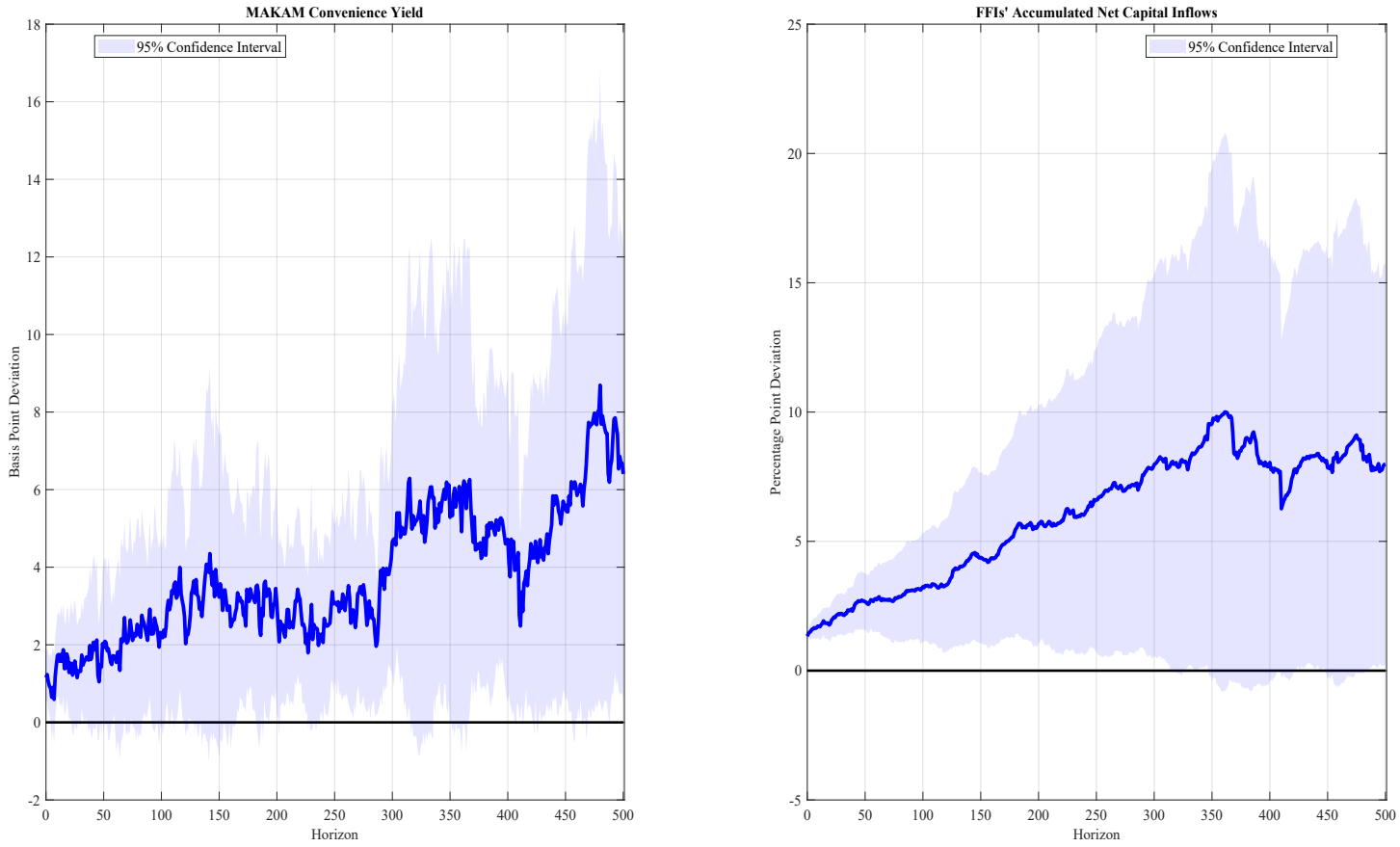

Notes: This figure presents the impulse responses (solid lines) to a GIV capital inflow shock of the MAKAM convenience yield and FFIs' accumulated MAKAM net capital inflows as share of outstanding MAKAM, where the number of lags in each FFI-level regressions is increased by 50%. Responses are normalized such that the peak response of the latter variable is 10 (i.e., 10-percentage-point increase as share of outstanding MAKAM), implying a 3.3-standard-deviation GIV capital inflow shock size. 95% confidence bands (shaded areas) are based on standard errors computed from the heteroskedasticity- and autocorrelation-consistent procedure of Newey and West (1987) with the truncation lag equal to $h+1$ (where $h = 0, 1, ..., 500$ is the local projection horizon). Horizons are on the x-axis (impact horizon (0) to 500th horizon). Values for MAKAM convenience yield variable are in basis point change units relative to the pre-shock value of the spread; those for the FFIs' accumulated MAKAM net capital inflows variable are in percentage-point change units relative to the pre-shock value of FFIs' market share.

Figure D.10: **Longer Lag Specification: FEVs Attributable to GIV Capital Inflow Shock: MAKAM Convenience Yield and FFIs' Accumulated MAKAM Net Capital Inflows.**

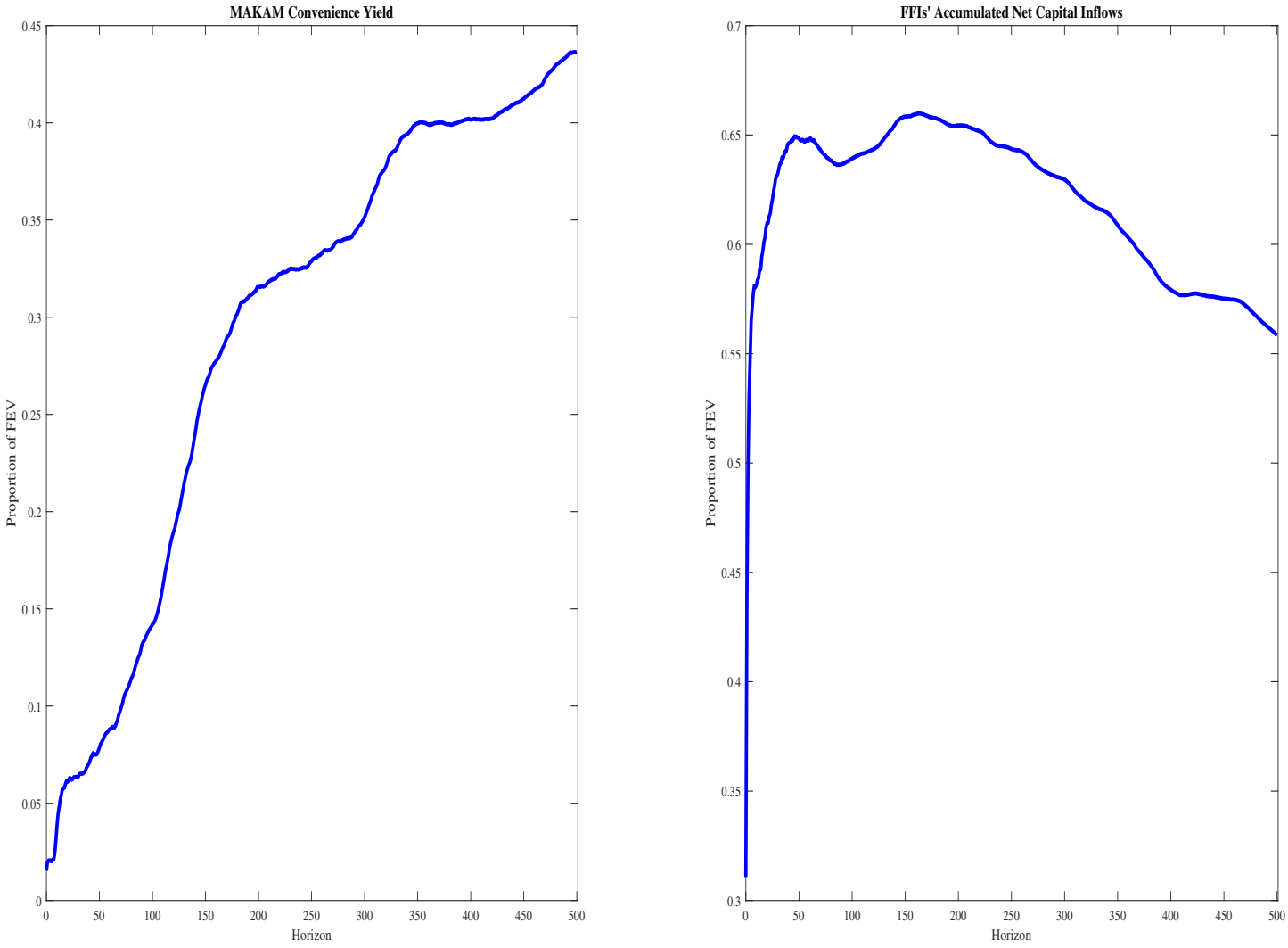

Notes: This figure presents the FEV shares of the variation in the MAKAM convenience yield and FFIs' accumulated MAKAM net capital inflow (as share of outstanding MAKAM) variables attributable to a one-standard-deviation GIV capital inflow shock, where the number of lags in each FFI-level regression is increased by 50%. Horizons are on the x-axis (impact horizon (0) to 500th horizon). FEV share is on the y-axis (in fractional terms).

Figure D.11: **Longer Lag Specification: Impulse Responses to GIV Capital Inflow Shock: Government Bond Convenience Yields.**

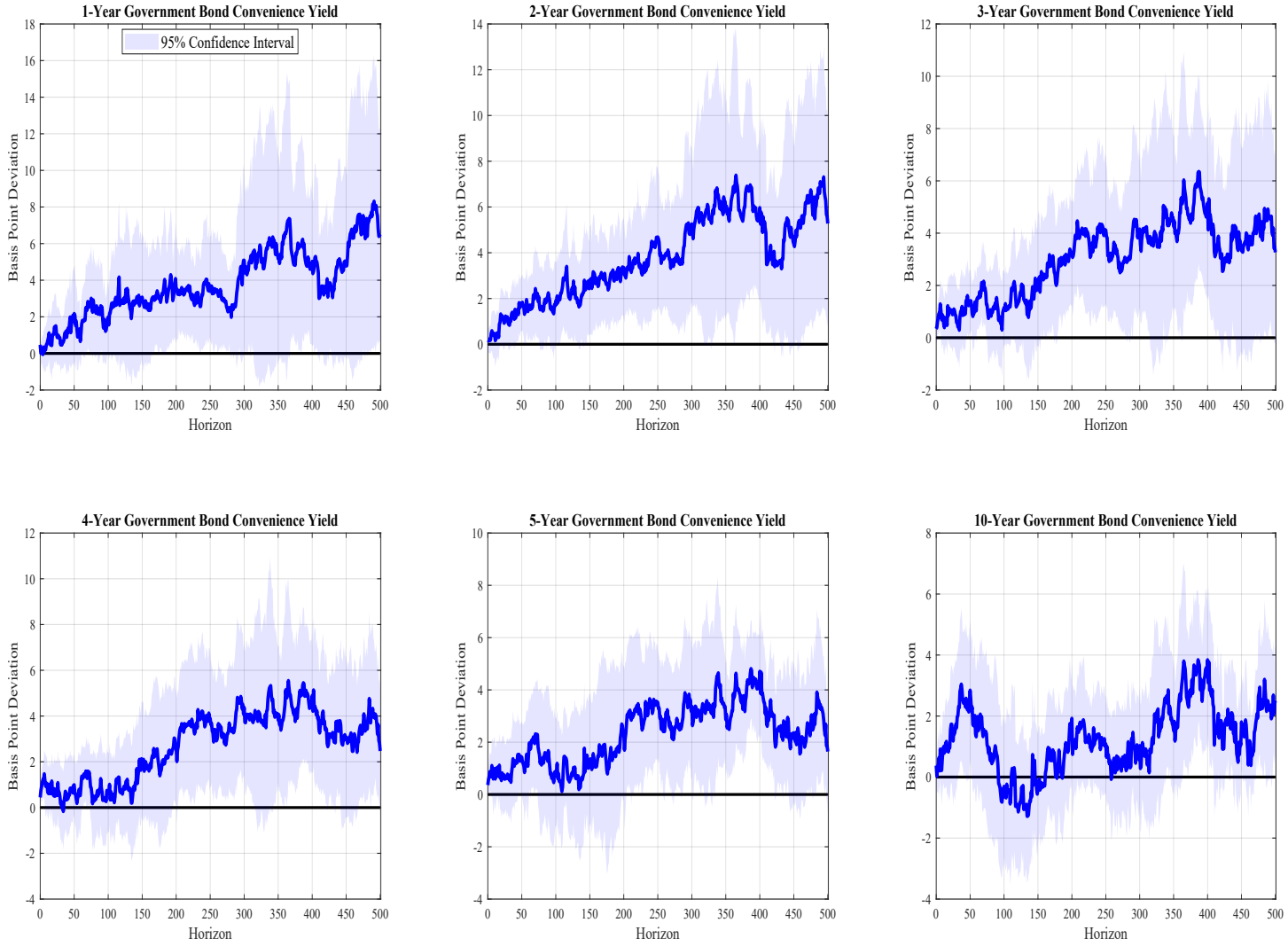

Notes: This figure presents the impulse responses (solid lines) to a GIV capital inflow shock of the 1- through 5-year and 10-year government bond convenience yields, where the number of lags in FFI-level regression is increased by 50%. Responses are normalized such that the peak response of FFIs' accumulated net capital inflows variable is 10 (i.e., 10-percentage-point increase as share of outstanding MAKAM), implying a 3.3-standard-deviation GIV capital inflow shock size. 95% confidence bands (dashed lines) are based on standard errors computed from the heteroskedasticity- and autocorrelation-consistent procedure of Newey and West (1987) with the truncation lag equal to $h+1$ (where $h = 0, 1, ..., 500$ is the local projection horizon). Horizons are on the x-axis (impact horizon (0) to 500th horizon). Values are in basis point change units relative to the pre-shock value of the spread variable.

Figure D.12: **Longer Lag Specification: FEVs Attributable to GIV Capital Inflow Shock: Government Bond Convenience Yields.**

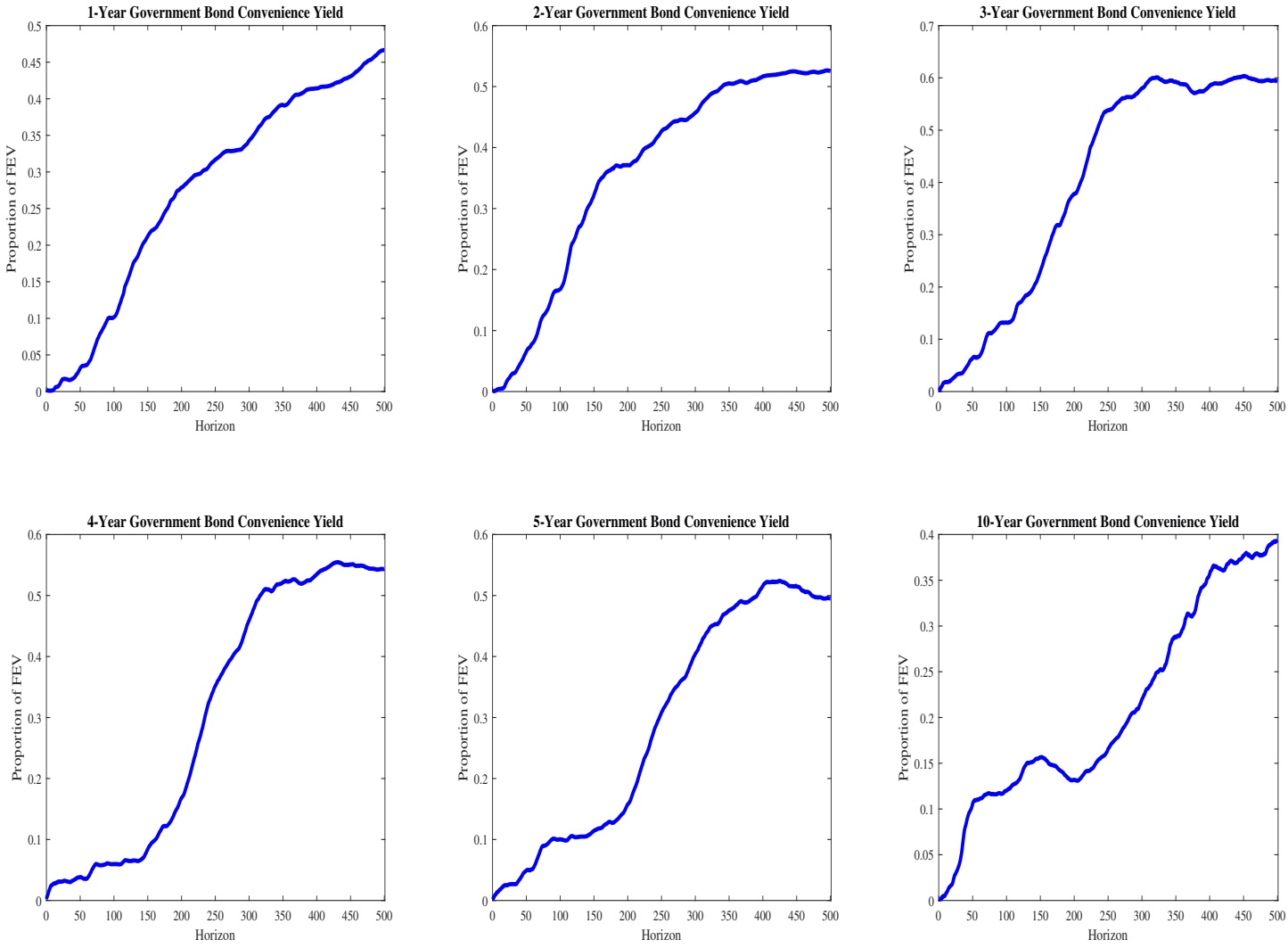

Notes: This figure presents the FEV shares of the variation in the government bond convenience yields attributable to a one-standard-deviation GIV capital inflow shock, where the number of lags in each FFI-level regression is increased by 50%. Horizons are on the x-axis (impact horizon (0) to 500th horizon). FEV share is on the y-axis (in fractional terms).

Figure D.13: **Longer Lag Specification: Impulse Responses to GIV Capital Inflow Shock: Corporate Bond Yield Spreads.**

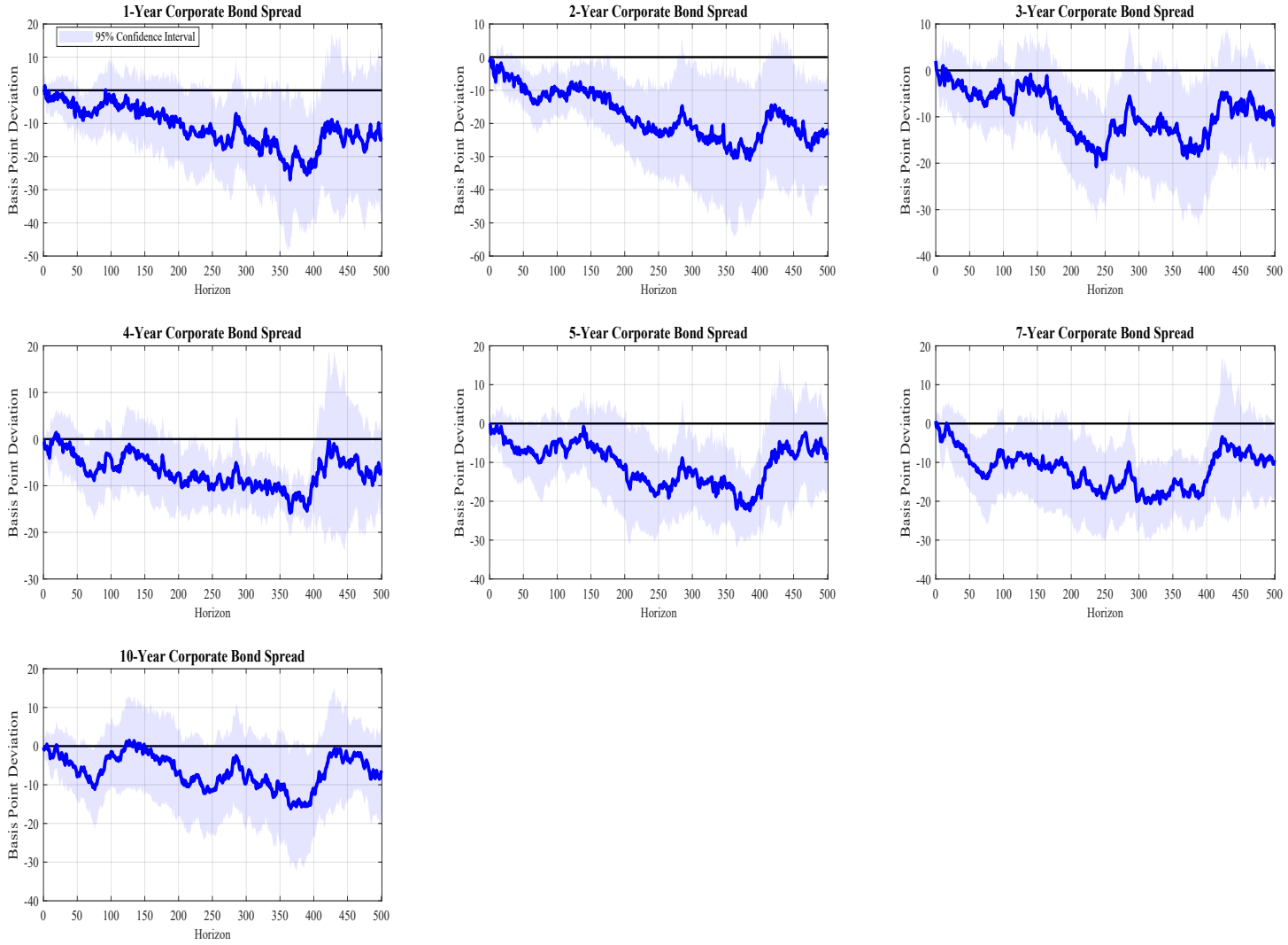

Notes: This figure presents the impulse responses (solid lines) to a GIV capital inflow shock of the 1- through 5-year and 7- and 10-year investment-grade corporate bond yield spreads (with respect to maturity-comparable IRS rates), where the number of lags in each FFI-level regression is increased by 50%. Responses are normalized such that the peak response of FFIs' accumulated net capital inflows variable is 10 (i.e., 10-percentage-point increase as share of outstanding MAKAM), implying a 3.3-standard-deviation GIV capital inflow shock size. 95% confidence bands (shaded areas) are based on standard errors computed from the heteroskedasticity- and autocorrelation-consistent procedure of Newey and West (1987) with the truncation lag equal to $h+1$ (where $h = 0, 1, ..., 500$ is the local projection horizon). Horizons are on the x-axis (impact horizon (0) to 500th horizon). Values are in basis point change units relative to the pre-shock value of the spread variable.

Figure D.14: **Longer Lag Specification: FEVs Attributable to GIV Capital Inflow Shock: Corporate Bond Yield Spreads.**

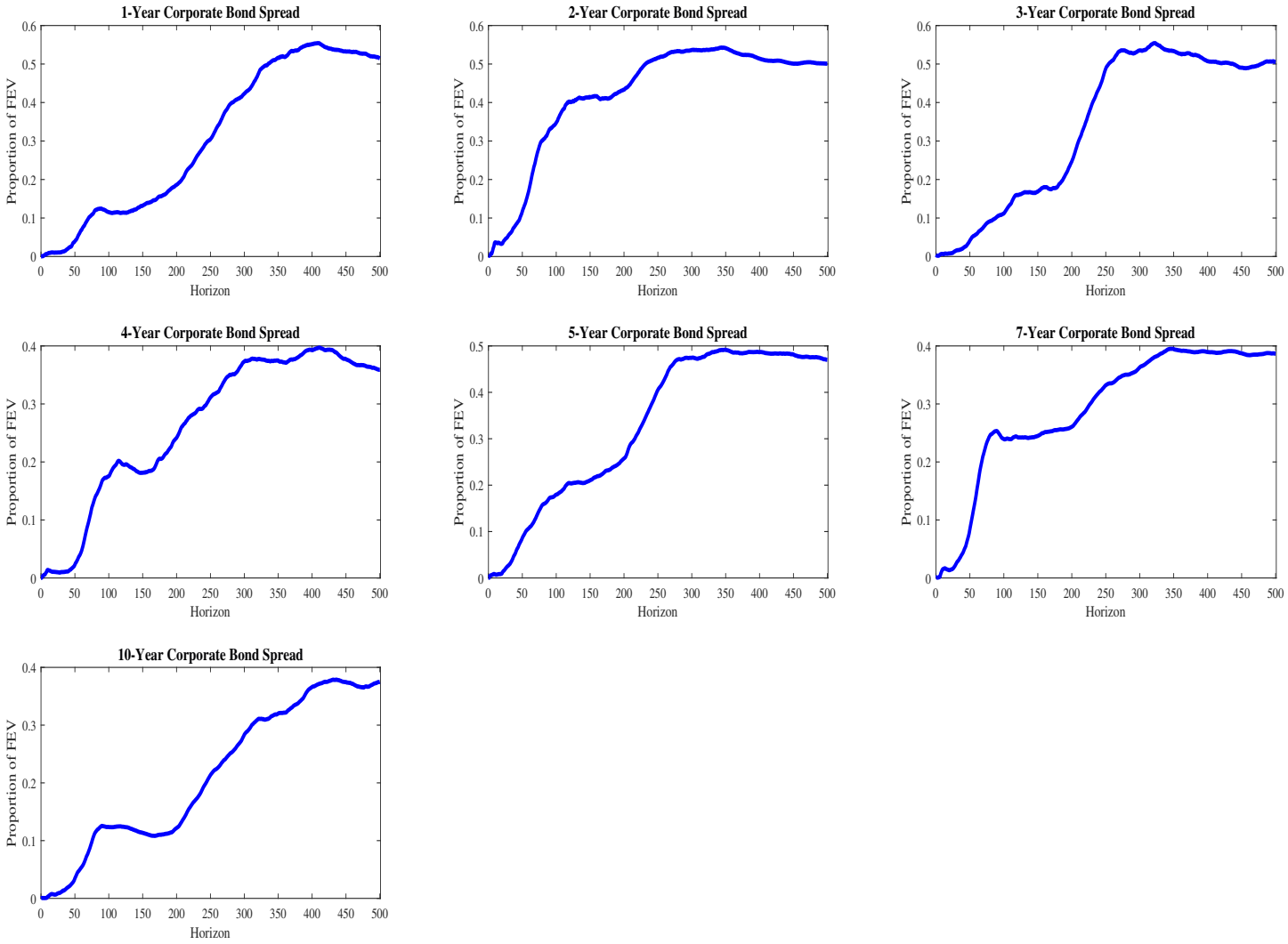

Notes: This figure presents the FEV shares of the variation in the corporate bond spread variables attributable to a one-standard-deviation GIV capital inflow shock, where the number of lags in each FFI-level regressions is increased by 50%. Horizons are on the x-axis (impact horizon (0) to 500th horizon). FEV share is on the y-axis (in fractional terms).

Figure D.15: **Longer Lag Specification: Impulse Responses to GIV Capital Inflow Shock: TA-35 Index.**

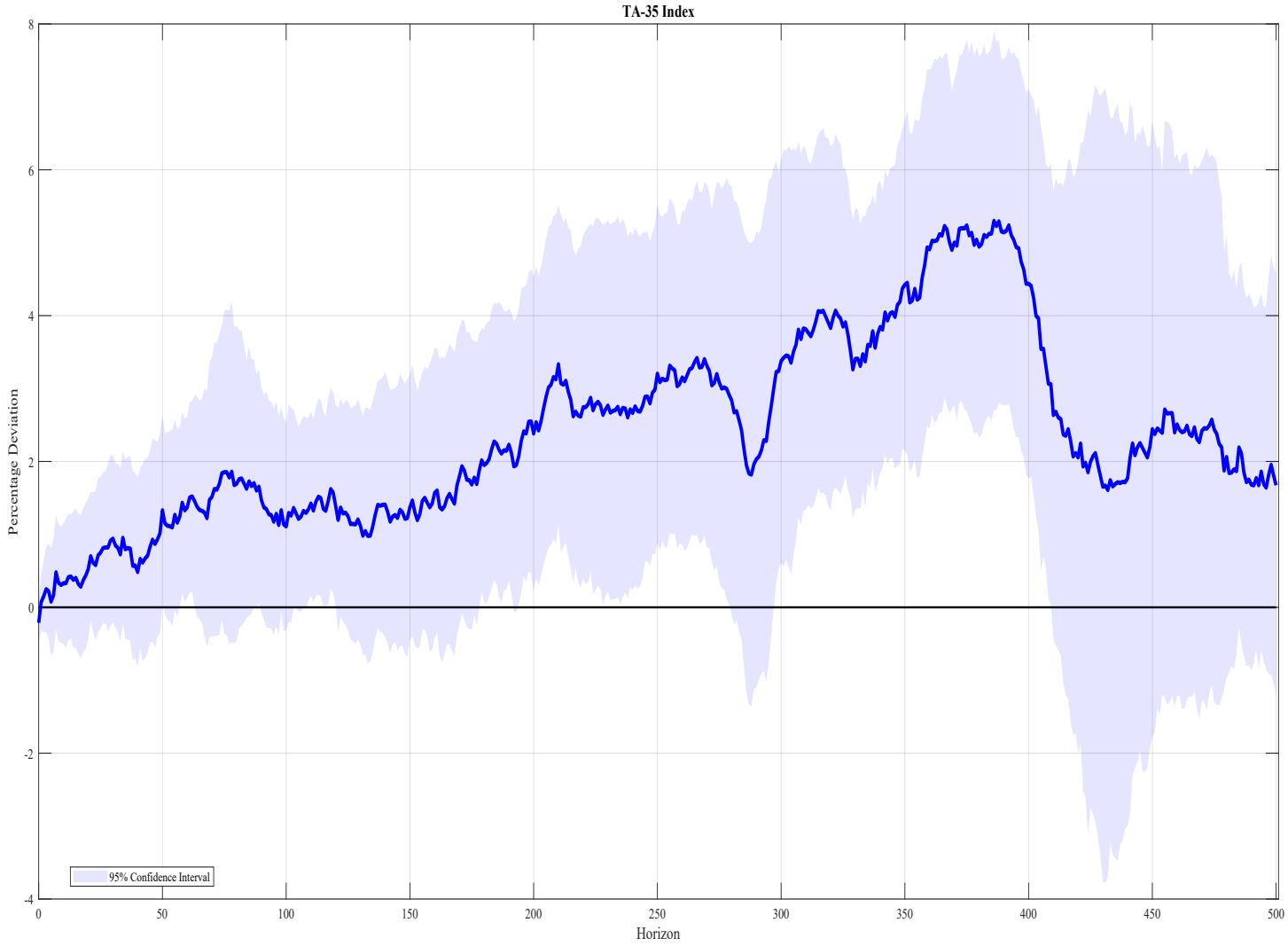

Notes: This figure presents the impulse responses (solid line) to a GIV capital inflow shock of the TA-35 stock price index, where the number of lags in each FFI-level regression is increased by 50%. Responses are normalized such that the peak response of FFIs' accumulated net capital inflows variable is 10 (i.e., 10-percentage-point increase as share of outstanding MAKAM), implying a 3.3-standard-deviation GIV capital inflow shock size. 95% confidence bands (shaded areas) are based on standard errors computed from the heteroskedasticity- and autocorrelation-consistent procedure of Newey and West (1987) with the truncation lag equal to $h+1$ (where $h = 0, 1, ..., 500$ is the local projection horizon). Horizons are on the x-axis (impact horizon (0) to 500th horizon). Values are in percentage point change units relative to the pre-shock value of the stock price index variable.

Figure D.16: **Longer Lag Specification: FEVs Attributable to GIV Capital Inflow Shock: TA-35 Index.**

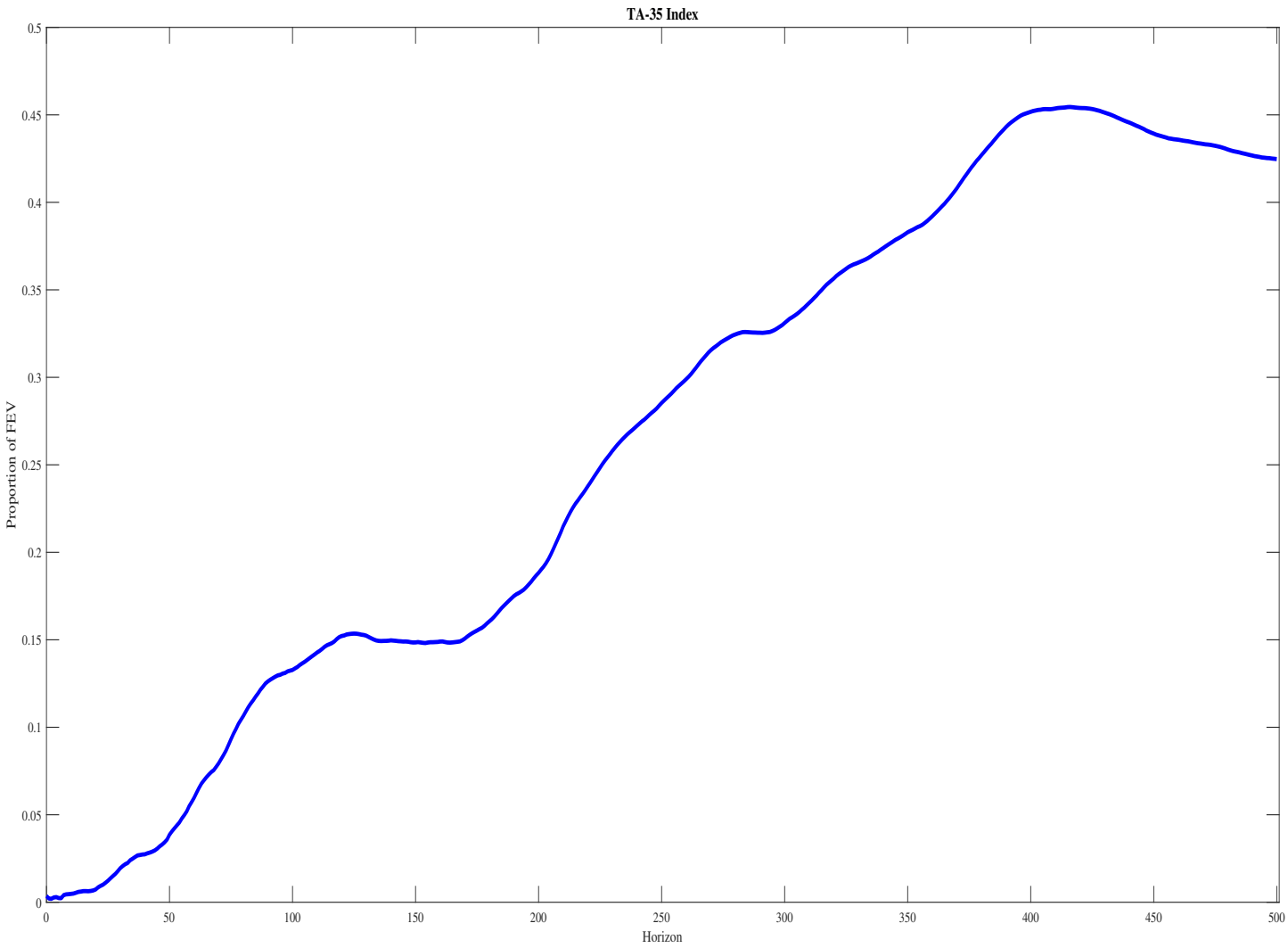

Notes: This figure presents the FEV shares of the variation in the TA-35 stock price index variable attributable to a one-standard-deviation GIV capital inflow shock, where the number of lags in each FFI-level regression is increased by 50%. Horizons are on the x-axis (impact horizon (0) to 500th horizon). FEV share is on the y-axis (in fractional terms).

Figure D.17: **Omission of Monetary Tightening Cycle Period: Impulse Responses to GIV Capital Inflow Shock: MAKAM Convenience Yield and FFIs' Accumulated MAKAM Net Capital Inflows.**

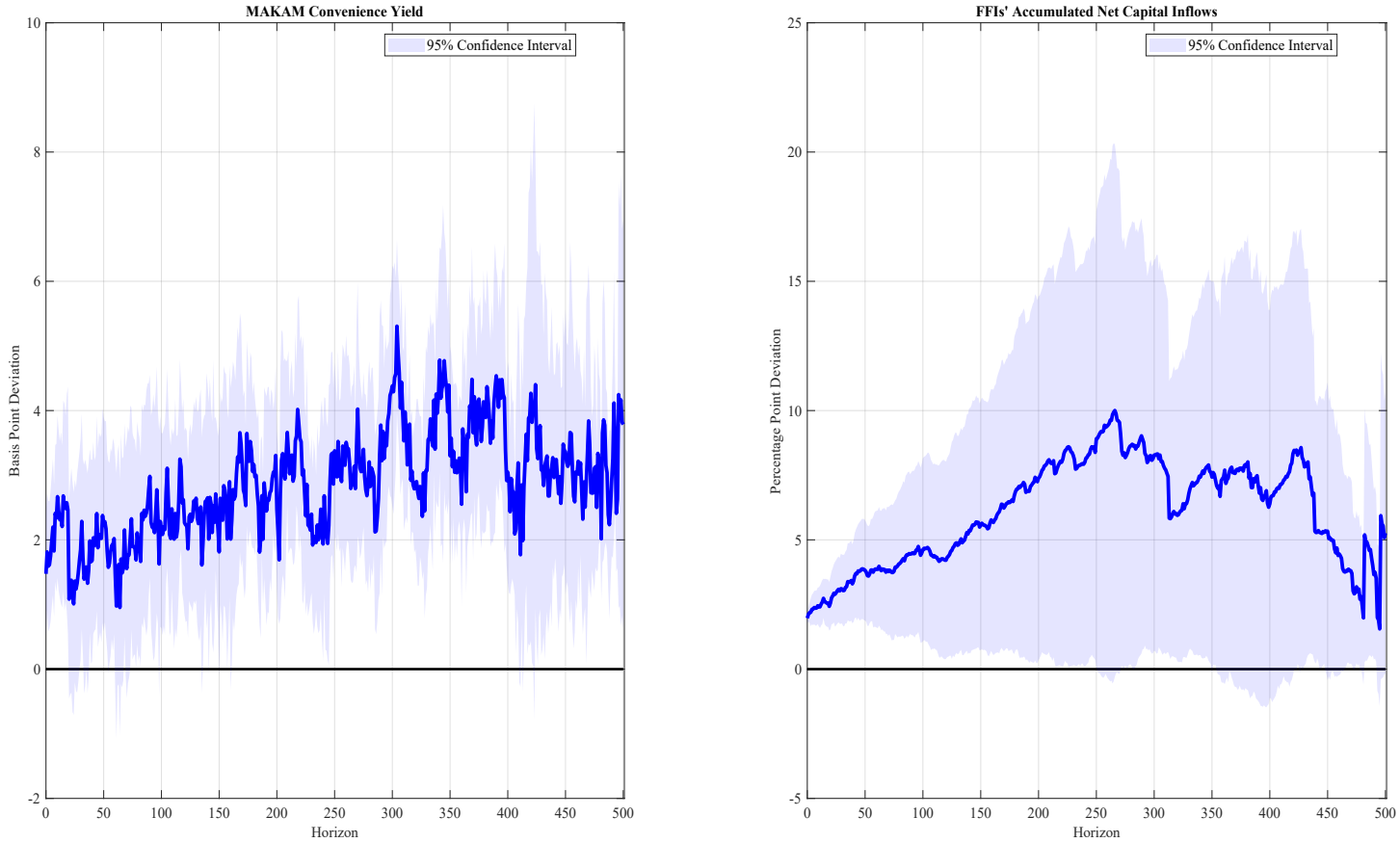

Notes: This figure presents the impulse responses (solid lines) to a GIV capital inflow shock of the convenience yield variable (MAKAM convenience yield) and FFIs' accumulated MAKAM net capital inflows as share of outstanding MAKAM, where the sample is truncated at 4/11/2022. Responses are normalized such that the peak response of the latter variable is 10 (i.e., 10-percentage-point increase as share of outstanding MAKAM), implying a 4.9-standard-deviation GIV capital inflow shock size. 95% confidence bands (shaded areas) are based on standard errors computed from the heteroskedasticity- and autocorrelation-consistent procedure of Newey and West (1987) with the truncation lag equal to $h+1$ (where $h = 0, 1, ..., 500$ is the local projection horizon). Horizons are on the x-axis (impact horizon (0) to 500th horizon). Values for MAKAM convenience yield variable are in basis point change units relative to the pre-shock value of the spread; those for the FFIs' accumulated MAKAM net capital inflows variable are in percentage-point change units relative to the pre-shock value of FFIs' market share.

Figure D.18: **Omission of Monetary Tightening Cycle Period: FEVs Attributable to GIV Capital Inflow Shock: MAKAM Convenience Yield and FFIs' Accumulated MAKAM Net Capital Inflows.**

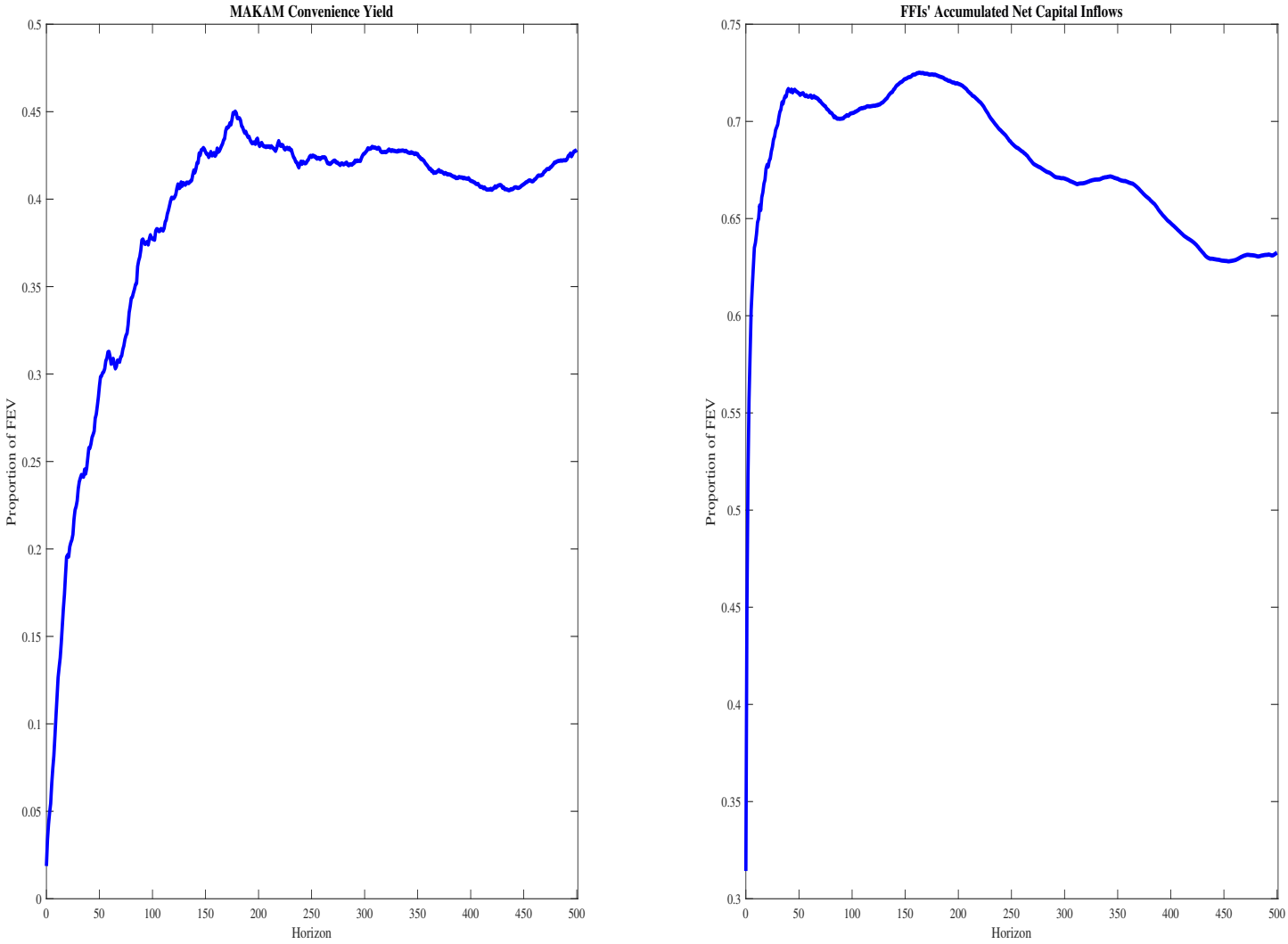

Notes: This figure presents the FEV shares of the variation in the MAKAM convenience yield and FFIs' accumulated MAKAM net capital inflow (as share of outstanding MAKAM) variables attributable to a one-standard-deviation GIV capital inflow shock, where the sample is truncated at 4/11/2022. Horizons are on the x-axis (impact horizon (0) to 500th horizon). FEV share is on the y-axis (in fractional terms).

Figure D.19: **Omission of Monetary Tightening Cycle Period: Impulse Responses to GIV Capital Inflow Shock: Government Bond Convenience Yields.**

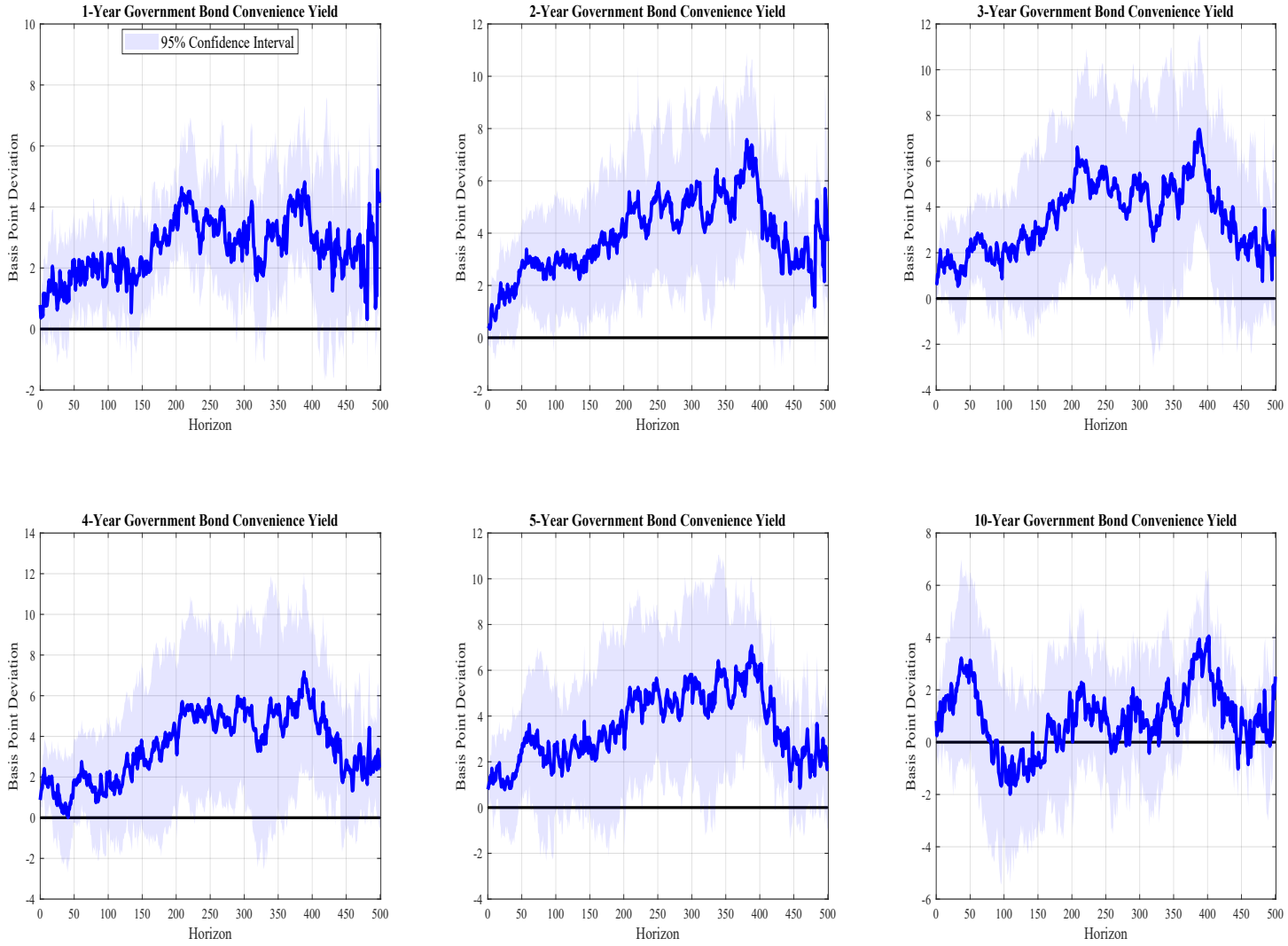

Notes: This figure presents the impulse responses (solid lines) to a GIV capital inflow shock of the 1- through 5-year and 10-year government bond yield spreads (with respect to maturity-comparable IRS rates), where the sample is truncated at 4/11/2022. Responses are normalized such that the peak response of FFIs' accumulated net capital inflows variable is 10 (i.e., 10-percentage-point increase as share of outstanding MAKAM), implying a 4.9-standard-deviation GIV capital inflow shock size. 95% confidence bands (dashed lines) are based on standard errors computed from the heteroskedasticity- and autocorrelation-consistent procedure of Newey and West (1987) with the truncation lag equal to $h+1$ (where $h = 0, 1, ..., 500$ is the local projection horizon). Horizons are on the x-axis (impact horizon (0) to 500th horizon). Values are in basis point change units relative to the pre-shock value of the spread variable.

Figure D.20: **Omission of Monetary Tightening Cycle Period: FEVs Attributable to GIV Capital Inflow Shock: Government Bond Convenience Yields.**

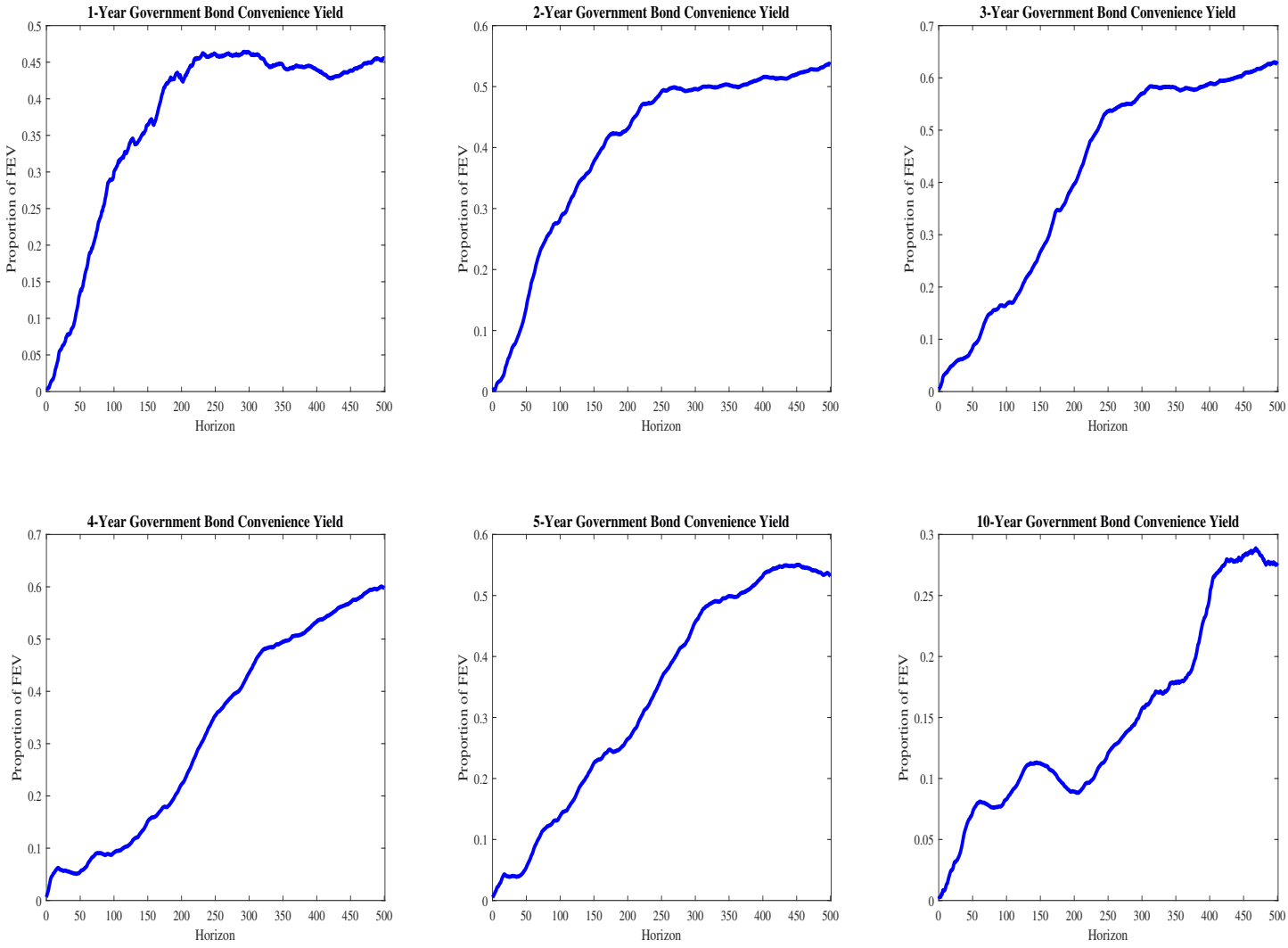

Notes: This figure presents the FEV shares of the variation in the government bond convenience yields attributable to a one-standard-deviation GIV capital inflow shock, where the sample is truncated at 4/11/2022. Horizons are on the x-axis (impact horizon (0) to 500th horizon). FEV share is on the y-axis (in fractional terms).

Figure D.21: **Omission of Monetary Tightening Cycle Period: Impulse Responses to GIV Capital Inflow Shock: Corporate Bond Yield Spreads.**

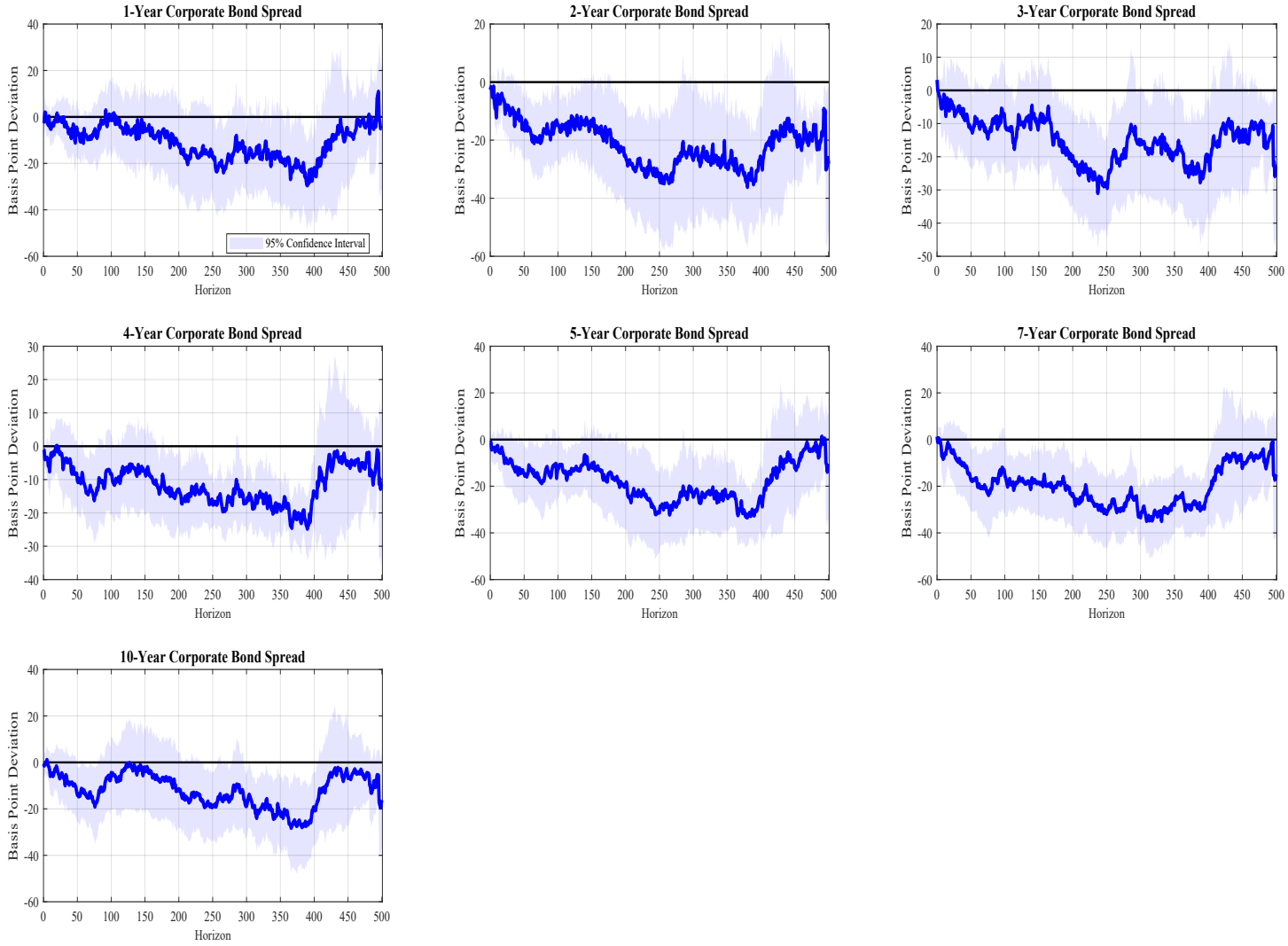

Notes: This figure presents the impulse responses (solid lines) to a GIV capital inflow shock of the 1- through 5-year and 7- and 10-year investment-grade corporate bond yield spreads (with respect to maturity-comparable IRS rates), where the sample is truncated at 4/11/2022. Responses are normalized such that the peak response of FFIs' accumulated net capital inflows variable is 10 (i.e., 10-percentage-point increase as share of outstanding MAKAM), implying a 4.9-standard-deviation GIV capital inflow shock size. 95% confidence bands (shaded areas) are based on standard errors computed from the heteroskedasticity- and autocorrelation-consistent procedure of Newey and West (1987) with the truncation lag equal to $h+1$ (where $h = 0, 1, ..., 500$ is the local projection horizon). Horizons are on the x-axis (impact horizon (0) to 500th horizon). Values are in basis point change units relative to the pre-shock value of the spread variable.

Figure D.22: **Omission of Monetary Tightening Cycle Period: FEVs Attributable to GIV Capital Inflow Shock: Corporate Bond Yield Spreads.**

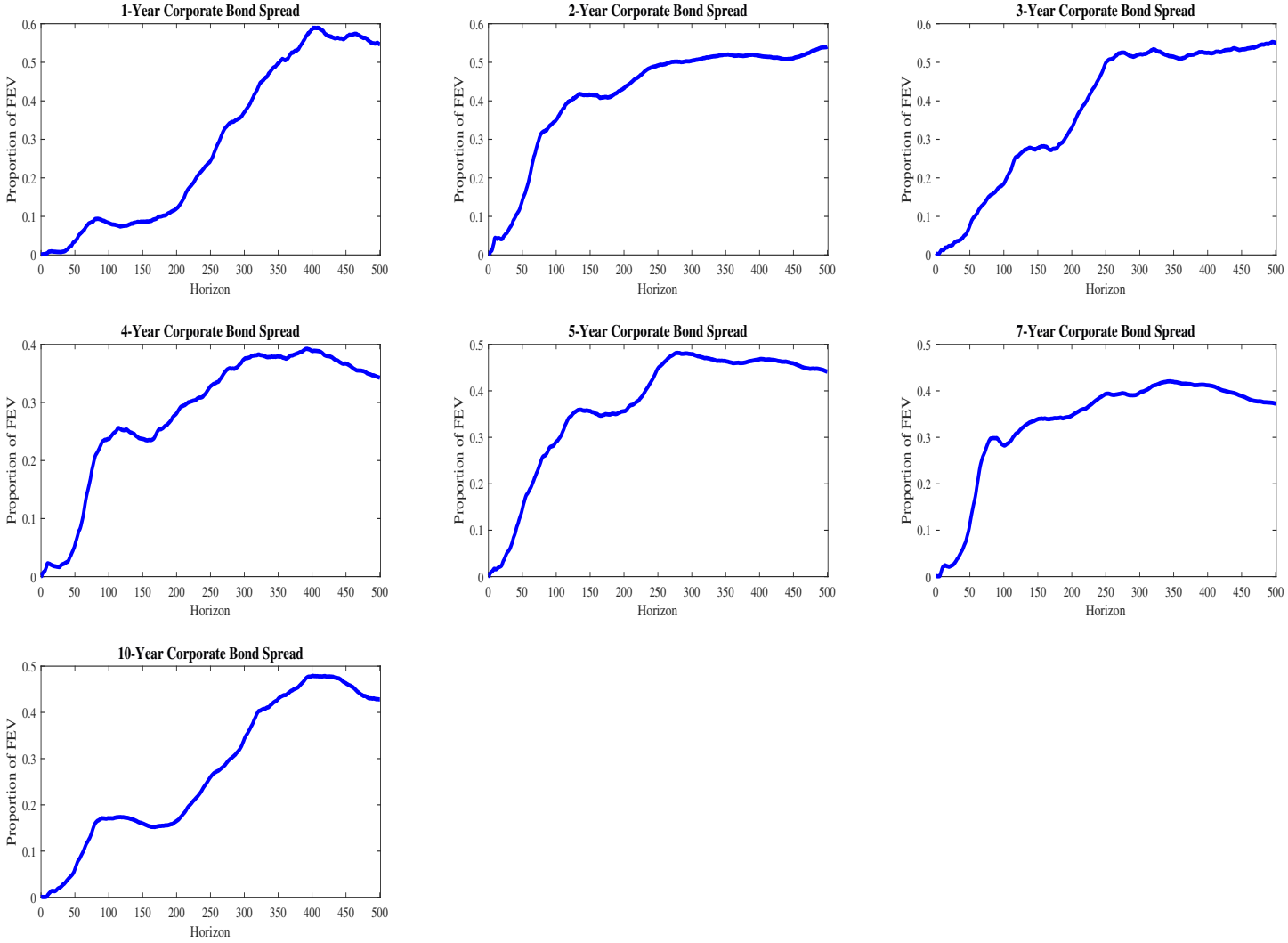

Notes: This figure presents the FEV shares of the variation in the corporate bond spread variables attributable to a one-standard-deviation GIV capital inflow shock, where the sample is truncated at 4/11/2022. Horizons are on the x-axis (impact horizon (0) to 500th horizon). FEV share is on the y-axis (in fractional terms).

Figure D.23: **Omission of Monetary Tightening Cycle Period: Impulse Responses to GIV Capital Inflow Shock: TA-35 Index.**

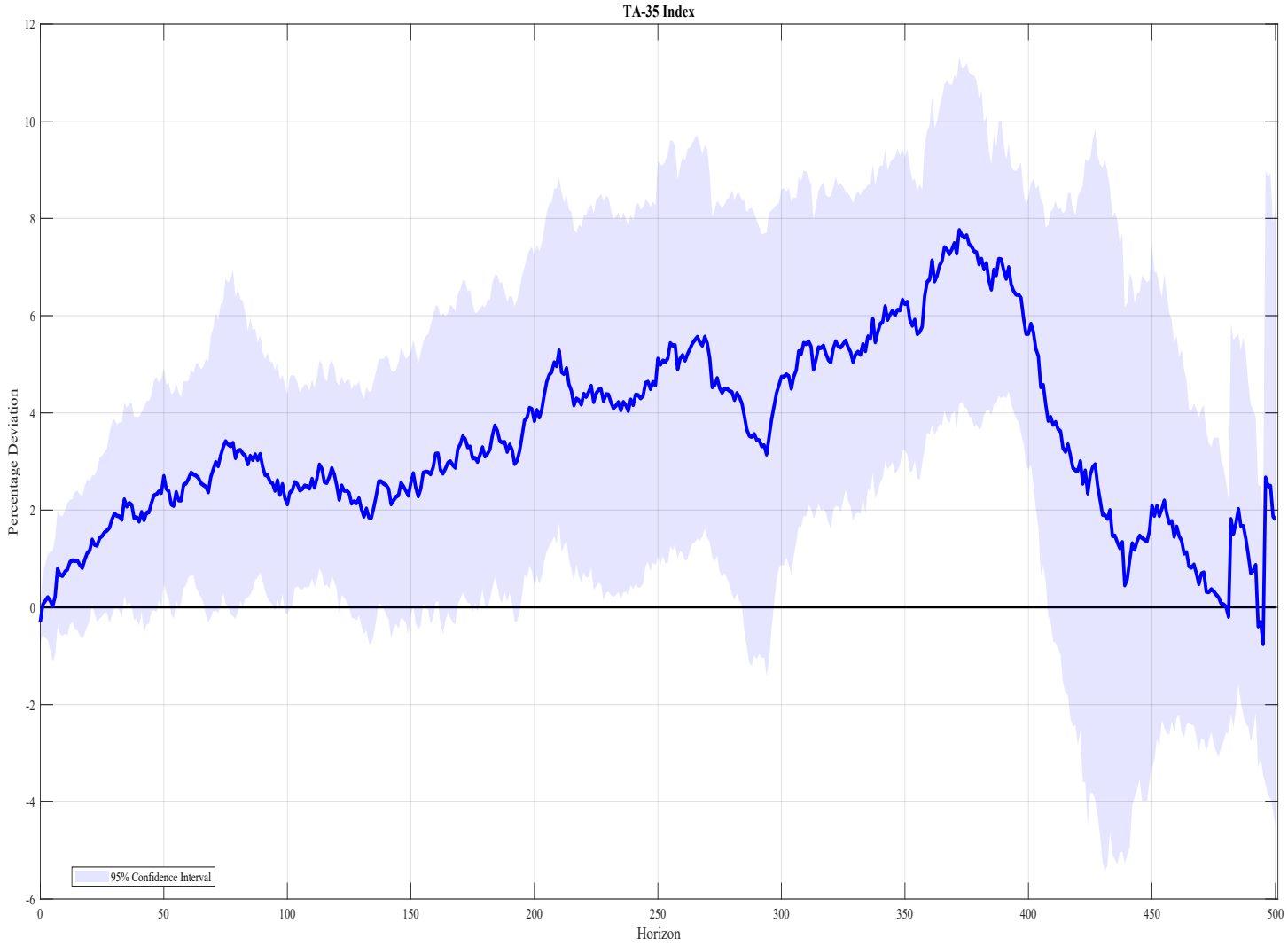

Notes: This figure presents the impulse responses (solid line) to a GIV capital inflow shock of the TA-35 stock price index, where the sample is truncated at 4/11/2022. Responses are normalized such that the peak response of FFIs' accumulated net capital inflows variable is 10 (i.e., 10-percentage-point increase as share of outstanding MAKAM), implying a 4.9-standard-deviation GIV capital inflow shock size. 95% confidence bands (shaded area) are based on standard errors computed from the heteroskedasticity- and autocorrelation-consistent procedure of Newey and West (1987) with the truncation lag equal to $h+1$ (where $h = 0, 1, ..., 500$ is the local projection horizon). Horizons are on the x-axis (impact horizon (0) to 500th horizon). Values are in basis point change units relative to the pre-shock value of the spread variable.

Figure D.24: **Omission of Monetary Tightening Cycle Period: FEVs Attributable to GIV Capital Inflow Shock: TA-35 Index.**

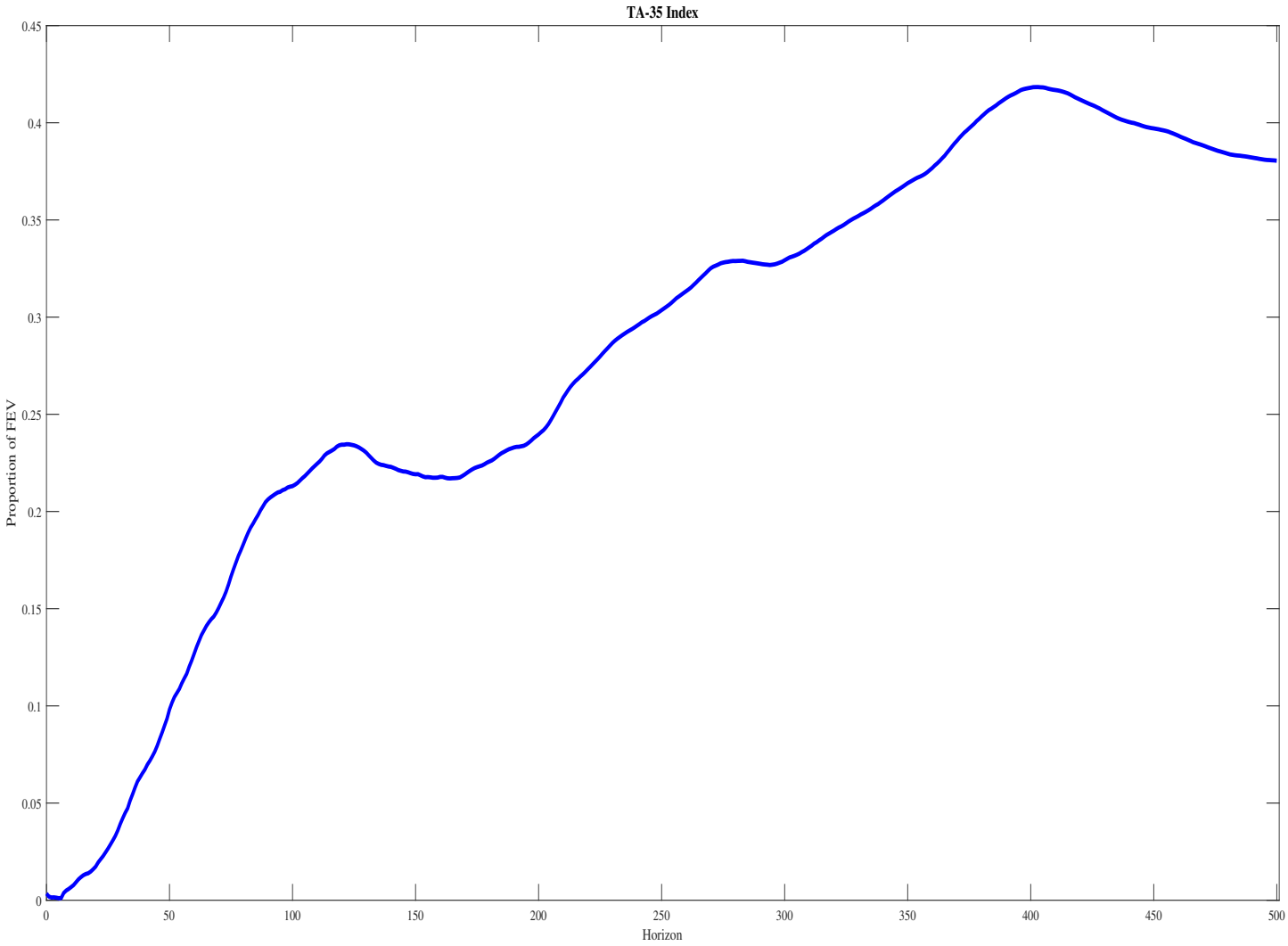

Notes: This figure presents the FEV shares of the variation in the TA-35 stock price index attributable to a one-standard-deviation GIV capital inflow shock, where the sample is truncated at 4/11/2022. Horizons are on the x-axis (impact horizon (0) to 500th horizon). FEV share is on the y-axis (in fractional terms).

Figure D.25: **Alternative Common Component Removal: Impulse Responses to GIV Capital Inflow Shock: MAKAM Convenience Yield and FFIs' Accumulated MAKAM Net Capital Inflows.**

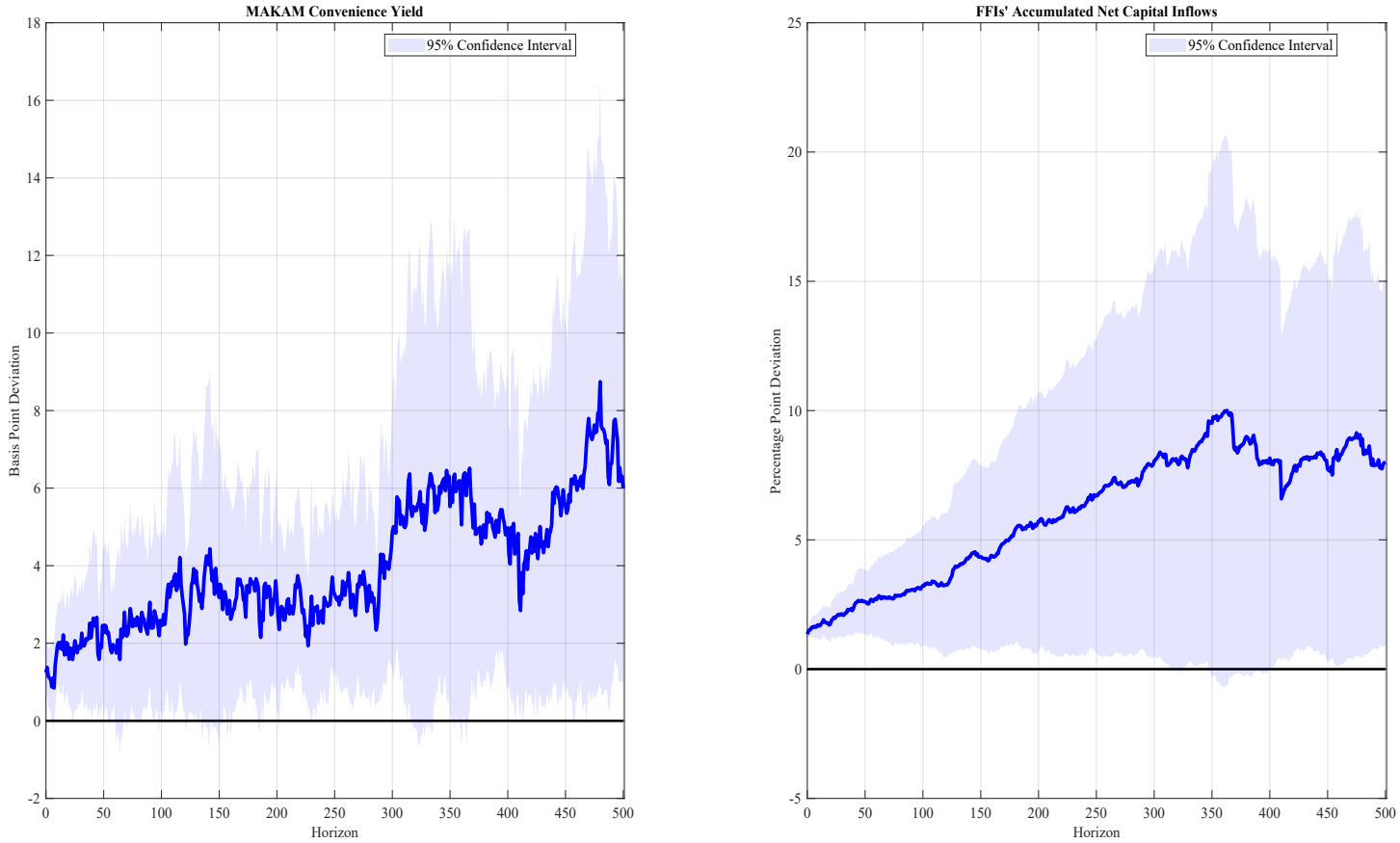

Notes: This figure presents the impulse responses (solid lines) to a GIV capital inflow shock of the MAKAM convenience yield and FFIs' accumulated MAKAM net capital inflows as share of outstanding MAKAM, where the common component removal in the GIV construction uses the equally-weighted-average of the FFI-level shocks instead of the inverse-variance-weighted one. Responses are normalized such that the peak response of FFIs' accumulated net capital inflows variable is 10 (i.e., 10-percentage-point increase as share of outstanding MAKAM), implying a 3.5-standard-deviation GIV capital inflow shock size. 95% confidence bands (shaded areas) are based on standard errors computed from the heteroskedasticity- and autocorrelation-consistent procedure of Newey and West (1987) with the truncation lag equal to $h+1$ (where $h = 0, 1, ..., 500$ is the local projection horizon). Horizons are on the x-axis (impact horizon (0) to 500th horizon). Values for MAKAM convenience yield variable are in basis point change units relative to the pre-shock value of the spread; those for the FFIs' accumulated MAKAM net capital inflows variable are in percentage-point change units relative to the pre-shock value of FFIs' market share.

Figure D.26: **Alternative Common Component Removal: FEVs Attributable to GIV Capital Inflow Shock: MAKAM Convenience Yield and FFIs' Accumulated MAKAM Net Capital Inflows.**

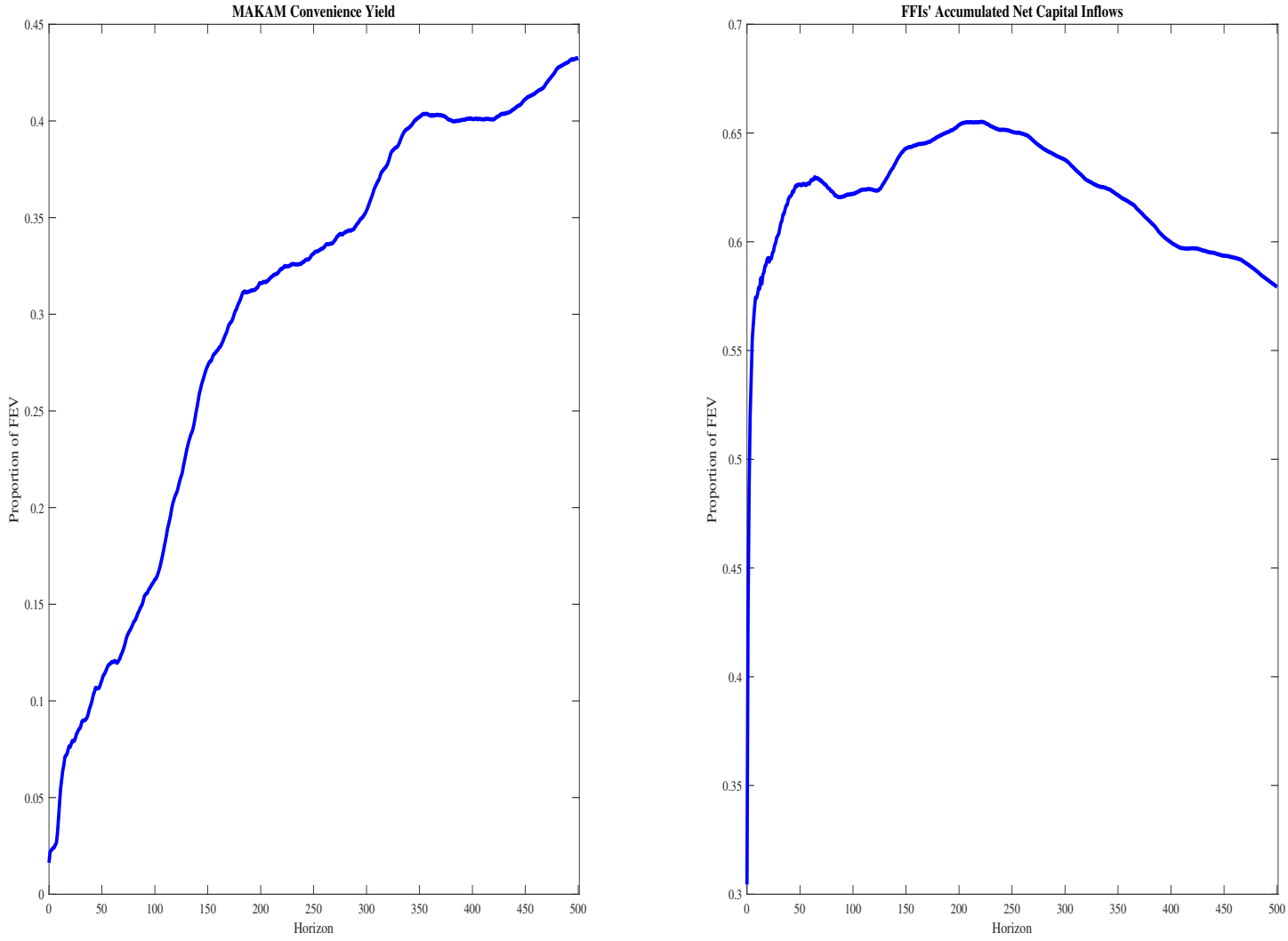

Notes: This figure presents the FEV shares of the variation in the MAKAM convenience yield and FFIs' accumulated MAKAM net capital inflow (as share of outstanding MAKAM) variables attributable to a one-standard-deviation GIV capital inflow shock, where the common component removal in the GIV construction uses the equally-weighted-average of the FFI-level shocks instead of the inverse-variance-weighted one. Horizons are on the x-axis (impact horizon (0) to 500th horizon). FEV share is on the y-axis (in fractional terms).

Figure D.27: **Alternative Common Component Removal: Impulse Responses to GIV Capital Inflow Shock: Government Bond Convenience Yields.**

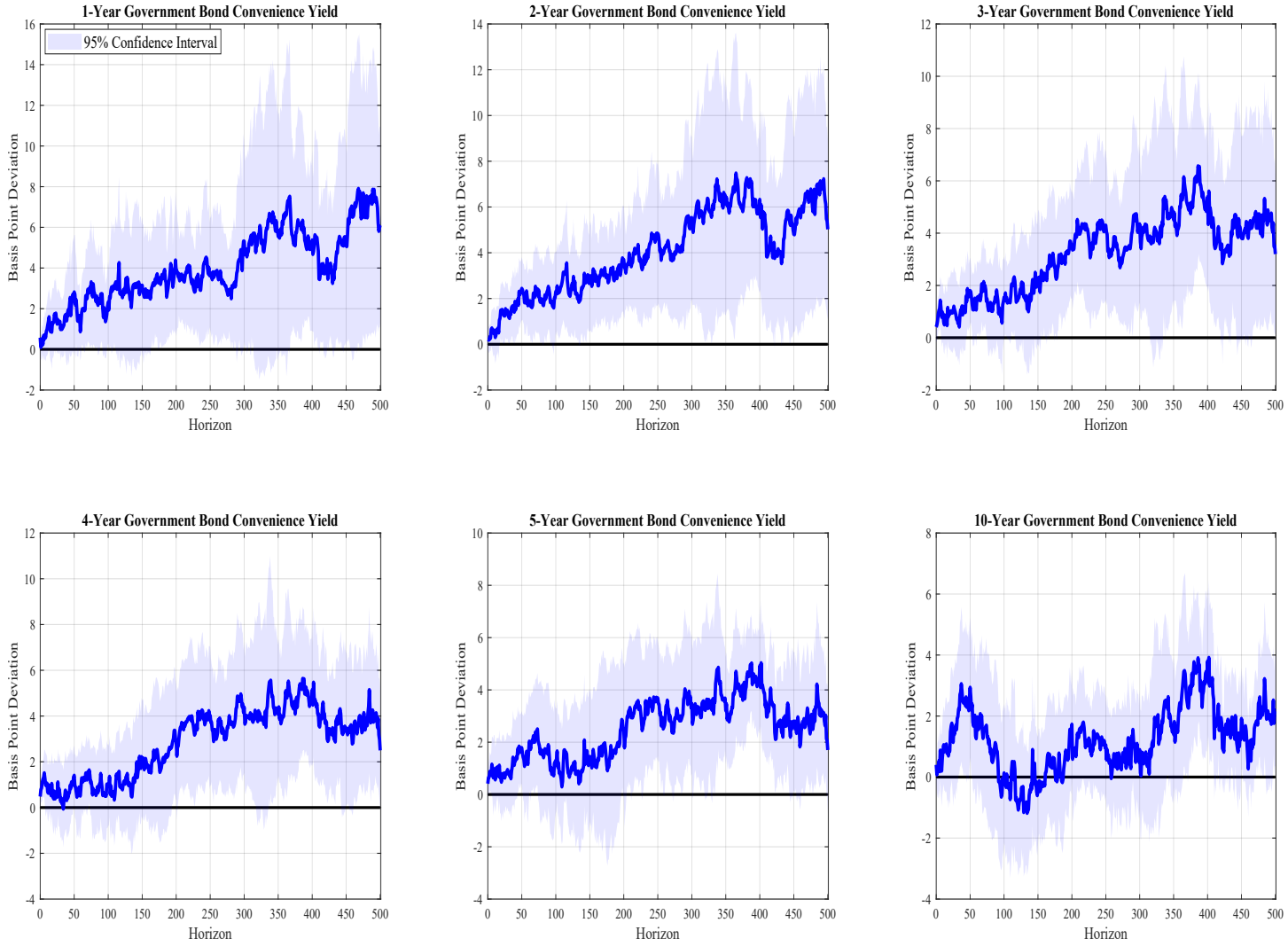

Notes: This figure presents the impulse responses (solid lines) to a GIV capital inflow shock of the 1- through 5-year and 10-year government bond yield spreads (with respect to maturity-comparable IRS rates), where the common component removal in the GIV construction uses the equally-weighted-average of the FFI-level shocks instead of the inverse-variance-weighted one. Responses are normalized such that the peak response of FFIs' accumulated net capital inflows variable is 10 (i.e., 10-percentage-point increase as share of outstanding MAKAM), implying a 3.5-standard-deviation GIV capital inflow shock size. 95% confidence bands (shaded areas) are based on standard errors computed from the heteroskedasticity- and autocorrelation-consistent procedure of Newey and West (1987) with the truncation lag equal to $h+1$ (where $h = 0, 1, ..., 500$ is the local projection horizon). Horizons are on the x-axis (impact horizon (0) to 500th horizon). Values are in basis point change units relative to the pre-shock value of the spread variable.

Figure D.28: **Alternative Common Component Removal: FEVs Attributable to GIV Capital Inflow Shock: Government Bond Convenience Yields.**

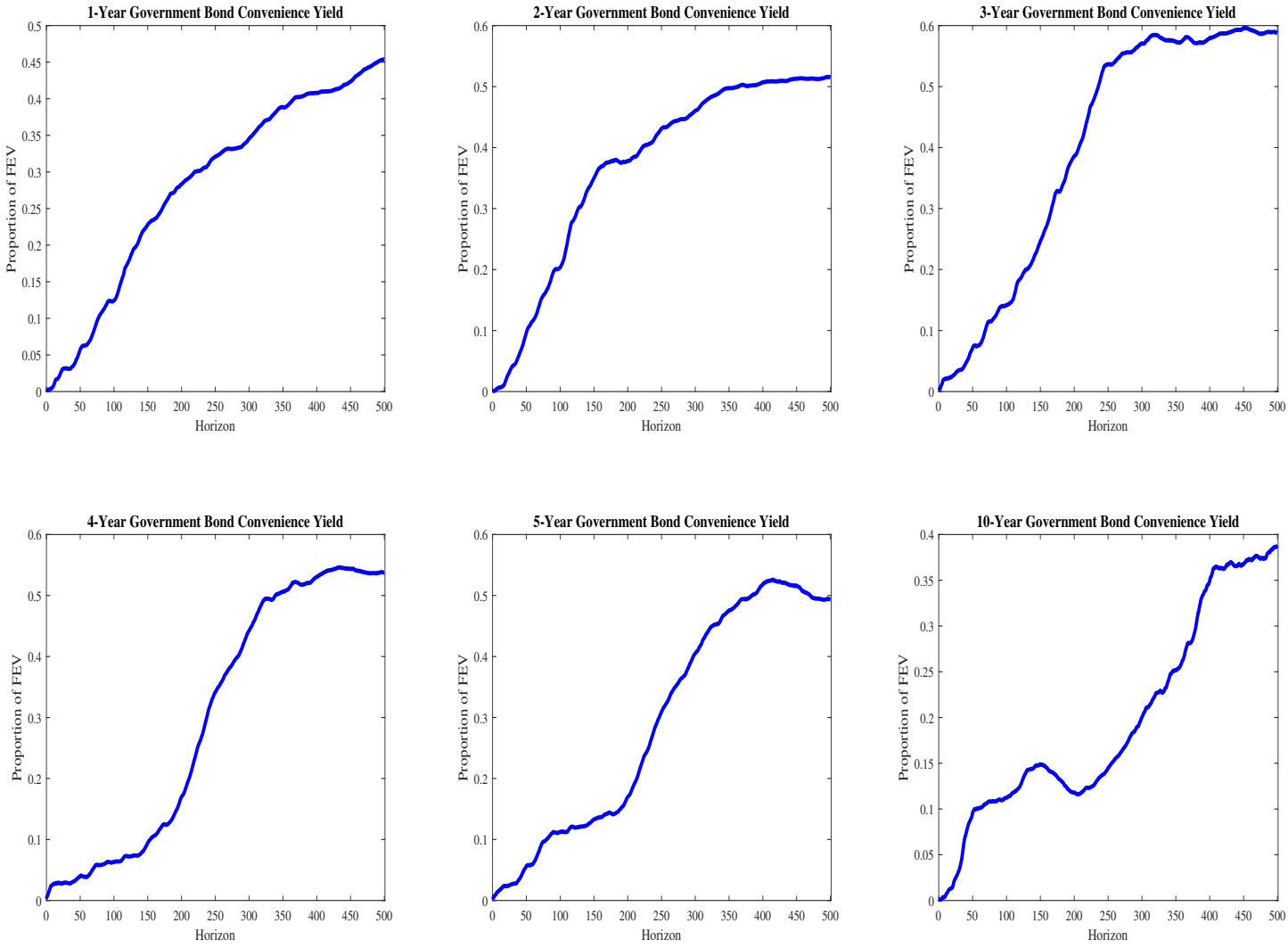

Notes: This figure presents the FEV shares of the variation in the government bond convenience yields attributable to a one-standard-deviation GIV capital inflow shock, where the common component removal in the GIV construction uses the equally-weighted-average of the FFI-level shocks instead of the inverse-variance-weighted one. Horizons are on the x-axis (impact horizon (0) to 500th horizon). FEV share is on the y-axis (in fractional terms).

Figure D.29: **Alternative Common Component Removal: Impulse Responses to GIV Capital Inflow Shock: Corporate Bond Yield Spreads.**

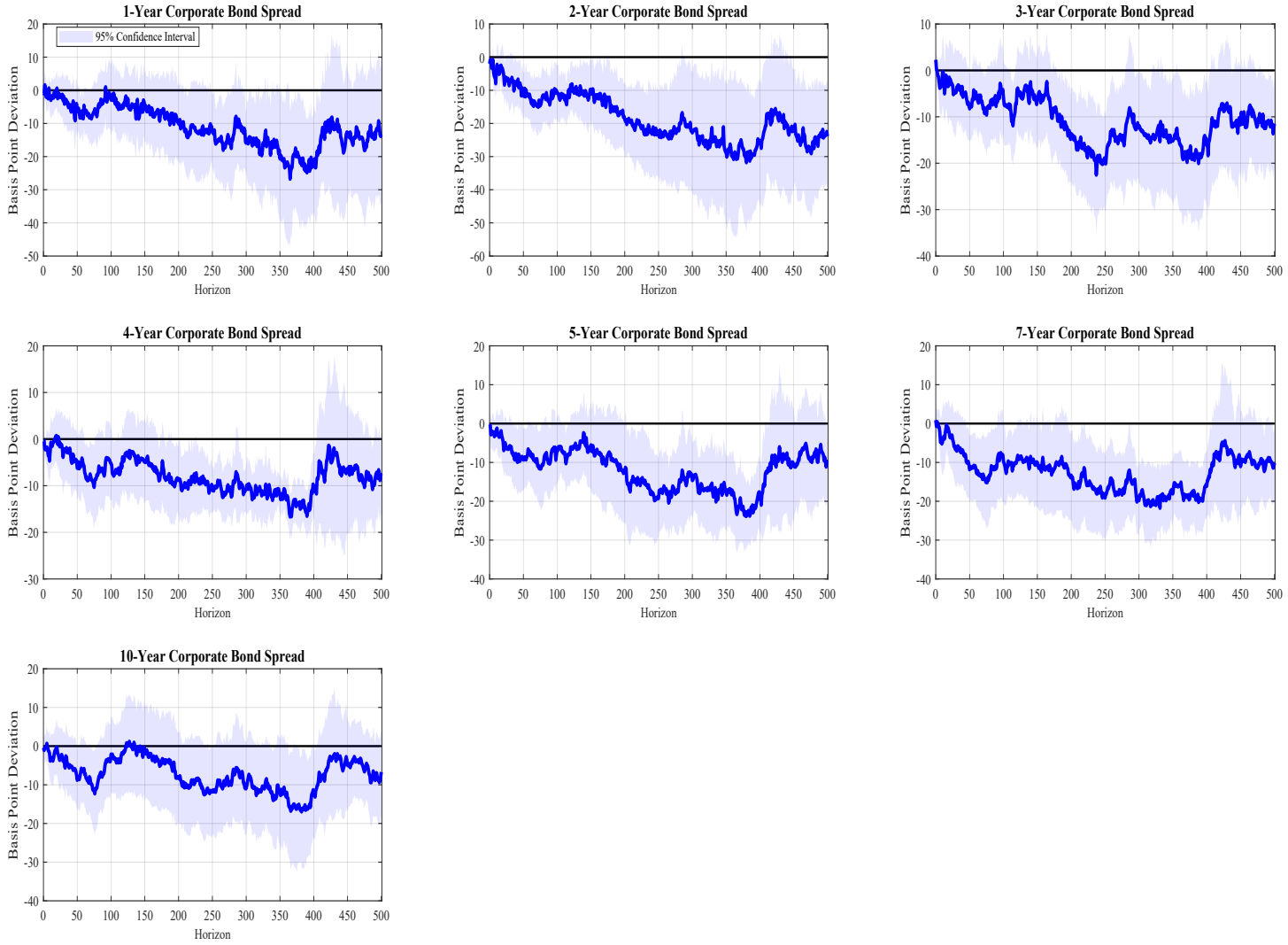

Notes: This figure presents the impulse responses (solid lines) to a GIV capital inflow shock of the 1- through 5-year and 7- and 10-year investment-grade corporate bond yield spreads (with respect to maturity-comparable IRS rates), where the common component removal in the GIV construction uses the equally-weighted-average of the FFI-level shocks instead of the inverse-variance-weighted one. Responses are normalized such that the peak response of FFIs' accumulated net capital inflows variable is 10 (i.e., 10-percentage-point increase as share of outstanding MAKAM), implying a 3.5-standard-deviation GIV capital inflow shock size. 95% confidence bands (shaded areas) are based on standard errors computed from the heteroskedasticity- and autocorrelation-consistent procedure of Newey and West (1987) with the truncation lag equal to $h+1$ (where $h = 0, 1, ..., 500$ is the local projection horizon). Horizons are on the x-axis (impact horizon (0) to 500th horizon). Values are in basis point change units relative to the pre-shock value of the spread variable.

Figure D.30: **Alternative Common Component Removal: FEVs Attributable to GIV Capital Inflow Shock: Corporate Bond Yield Spreads.**

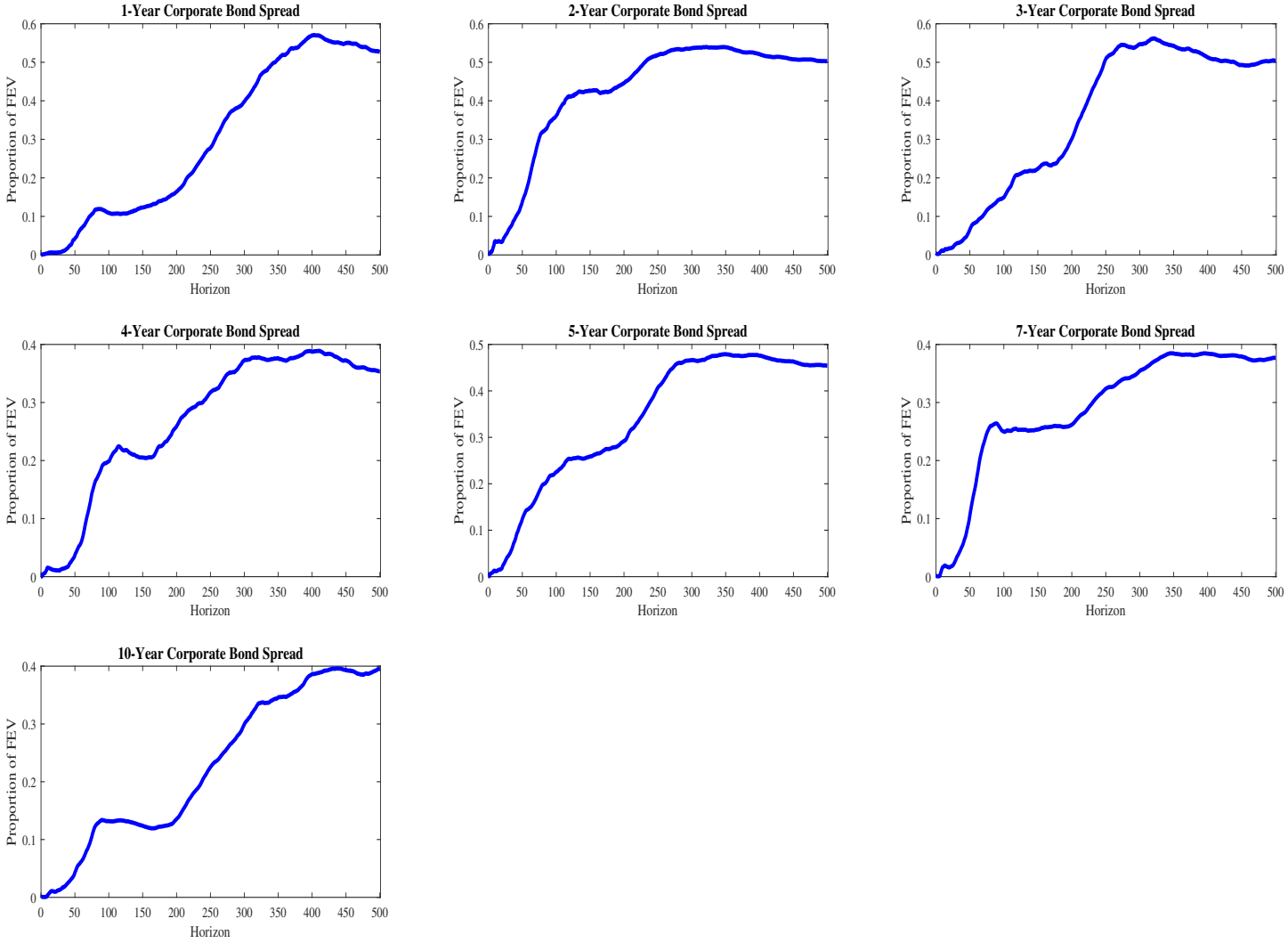

Notes: This figure presents the FEV shares of the variation in the corporate bond spread variables attributable to a one-standard-deviation GIV capital inflow shock, where the common component removal in the GIV construction uses the equally-weighted-average of the FFI-level shocks instead of the inverse-variance-weighted one. Horizons are on the x-axis (impact horizon (0) to 500th horizon). FEV share is on the y-axis (in fractional terms).

Figure D.31: **Alternative Common Component Removal: Impulse Responses to GIV Capital Inflow Shock: TA-35 Index.**

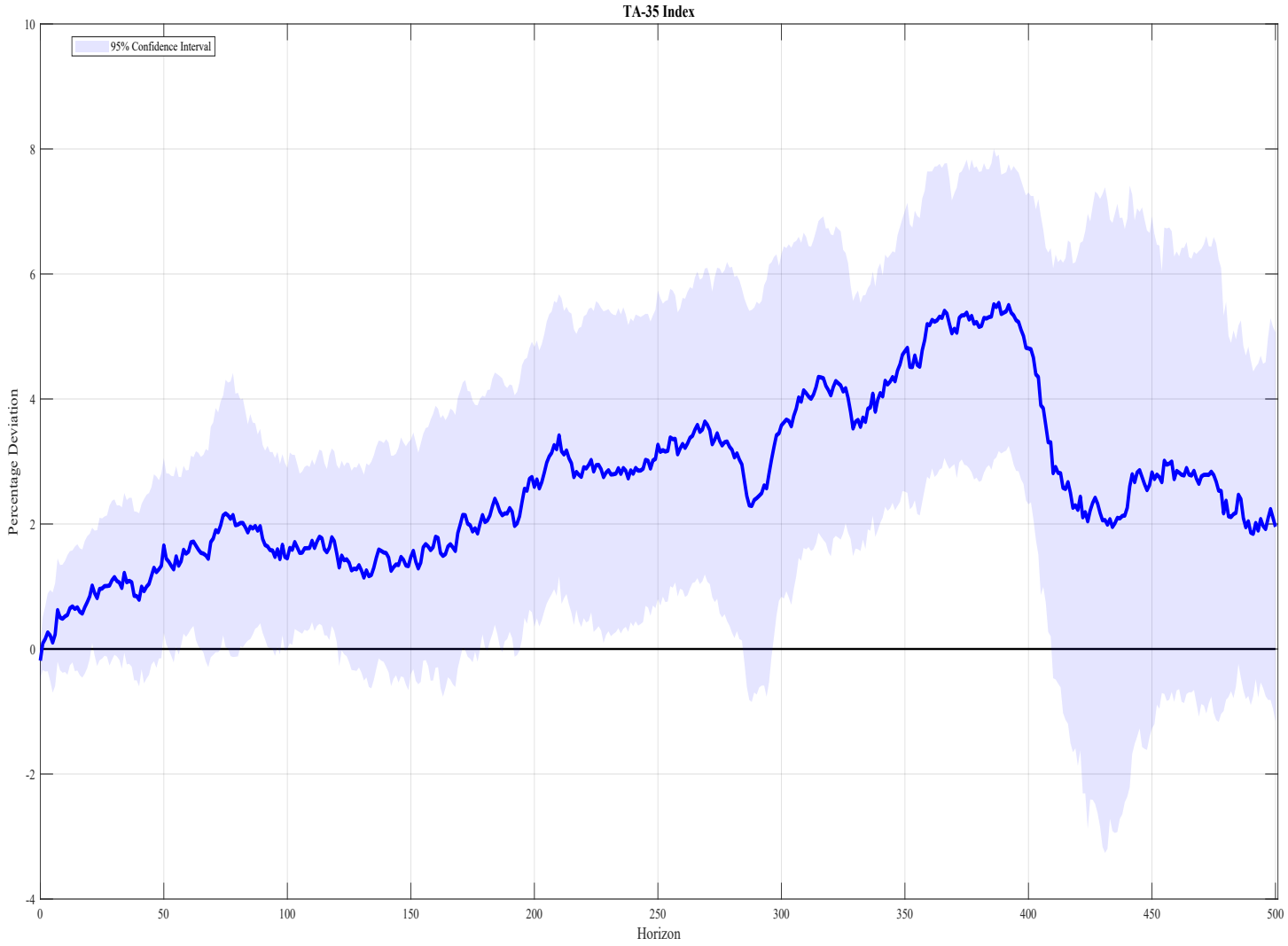

Notes: This figure presents the impulse responses (solid line) to a GIV capital inflow shock of the TA-35 stock price index, where the common component removal in the GIV construction uses the equally-weighted-average of the FFI-level shocks instead of the inverse-variance-weighted one. Responses are normalized such that the peak response of FFIs' accumulated net capital inflows variable is 10 (i.e., 10-percentage-point increase as share of outstanding MAKAM), implying a 3.5-standard-deviation GIV capital inflow shock size. 95% confidence bands (shaded area) are based on standard errors computed from the heteroskedasticity- and autocorrelation-consistent procedure of Newey and West (1987) with the truncation lag equal to $h+1$ (where $h = 0, 1, ..., 500$ is the local projection horizon). Horizons are on the x-axis (impact horizon (0) to 500th horizon). Values are in basis point change units relative to the pre-shock value of the spread variable.

Figure D.32: **Alternative Common Component Removal: FEVs Attributable to GIV Capital Inflow Shock: TA-35 Index.**

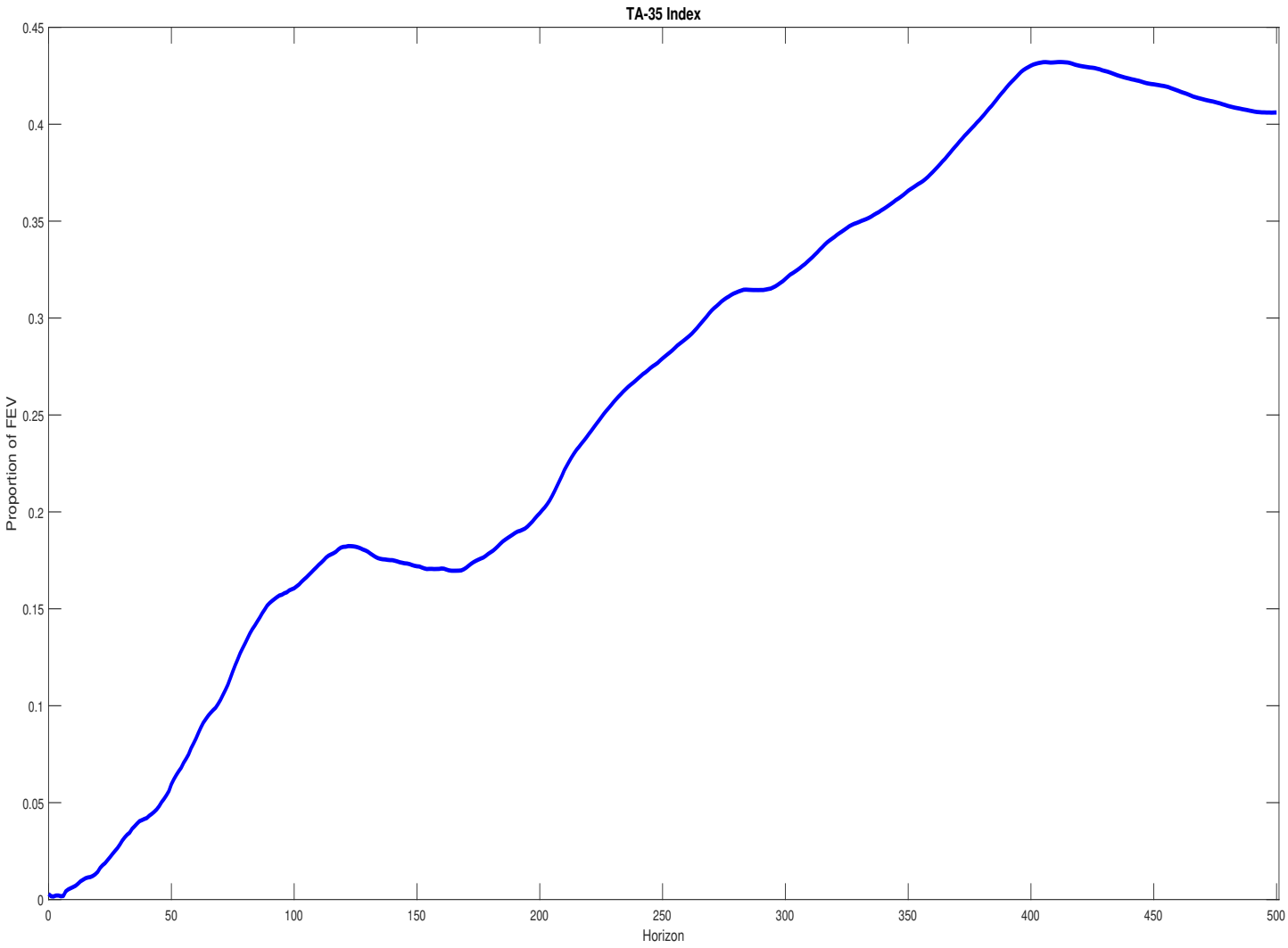

Notes: This figure presents the FEV shares of the variation in the TA-35 stock price index attributable to a one-standard-deviation GIV capital inflow shock, where the common component removal in the GIV construction uses the equally-weighted-average of the FFI-level shocks instead of the inverse-variance-weighted one. Horizons are on the x-axis (impact horizon (0) to 500th horizon). FEV share is on the y-axis (in fractional terms).

Figure D.33: **Controlling for Unobserved Custody-Based Flows: Impulse Responses to GIV Capital Inflow Shock: MAKAM Convenience Yield and FFIs' Accumulated MAKAM Net Capital Inflows.**

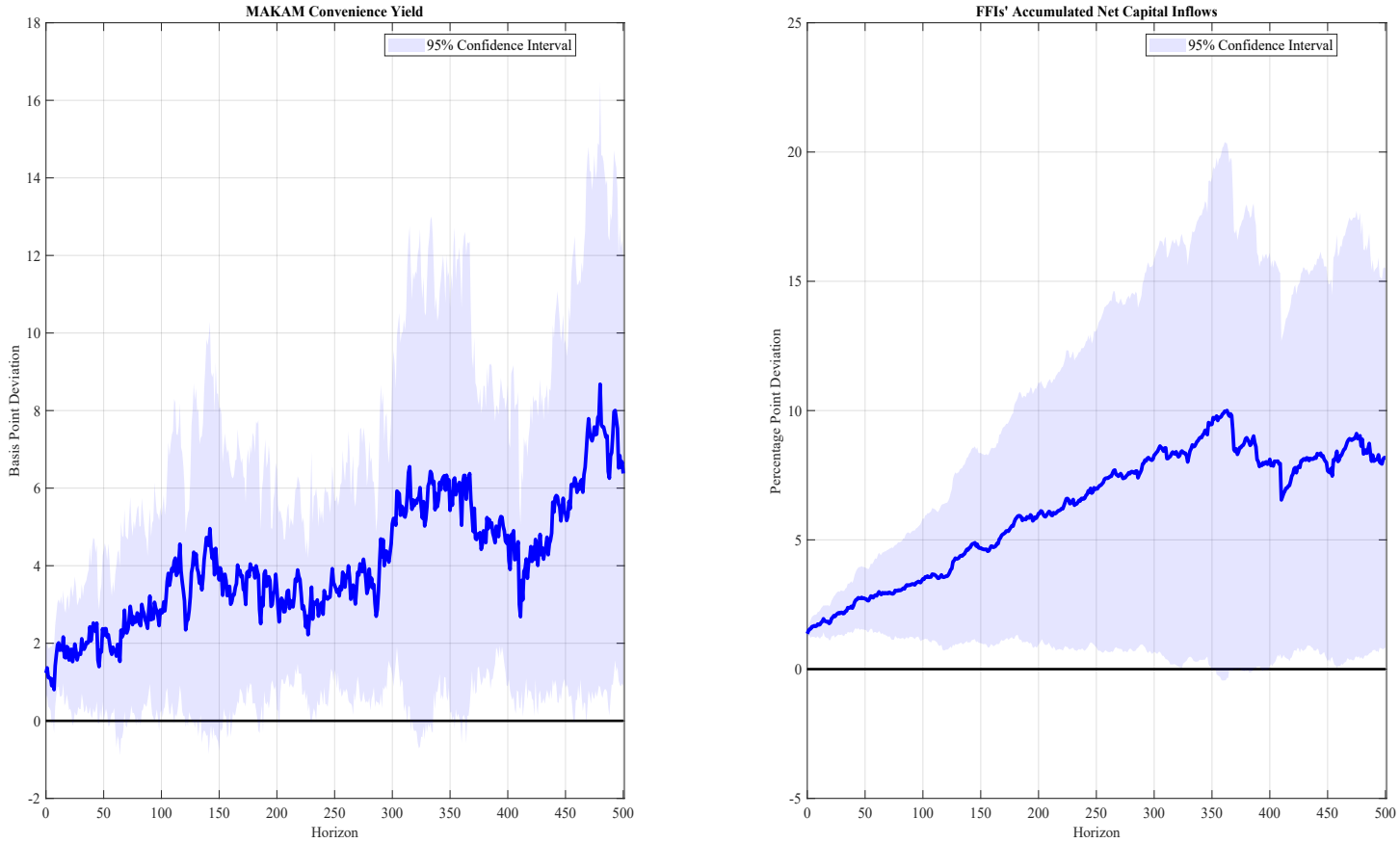

Notes: This figure presents the impulse responses (solid lines) to a GIV capital inflow shock of the MAKAM convenience yield and FFIs' accumulated MAKAM net capital inflows as share of outstanding MAKAM, where the custody bank FFI's flows are included in the FFI-level regressions. Responses are normalized such that the peak response of FFIs' accumulated net capital inflows variable is 10 (i.e., 10-percentage-point increase as share of outstanding MAKAM), implying a 3.4-standard-deviation GIV capital inflow shock size. 95% confidence bands (dashed lines) are based on standard errors computed from the heteroskedasticity- and autocorrelation-consistent procedure of Newey and West (1987) with the truncation lag equal to $h+1$ (where $h = 0, 1, ..., 500$ is the local projection horizon). Horizons are on the x-axis (impact horizon (0) to 500th horizon). Values for MAKAM convenience yield variable are in basis point change units relative to the pre-shock value of the spread; those for the FFIs' accumulated MAKAM net capital inflows variable are in percentage-point change units relative to the pre-shock value of FFIs' market share.

Figure D.34: **Controlling for Unobserved Custody-Based Flows: FEVs Attributable to GIV Capital Inflow Shock: MAKAM Convenience Yield and FFIs' Accumulated MAKAM Net Capital Inflows.**

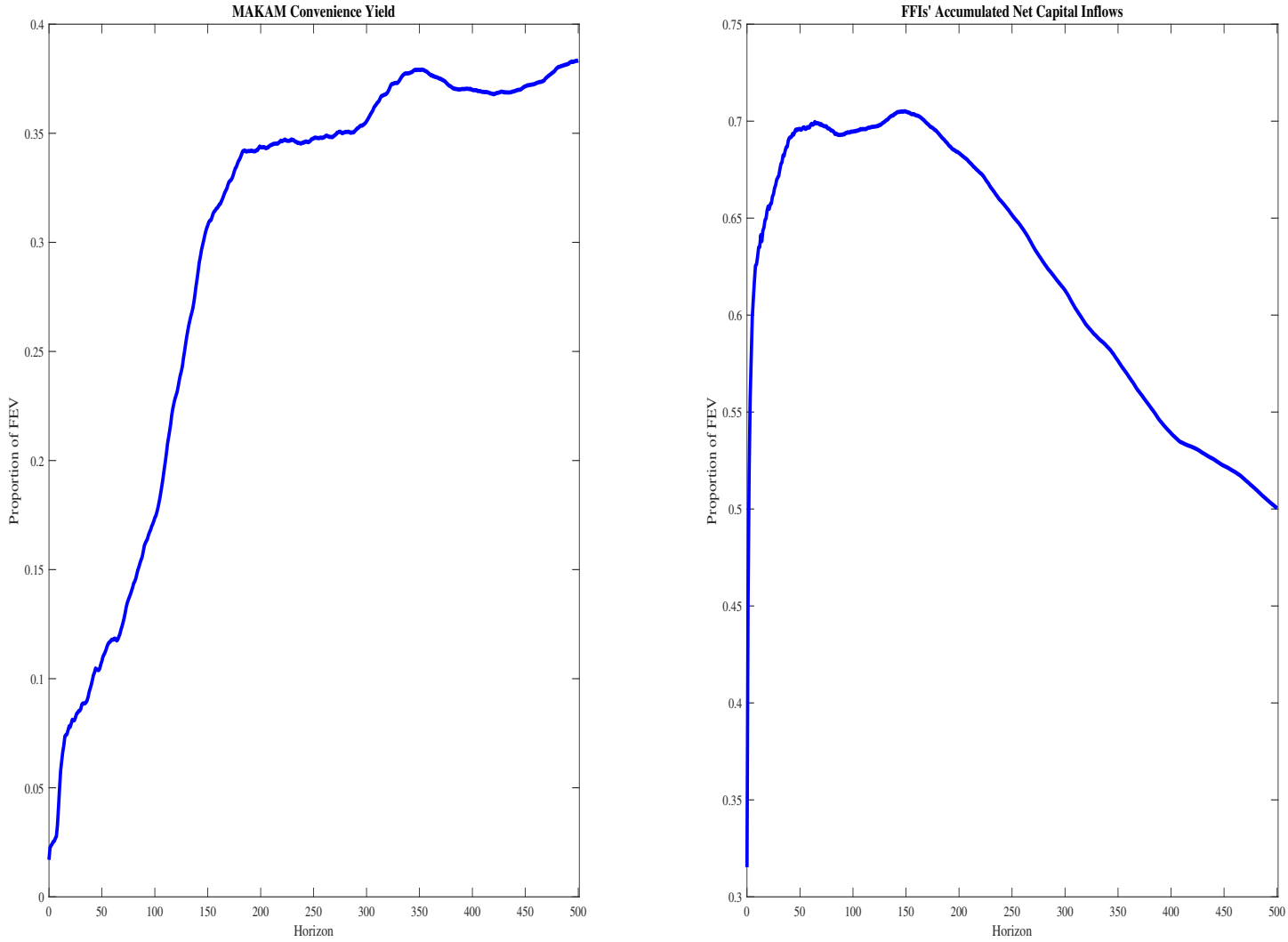

Notes: This figure presents the FEV shares of the variation in the MAKAM convenience yield and FFIs' accumulated MAKAM net capital inflow (as share of outstanding MAKAM) variables attributable to a one-standard-deviation GIV capital inflow shock, where the custody bank FFI's flows are included in the FFI-level regressions. Horizons are on the x-axis (impact horizon (0) to 500th horizon). FEV share is on the y-axis (in fractional terms).

Figure D.35: **Controlling for Unobserved Custody-Based Flows: Impulse Responses to GIV Capital Inflow Shock: Government Bond Convenience Yields.**

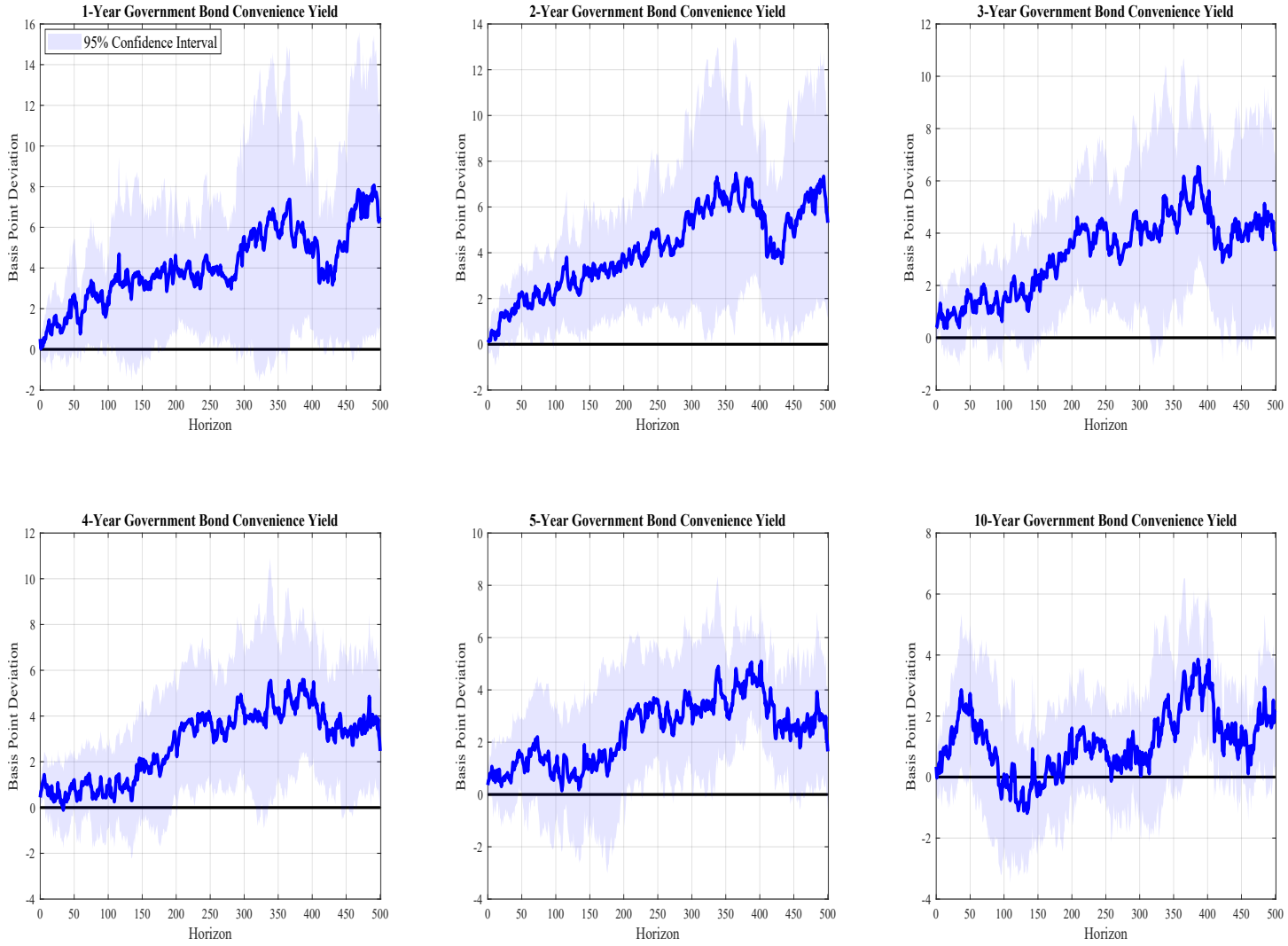

Notes: This figure presents the impulse responses (solid lines) to a GIV capital inflow shock of the 1- through 5-year and 10-year government bond convenience yields, where the custody bank FFI's flows are included in the FFI-level regressions. Responses are normalized such that the peak response of FFIs' accumulated net capital inflows variable is 10 (i.e., 10-percentage-point increase as share of outstanding MAKAM), implying a 3.4-standard-deviation GIV capital inflow shock size. 95% confidence bands (dashed lines) are based on standard errors computed from the heteroskedasticity- and autocorrelation-consistent procedure of Newey and West (1987) with the truncation lag equal to $h+1$ (where $h = 0, 1, ..., 500$ is the local projection horizon). Horizons are on the x-axis (impact horizon (0) to 500th horizon). Values are in basis point change units relative to the pre-shock value of the spread variable.

Figure D.36: **Controlling for Unobserved Custody-Based Flows: FEVs Attributable to GIV Capital Inflow Shock: Government Bond Convenience Yields.**

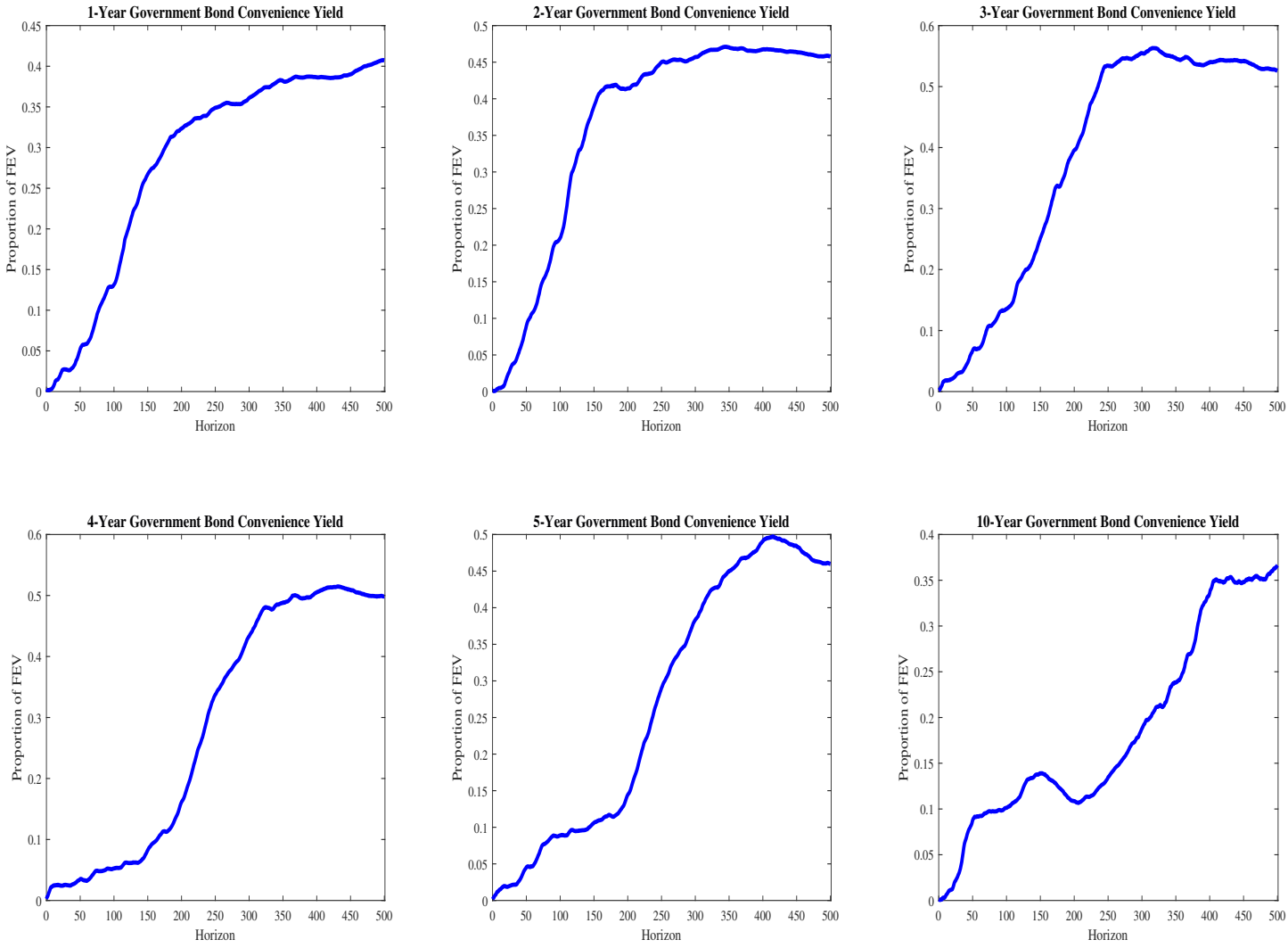

Notes: This figure presents the FEV shares of the variation in the government bond convenience yields attributable to a one-standard-deviation GIV capital inflow shock, where the custody bank FFI's flows are included in the FFI-level regressions. Horizons are on the x-axis (impact horizon (0) to 500th horizon). FEV share is on the y-axis (in fractional terms).

Figure D.37: **Controlling for Unobserved Custody-Based Flows: Impulse Responses to GIV Capital Inflow Shock: Corporate Bond Yield Spreads.**

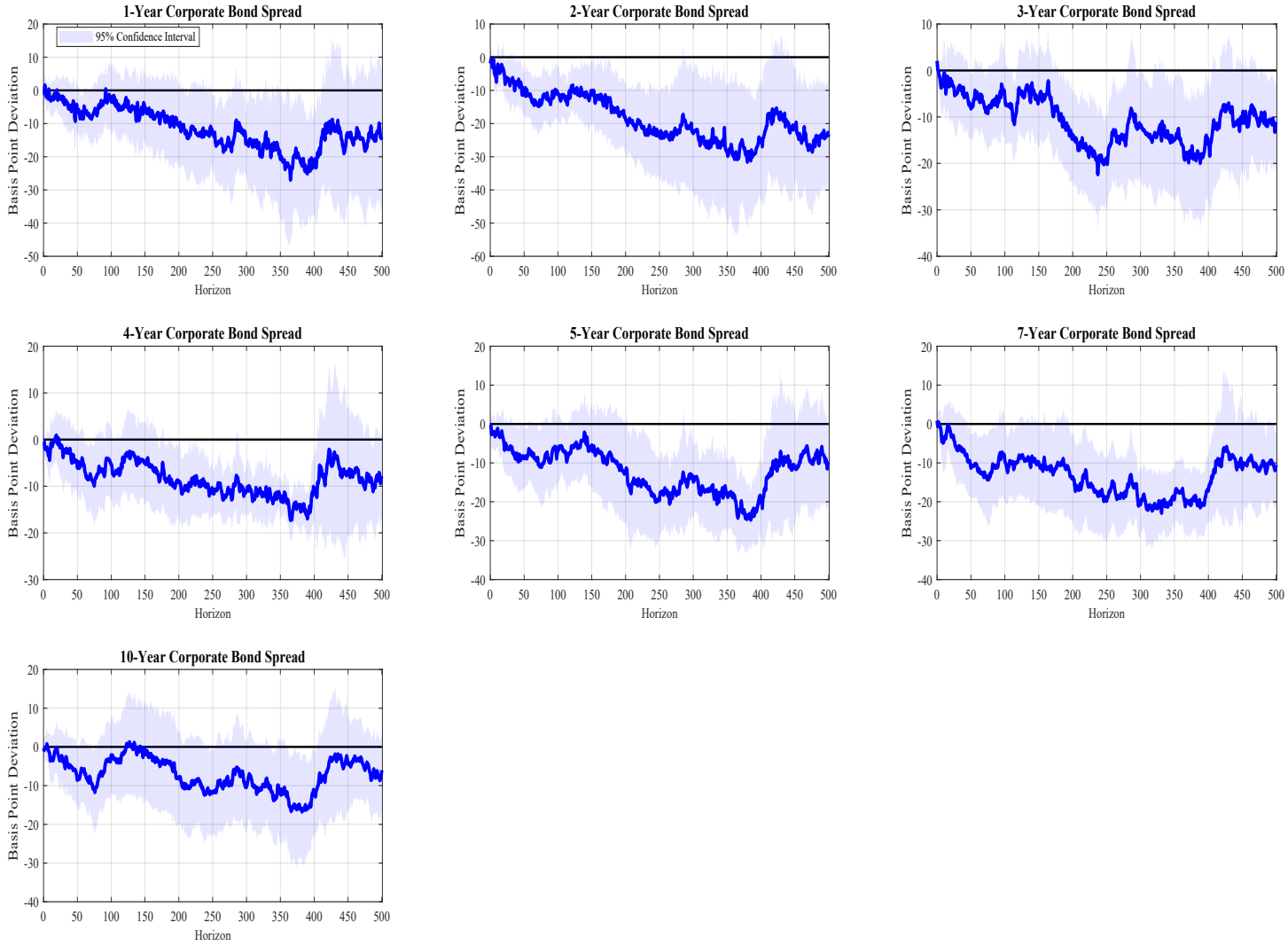

Notes: This figure presents the impulse responses (solid lines) to a GIV capital inflow shock of the 1- through 5-year and 7- and 10-year investment-grade corporate bond yield spreads (with respect to maturity-comparable IRS rates), where the custody bank FFI's flows are included in the FFI-level regressions. Responses are normalized such that the peak response of FFIs' accumulated net capital inflows variable is 10 (i.e., 10-percentage-point increase as share of outstanding MAKAM), implying a 3.4-standard-deviation GIV capital inflow shock size. 95% confidence bands (dashed lines) are based on standard errors computed from the heteroskedasticity- and autocorrelation-consistent procedure of Newey and West (1987) with the truncation lag equal to $h+1$ (where $h = 0, 1, ..., 500$ is the local projection horizon). Horizons are on the x-axis (impact horizon (0) to 500th horizon). Values are in basis point change units relative to the pre-shock value of the spread variable.

Figure D.38: **Controlling for Unobserved Custody-Based Flows: FEVs Attributable to GIV Capital Inflow Shock: Corporate Bond Yield Spreads.**

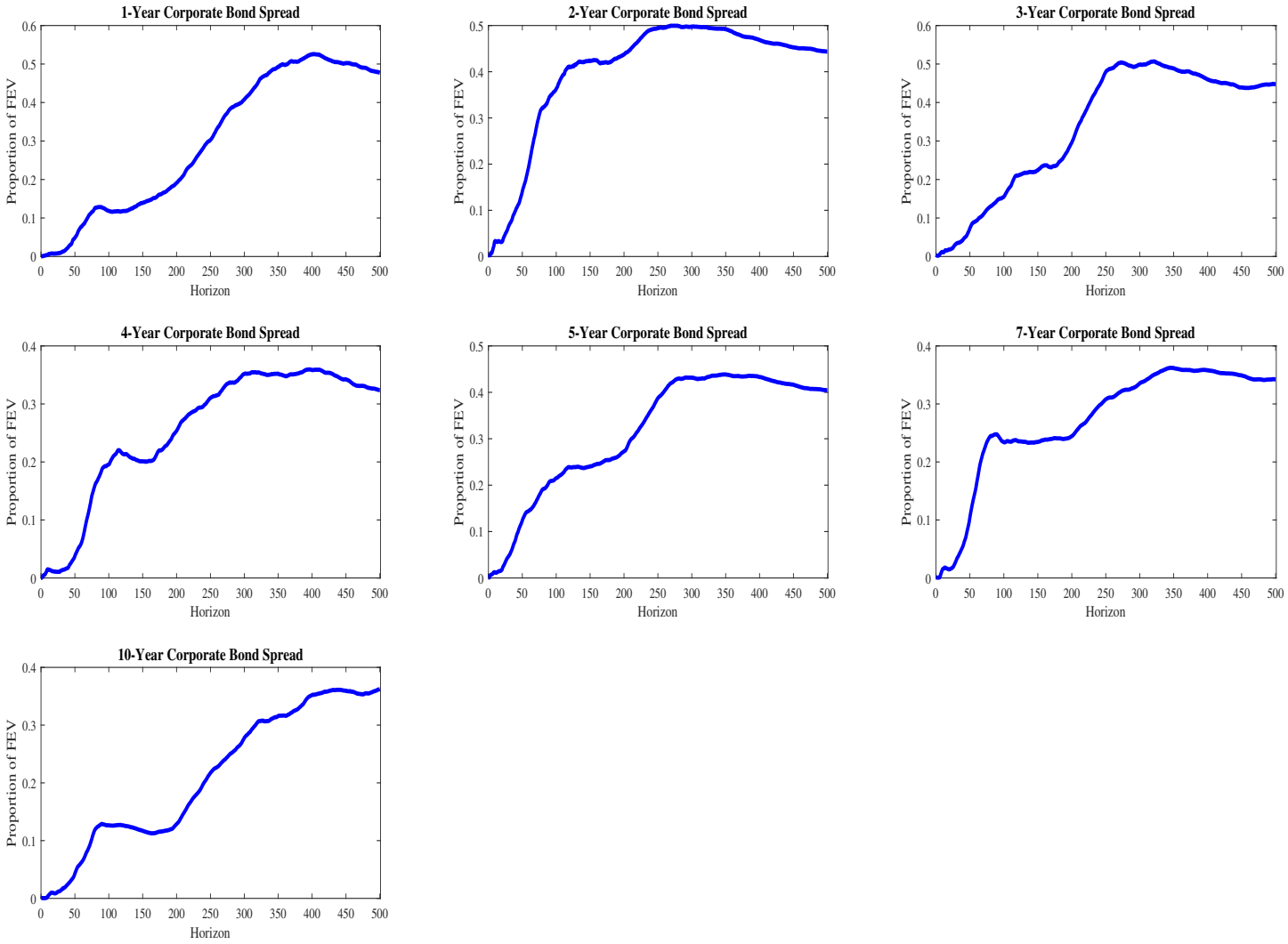

Notes: This figure presents the FEV shares of the variation in the corporate bond spread variables attributable to a one-standard-deviation GIV capital inflow shock, where the custody bank FFI's flows are included in the FFI-level regressions. Horizons are on the x-axis (impact horizon (0) to 500th horizon). FEV share is on the y-axis (in fractional terms).

Figure D.39: **Controlling for Unobserved Custody-Based Flows: Impulse Responses to GIV Capital Inflow Shock: TA-35 Index.**

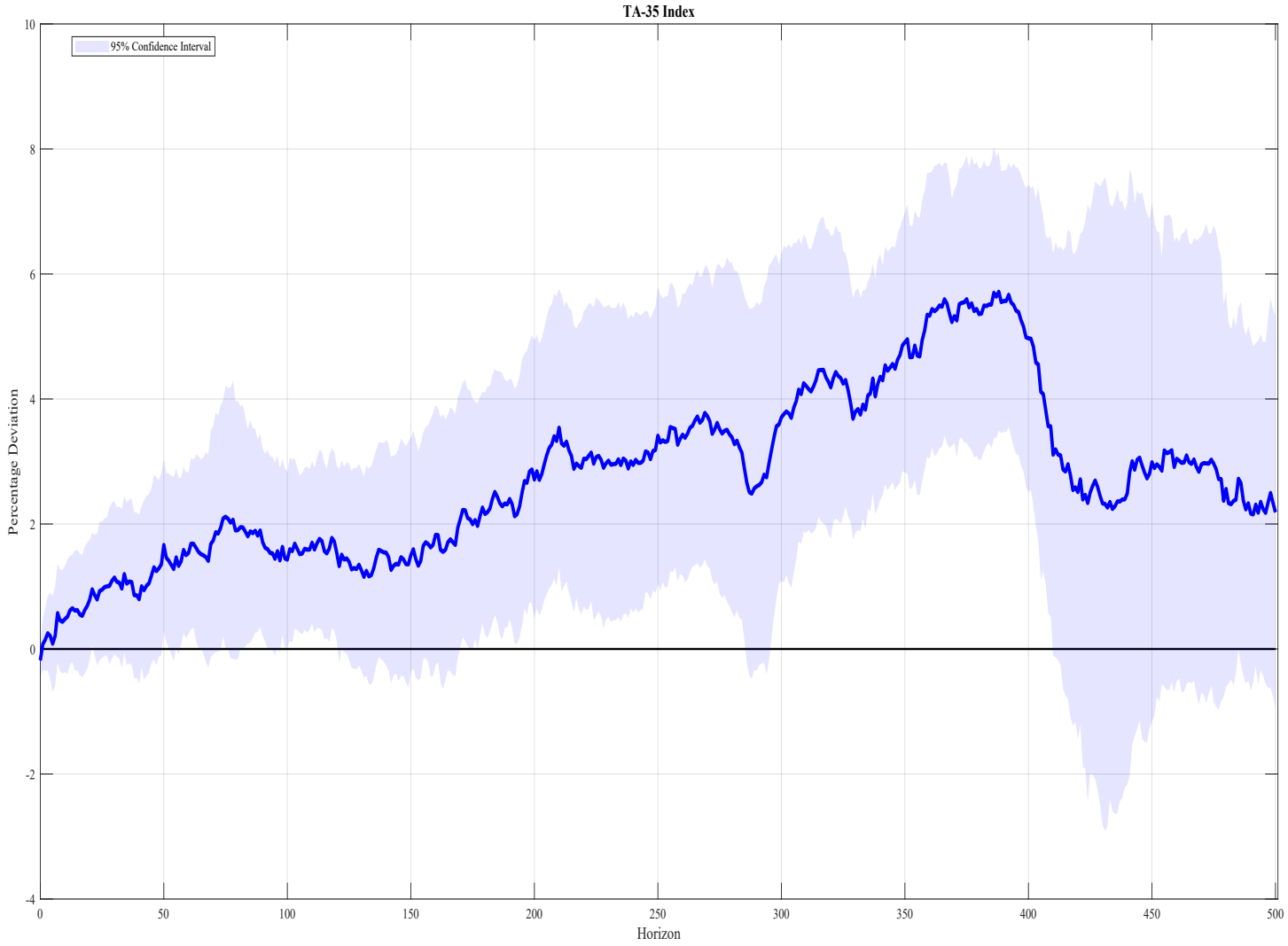

Notes: This figure presents the impulse responses (solid lines) to a GIV capital inflow shock of the TA-35 stock price index, where the custody bank FFI's flows are included in the FFI-level regressions. Responses are normalized such that the peak response of FFIs' accumulated net capital inflows variable is 10 (i.e., 10-percentage-point increase as share of outstanding MAKAM), implying a 3.4-standard-deviation GIV capital inflow shock size. 95% confidence bands (dashed lines) are based on standard errors computed from the heteroskedasticity- and autocorrelation-consistent procedure of Newey and West (1987) with the truncation lag equal to $h+1$ (where $h = 0, 1, ..., 500$ is the local projection horizon). Horizons are on the x-axis (impact horizon (0) to 500th horizon). Values are in basis point change units relative to the pre-shock value of the spread variable.

Figure D.40: **Controlling for Unobserved Custody-Based Flows: FEVs Attributable to GIV Capital Inflow Shock: TA-35 Index.**

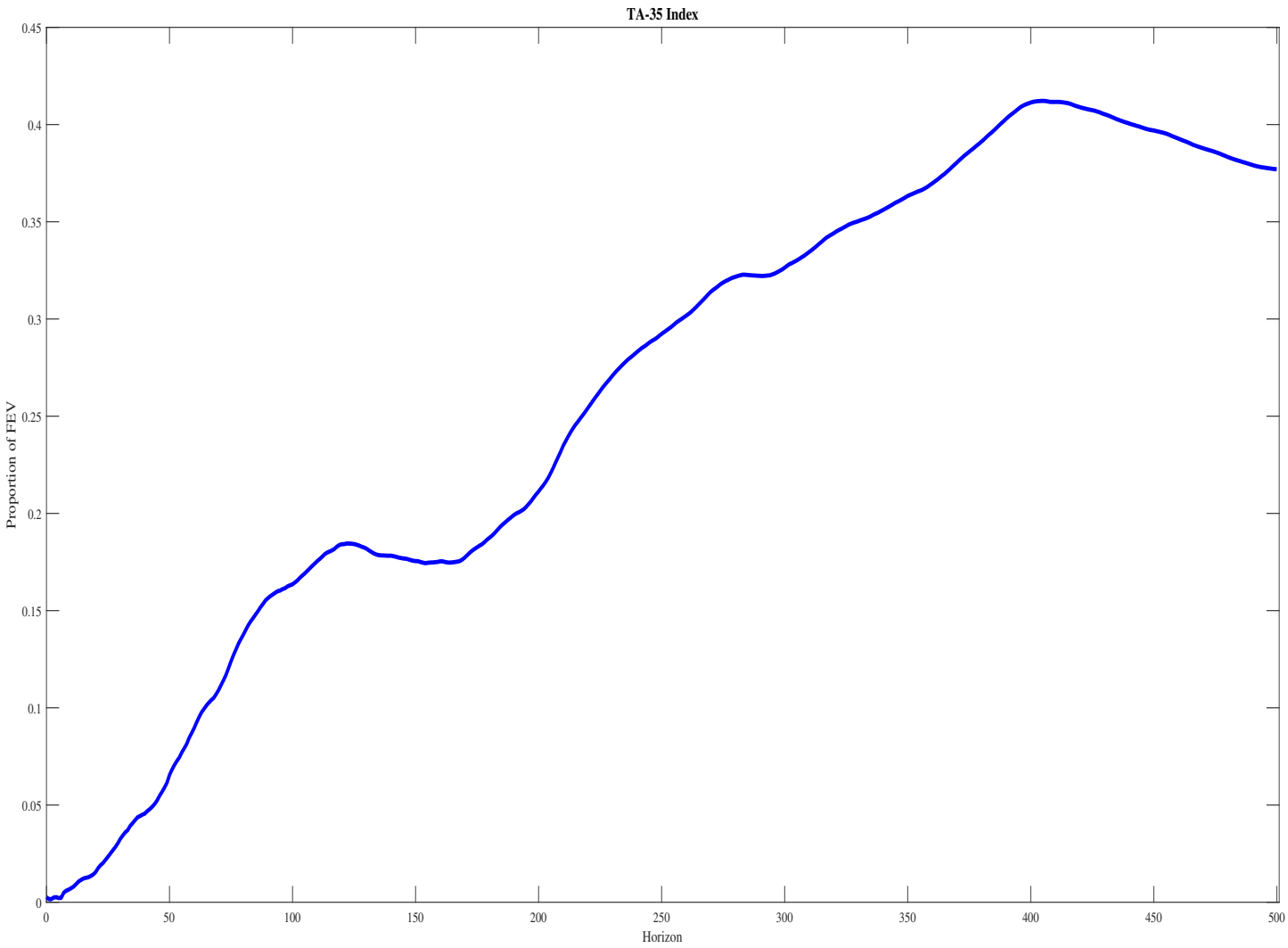

Notes: This figure presents the FEV shares of the variation in the TA-35 stock price index attributable to a one-standard-deviation GIV capital inflow shock, where the custody bank FFI's flows are included in the FFI-level regressions. Horizons are on the x-axis (impact horizon (0) to 500th horizon). FEV share is on the y-axis (in fractional terms).

References

Anderson, A. G., Du, W. and Schlusche, B.: 2024, Arbitrage Capital of Global Banks, *The Journal of Finance (forthcoming)* .

BCBS and BIS: 2013, *Basel III: the Liquidity Coverage Ratio and Liquidity Risk Monitoring Tools*, Bank for International Settlements.

Duffie, D.: 2010, Presidential address: Asset price dynamics with slow-moving capital, *The Journal of Finance* **65**(4), 1237–1267.

Gabaix, X. and Koijen, R. S. J.: 2024, Granular instrumental variables, *Journal of Political Economy* **132**(7), 2274–2303.

Gorodnichenko, Y. and Lee, B.: 2020, Forecast error variance decompositions with local projections, *Journal of Business & Economic Statistics* **38**(4), 921–933.

Gray, M. S. and Pongsaparn, M. R.: 2015, *Issuance of central bank securities: International experiences and guidelines*, International Monetary Fund.

Ivashina, V., Scharfstein, D. S. and Stein, J. C.: 2015, Dollar Funding and the Lending Behavior of Global Banks, *The Quarterly Journal of Economics* **130**(3), 1241–1281.

Mitchell, M., Pedersen, L. H. and Pulvino, T.: 2007, Slow moving capital, *American Economic Review* **97**(2), 215–220.

Nagel, S.: 2016, The liquidity premium of near-money assets, *The Quarterly Journal of Economics* **131**(4), 1927–1971.

Newey, W. K. and West, K. D.: 1987, A simple, positive semi-definite, heteroskedasticity and autocorrelation consistent covariance matrix, *Econometrica* **55**(3), 703–708.

Rime, D., Schrimpf, A. and Syrstad, O.: 2022, Covered Interest Parity Arbitrage, *The Review of Financial Studies* **35**(11), 5185–5227.